

Flexible Runway Scheduling with non-linear Noise Restrictions using a Tabu Search Algorithm

Sam Lagerwij



Flexible Runway Scheduling with non-linear Noise Restrictions using a Tabu Search Algorithm

by

Sam Lagerwijn

to obtain the degree of Master of Science
at the Delft University of Technology,
to be defended publicly on Tuesday March 19th, 2024.

Student number: 4658418
Project duration: March 2023 – March 2024
Thesis committee: Dr. A. Bombelli TU Delft, Chairman
Ir. P.C. Roling TU Delft, Daily Supervisor
Dr. Ir. J. Ellerbroek TU Delft, Examiner

An electronic version of this thesis is available at <http://repository.tudelft.nl/>.
Cover image retrieved from: <https://nieuws.klm.com/beeldmateriaal/> on February 1st, 2024

Acknowledgements

This thesis ends my time at the faculty of Aerospace Engineering in Delft. I have been interested in aircraft and the whole aviation industry for as long as I can remember. So choosing this university and study was an easy choice for me. Aerospace Engineering at Delft University of Technology. After more than six years I can proudly say that I managed to finish my academic journey at the same university and study. The past year was not always easy, and sometimes a little bit lonely, but I am proud of the results presented in this paper.

I would like to express my gratitude to my supervisor Paul Roling for his support during the entire thesis project. Thank you for the valuable feedback and insights you gave during our meetings. You always had some ideas when I was stuck, and your contributions significantly improved the overall quality of this thesis. Furthermore, I would like to thank Alessandro Bombelli for his feedback during the various milestone meetings. Your attention to detail and valuable ideas contributed to having a clear story that is understandable for everyone.

Thank you to all the friends I made during my time in Delft, both in my bachelor's and my master's. You all made my time in Delft enjoyable, and I appreciate having some distractions besides the hard studying. I would specifically like to thank Vincent, it was always a pleasure to work together in group projects and to be on the same page on most subjects. You were always available for help, and your feedback and advice during the times I was stuck or doubting about my methodology improved the quality of my thesis report.

Thank you Juliette for being at my side during the whole thesis process. I'm thankful that you were always there for me during the good times and sometimes the less good times. You always ensured me that I was going in the right direction, and kept me motivated. I will be forever grateful for that.

Thank you to all my friends at home for all the good times I had besides studying. To have a chat together after a long day of thesis work was always enjoyable for me. Thank you for that.

Finally, I would like to thank my parents for always supporting me during my entire education. I am happy to celebrate this great moment in my life with you.

Sam Lagerwijn
Naaldwijk, March 2024

Contents

List of Figures	vii
List of Tables	ix
List of Abbreviations	xi
Introduction	xv
I Scientific Paper	1
II Literature Study	
previously graded under AE4020	25
1 Introduction	27
1.1 Background Runway Scheduling	27
1.2 Research Context	27
1.3 Report Structure	28
2 Airport Capacity	29
2.1 Background Information	29
2.2 Runway Capacity Measures and Delay	29
2.3 Runway Capacity Factors	31
2.3.1 Runway Dependencies.	31
2.3.2 Runway Occupancy Time	33
2.3.3 Separation	33
2.3.4 Aircraft Mix and Sequencing.	34
2.3.5 Weather and Wind Conditions	35
2.4 Holding Techniques.	35
2.5 RECAT-EU	35
2.6 Runway Operation Modelling.	37
2.6.1 Arrival Mode	37
2.6.2 Departure Mode	38
2.6.3 Maximum Throughput Capacity.	38
2.7 Decision-support Tools	38
2.8 Airfield Capacity Models	38
2.8.1 Macroscopic Models.	39
2.8.2 Mesoscopic Models	40
2.8.3 Microscopic Models	40
3 Fuel Burn Modelling	43
3.1 Airline Fuel Economics	43
3.1.1 Airline Cost Structure	43
3.1.2 Aviation Fuel Cost	44
3.2 Existing Fuel Burn Models	45
3.2.1 Base of Aircraft Data	45
3.2.2 Aviation Environmental Design Tool.	46
3.2.3 Boeing Fuel Flow Method 2	47
3.2.4 Senzig-Fleming-Iovinelli (SFI) Model	47
3.3 Optimal Control and Fuel Consumption	48
3.3.1 Aircraft Trajectory Optimisation Problem	48
3.3.2 Solving the ATOP.	48
3.3.3 Implementation of the ATOP in The Runway Scheduling Model	49

4	Noise Modelling	51
4.1	Sources of Aircraft Noise	51
4.1.1	Airframe Noise	51
4.1.2	Engine Noise	51
4.2	Aircraft Noise Calculation	52
4.2.1	Weighted Sound Pressure Level	52
4.2.2	Sound Exposure Level	52
4.2.3	Day-Evening-Night Average Level	53
4.3	Noise Annoyance and Mitigation	53
4.3.1	Measurement of Annoyance	53
4.3.2	Balanced Approach	54
4.3.3	Noise Regulations at Schiphol Airport	57
4.4	Noise Modelling Tools	57
4.4.1	Integrated Noise Model	57
4.4.2	AEDT	58
4.4.3	Dutch Aircraft Noise Model (NRM)	58
4.4.4	ECAC Noise Model	59
5	Mathematical Problems and Solving Methods	61
5.1	Mathematical Models	61
5.2	Solving Methods	62
5.2.1	Exact Solving Methods	62
5.2.2	Metaheuristics	64
5.3	Receding Horizon Control	65
6	Research Proposal	67
6.1	Discussion Literature	67
6.1.1	Fuel	67
6.1.2	Noise	68
6.1.3	Optimal Control and Trajectory	68
6.1.4	Optimisation Method	68
6.2	Research Objective and Context	69
6.3	Research Questions	69
III	Supporting work	71
1	Previous Work	73
1.1	Flexible Runway Scheduling Model	73
1.1.1	Objective Function	73
1.1.2	Constraints	73
2	Additional Results	75
2.1	90-minute flight schedule	75
2.2	Six-hour flight schedule	77
2.3	Daytime flight schedule	78
2.4	Full day flight schedule	80
3	Verification & Validation	83
3.1	Verification	83
3.1.1	Separation	83
3.2	Validation	84
3.2.1	Handhavingspunten	84
3.2.2	Fuel flow and AEDT	85
	Bibliography	87

List of Figures

2.1	Delay as a function of capacity and demand [44]	31
2.2	Operations on converging and diverging runways[105].	32
2.3	Operations on intersecting runways [105].	32
2.4	Comparison of FCFS and CPS [52]	34
2.5	Categorisation process and criteria for assigning an existing aircraft into RECAT-EU scheme[91]	36
2.6	Runway capacity modelling for arrival mode [22]	37
3.1	Total Operating Cost breakdown	43
3.2	Passenger airlines operating costs United States 2019 [3]	44
3.3	Jet fuel price developments, Jet Fuel & Crude Oil price (\$/barrel)[47]	44
3.4	Results of the lexicographic approach[95]	49
4.1	Overview of main aircraft noise sources[32]	52
4.2	Percentage of highly annoyed people versus L_{DEN} for various airports[37]	54
4.3	The four principal elements of the Balanced Approach to Aircraft Noise Management[50]	54
4.4	The ICAO Noise Standards for aeroplanes [51]	55
5.1	Overview of Optimisation Techniques	62
5.2	Example of RHC for the RSP [111]	66
2.1	Additional results fuel optimization 90-minute flight schedule	75
2.2	Additional results noise optimization 90-minute flight schedule	76
2.3	Additional results fuel optimization six-hour flight schedule	77
2.4	Additional results noise optimization six-hour flight schedule	78
2.5	Pareto Front daytime flight schedule	78
2.6	Additional results fuel optimization daytime flight schedule	79
2.7	Additional results noise optimization daytime flight schedule	80
2.8	Pareto Front full-day flight schedule	80
2.9	Additional results fuel optimization full-day flight schedule	81
2.10	Additional results noise optimization full-day flight schedule	82
3.1	Handhavingspunten Amsterdam Airport Schiphol [53]	84

List of Tables

2.1	Classification of Runway Capacity Factors[92]	31
2.2	ICAO Wake Turbulence Categories [82]	33
2.3	Distance-based separation minima [82]	34
2.4	Time-based separation minima [82]	34
2.5	RECAT-EU separation in NM / seconds [91]	36
2.6	Runway Occupancy Times for the RECAT-EU categories [57]	36
2.7	Overview of airport capacity models [72], [79]	39
4.1	Day-evening-night average level penalties[21]	53
4.2	Criteria of equality[107]	57
6.1	Overview of potential research for the Thesis	67
6.2	Trade-off between selected metaheuristic algorithms	69
3.1	Part of balanced flight schedule	83
3.2	Validation handhavingspunten full day $\alpha = 0.2$	85

List of Abbreviations

AAS	Amsterdam Airport Schiphol
ACATS	Airport Capacity Analysis Through Simulation
ACO	Ant Colony Optimisation
AEDT	Aviation Environmental Design Tool
AEL	Acoustic Energy Level
ALP	Aircraft Landing Problem
AMAN	Arrival MANager
AND	Approximate Network Delays
APM	Aircraft Performance Model
AROT	Arrival Runway Occupancy Time
ARPM	Airline Procedure Model
ARSP	Aircraft Runway Scheduling Problem
ASP	Aircraft Scheduling Problem
ATM	Air Traffic Management
ATOP	Aircraft Trajectory Optimization Problem
ATP	Aircraft Take-off Problem
BADA	Base of Aircraft Data
BT	Buffer Time
CAA	Australian Civil Aviation Authority
CCO	Continuous Climb Operations
CDA	Continuous Descent Arrival
CPS	Constrained Position Shifting
CTAS	Center-TRACON Automation System
DBS	Distance-Based Separation
DENL	Day-Evening-Night Level
DMAN	Departure MANager
DOC	Direct Operating Cost
DROT	Departure Runway Occupancy Time
ECAC	European Civil Aviation Conference
EPN	Effective Perceived Noise

ETA	Estimated Time of Arrival
ETT	Estimated Take-off Time
FAA	Federal Aviation Administration
FAF	Final Approach Fix
FCFS	First-Come First-Served
FRSM	Flexible Runway Scheduling Model
GA	Genetic Algorithms
HA	Highly Annoyed
HAP	Highly Annoyed People
IAF	Initial Approach Fix
ICAO	International Civil Aviation Organization
IDT	Inter-Departure Time
INM	Integrated Noise Model
IOC	Indirect Operating Cost
KPI	Key Performance Indicator
LOS	Level of Service
MACAD	Mantea Airfield Capacity and Delay
MILP	Mixed Integer Linear Programming
MIP	Mixed Integer Programming
MTC	Maximum Throughput Capacity
MTOW	Maximum Take-Off Weight
MVA	Minimum Vectoring Altitude
NADP	Noise Abatement Departure Procedure
NM	Nautical Mile
NNC	Non-Noise Certificated
NPD	Noise-Power-Distance
NPR	Noise Preferential Routes
NRM	Nederlands Rekenmodel
PBN	Performance Based Navigation
PHCAP	Practical Hourly Capacity
RECAT-EU	European wake turbulence categories re-categorisation
RHC	Receding Horizon Control
ROC	Rate of Climb
ROD	Rate of Descent

ROT	Runway Occupancy Time
ROTA	Runway Occupancy Time of Arrival
ROTD	Runway Occupancy Time of Departure
RSP	Runway Scheduling Problem
SA	Simulated Annealing
SARPs	Standards and Recommended Practices
SDP	Sleep Disturbed People
SEL	Sound exposure Level
SFI	Senzig-Fleming-Iovinelli
SID	Standard Instrument Departure
SIMMOD	Airport and Airspace Simulation Model
SLT	Scheduled Landing Time
SOT	Scheduled Operating Time
SPL	Sound Pressure Level
TAAM	Total Airspace & Airport Modeller
TAP	Terminal Area Productivity
TBS	Time-Based Separation
TEM	Total Energy Model
TMA	Terminal Manoeuvring Area
TOC	Total Operating Cost
TS	Tabu Search
TSFC	Thrust Specific Fuel Consumption
VDOC	Variable Direct Operating Cost
VMC	Visual Meteorological Conditions
VND	Variable Neighbourhood Descent
WTC	Wake Turbulence Category
WV	Wake vortex

Introduction

With the demand for air travel projected to double by 2040 at an annual average rate of 3.4%[\[48\]](#), airport capacity is emerging as a crucial constraint in air transport operations. While the conventional response might involve the construction of new airports or expanding existing ones, such measures often carry the potential for adverse environmental impacts on nearby communities. This concern has led to the implementation of noise regulations, restricting the maximum allowable exposure to aircraft noise for residents. Beyond noise, airports struggle with additional environmental challenges, notably fuel consumption and associated emissions.

In response to these challenges, a model was developed at Delft University of Technology by Delsen[\[24\]](#). This model, designed to concurrently optimize fuel burn and minimize noise annoyance while efficiently scheduling flights to runways and respecting airport capacity, has undergone subsequent refinements led by van der Meijden [\[106\]](#) and Abbenhuis [\[1\]](#), shaping its continued evolution. However, the existing model is not without limitations, particularly in terms of computational performance and the accurate modeling of noise annoyance.

This research aims to enhance the existing model, aiming for increased computational performance for practical implementation in day-to-day operations. Moreover, the objective is to present a more accurate depiction of noise annoyance stemming from the allocation of flights to runways, with a specific emphasis on mitigating environmental impacts on nearby communities. The potential improvements hold the potential to increase airport capacity while adhering to stringent environmental regulations.

As the aviation industry prepares for a future with greater demands for air travel, this research aims to provide valuable insights and contribute significantly to the discussion on sustainable airport operations. By addressing issues such as efficiency, noise reduction, and environmental concerns, the research hopes to offer a strong framework for optimizing airport operations to meet the evolving global aviation needs.

The report is structured as follows. In [Part I](#), the scientific paper is outlined, encompassing the methodology, results, and conclusions. Moving on to [Part II](#), the literature review is presented, articulating the motivation for this research and discussing the identified literature. Finally, [Part III](#) encompasses all supporting work, including the previous research on which this study is built, along with verification and validation processes and additional results.

I

Scientific Paper

Flexible Runway Scheduling with non-linear Noise Restrictions using a Tabu Search Algorithm

Sam Lagerwijn*

Delft University of Technology, Delft, The Netherlands

Abstract

In response to the growing demand for air travel, major airports are approaching critical thresholds in their infrastructure capacity. As the transportation sector continues to expand, it is increasingly important to address environmental concerns that arise from aspects, such as noise annoyance and fuel consumption. This paper aims to enhance the existing Flexible Runway Scheduling Model (FRSM) by integrating a tabu search algorithm with Receding Horizon Control (RHC), introducing non-linear noise restrictions, and implementing more sophisticated fuel burn modeling. The main goal is to evaluate how certain improvements affect the FRSM. To achieve this, a methodology has been developed that uses a multi-objective tabu search algorithm to minimize both fuel consumption and noise annoyance while assigning flights to runways. This study provides a comprehensive analysis of Amsterdam Airport Schiphol (AAS) across different scenarios, ranging from a 1.5-hour flight schedule to a full-day simulation, revealing significant findings. For the 1.5-hour and six-hour scenarios, the tabu search algorithm achieves a 55% and 87.3% reduction in computational time with marginal losses of 0.73% and 0.19% in solution accuracy for fuel burn optimization. Throughout all scenarios, the tabu search algorithm consistently results in a reduction of highly annoyed individuals ranging from 2.14% up to 62.5% compared to the existing FRSM, demonstrating its effectiveness. Moreover, the algorithm minimizes the impact on the flight schedule in terms of delay. Notably, as the flight schedule length increases, the performance of the tabu search algorithm improves compared to the existing FRSM. A sensitivity analysis optimization horizon indicates a positive effect on results, albeit with an associated computational cost. In conclusion, this study showcases the positive impacts of the remodeled FRSM, enabling a faster and more accurate trade-off. The research findings provide valuable insights for optimizing runway scheduling at major airports while balancing efficiency gains with environmental considerations.

Keywords: Runway capacity, Scheduling Model, Tabu Search, Metaheuristics, Noise Annoyance, Fuel Consumption, Receding Horizon Control

1 Introduction

In today's changing world of global air travel, the air transport industry is recovering from the disruptions caused by the COVID-19 pandemic. The industry is working hard to recover, and the predictions show a strong comeback. Year-on-year, the industry experienced a 40.1% increase in passenger traffic measured in revenue passenger-kilometers (RPKs), and by September 2023 the industry reached 92.9% of pre-pandemic levels [IATA, 2023]. These signs of recovery forecast a future recovery wherein the demand for air travel is anticipated to double by the year 2040, growing at an annual average rate of 3.4%.

As demand continues to rise, major airports are approaching the maximum capacity of their infrastructure and environmental thresholds due to escalating air traffic volumes. Runways are often recognized as the primary bottlenecks within airport infrastructure, significantly contributing to delays. The airport its overall capacity heavily relies on the operational efficiency of its runways. Constructing new airports or expanding existing ones stands as a potential remedy for congestion. However, these actions may result in adverse environmental effects on nearby communities, as highlighted by [Visser et al., 2008].

In recent years, the population residing near airports has increased, implying a larger number of people affected by aircraft-induced noise, as noted in the analysis by [Ganic et al., 2015]. Aircraft noise has become a significant source of concern for local communities, impacting both current airport operations and efforts to enhance airport capacity. Consequently, it has become a critical issue that significantly influences future traffic growth. The need for increased airport capacity alongside reduced noise disturbance and greater full efficiency led to the development of a new model. Delsen initially proposed a flexible runway allocation method [Delsen, 2016], proving its effectiveness in optimizing and trading off fuel burn and noise emission without using a preference list. Subsequent improvements by Van Der Meijden led to a more precise aircraft representation in the model,

*Msc Student, Sustainable Air Transport, Faculty of Aerospace Engineering, Delft University of Technology

eliminating consideration for only two types of aircraft and implementing pair-wise separation [van der Meijden, 2017]. Recent research performed by [Abbenhuis, 2021] transformed the model from an allocation to a scheduling model. This change involved altering decision and auxiliary variables making the scheduling model more suitable for complex runway systems. Furthermore, assigning continuous delays to the scheduled flights prevents the model from becoming infeasible. Regarding noise modeling, the Aviation Environmental Design Tool (AEDT) is used to estimate the noise. However, the current model still faces challenges concerning computational performance, noise limits, and fuel burn modeling. Currently, the Flexible Runway Scheduling Model (FRSM) is modeled as a Mixed-Integer Linear Programming (MILP) problem. This research aims to remodel the existing flexible runway scheduling model by employing a different modeling approach. This will allow for an assessment of how utilizing a different solving method impacts the current model. Furthermore, non-linear and more detailed constraints can be incorporated for noise disturbance and fuel consumption.

Literature offers several approaches to address the Runway Scheduling Problem (RSP) beyond employing MILP methods. Genetic algorithms, tabu search, and simulated annealing are prominently featured in existing literature. Additionally, other metaheuristics, such as ant colony optimization (ACO) and variable neighborhood descent have been utilized.

For this research, a deterministic approach has been chosen due to its easy implementation, adeptness in navigating extensive solution spaces, effectively overcoming local optima, and delivering near-optimal, high-quality solutions. Previous literature highlights three notable applications of tabu search in addressing the RSP. In research performed by [Atkin et al., 2007], the focus was on optimizing take-off scheduling to maximize runway throughput. They employed various metaheuristics (steepest descent, tabu search, and simulated annealing) and evaluated their performance, with the tabu search displaying slightly superior results. In a broader context, [Soykan and Rabadi, 2016] proposed a tabu search-based approach for the general RSP across multiple independent runways, utilizing a two-step methodology: the first step involved computing an initial solution through a greedy approach, followed by a tabu search algorithm to enhance the initial solution. Further research by [Soykan and Rabadi, 2022] emphasized multi-objective runway operations scheduling. Their approach involved solving the problem through a hybrid tabu/scatter search algorithm. Results showcased the effectiveness of the proposed model, indicating computational times suitable for practical applications. Since the tabu models have solely undergone testing with relatively small flight schedules and in less complex airport environments, the computational demands are likely to remain considerably high. To address this challenge, an approach incorporating a receding horizon control (RHC) strategy is adopted in this research. This strategy, as demonstrated by [Zhan et al., 2010], integrated an ACO variant known as an ant colony system with RHC to resolve the RSP for a single runway. Subsequent enhancements by [Wu et al., 2019] to Zhan his model specifically target the resolution of the multi-runway RSP. Their research indicates a substantial reduction in computational complexity, demonstrating that the proposed approach yields reasonable results.

However, the literature has not yet fully explored the combination of a multi-objective tabu search algorithm in combination with an RHC strategy. Therefore, this research focuses on enhancing the FRSM by addressing its shortcomings. Implementing a tabu search algorithm as the new modeling method has the potential to demonstrate its impact on the model. An additional advantage of this algorithm is its capability to incorporate non-linear elements, thereby improving the representation of noise annoyance, which exhibits a non-linear relationship. Additionally, utilizing a sliding time window approach can reduce the computational burden of the model, resulting in reduced computation time. This enhancement enables quicker evaluation of flight schedules and the possibility to handle larger schedules compared to the previous model.

This paper is structured in the following way. First, the methodology is presented in section 2, including information about separation modeling, fuel burn, noise annoyance, and the tabu search algorithm. Second, the case studies are described in section 3. section 4 presents the results of the case study and sensitivity analysis. section 5 provides a detailed discussion of the obtained results. Finally, section 6 presents the conclusions drawn from this study, and section 7 provides recommendations based on the findings.

2 Methodology

This study aims to develop an improved FRSM by employing an alternative optimization technique and refining fuel burn and noise modeling alongside a sliding time window. The methodology is divided into distinct parts, starting with separation modeling, and then progressing to fuel burn and noise annoyance modeling. The subsequent phase of the methodology focuses on the mathematical model and the tabu search algorithm.

2.1 Single Runway Separation Modeling

Separation modeling plays an important role in runway scheduling. Minimum separation is dependent on operation type, weight class, and runway. The separation modeling is based on the research performed by [Abbenhuis, 2021] and [van der Klugt, 2012]. The separation is determined by considering a leading and following aircraft.

Four distinct combinations on a single runway arise from these aircraft: two consecutive arrivals, two consecutive departures, an arrival followed by a departure, and a departure followed by an arrival. For these combinations, different equations are applied to calculate the separation time, which varies based on the specific runways in use.

When dealing with two consecutive arrivals on a single runway, the minimum separation time $T_{i,j}$ is dependent on the approach speed of the two aircraft. If the approach speed of flight V_i is smaller than flight V_j , Equation 1 is used. Conversely, if V_i is larger than V_j , Equation 2 is used to compute the separation time. Here, n represents the common approach path, and the required longitudinal separation $s_{i,j}$ is determined in compliance with RECAT-EU regulations[Rooseleer et al., 2018]. For both equations, the separation time is the maximum of the required longitudinal separation and the Arrival Runway Occupancy Time (AROT).

$$T_{i,j} = \max \left[\frac{s_{i,j}}{V_j}, AROT_i \right] \quad (1)$$

$$T_{i,j} = \max \left[\frac{n + s_{i,j}}{V_j} - \frac{n}{V_i}, AROT_i \right] \quad (2)$$

These two consecutive arrivals can also take place in opposite directions on the same runway. In this case, the minimum separation time is determined by the Minimum Vectoring Altitude (MVA), the Rate of Descent (ROD), and a communication buffer, \bar{c} , as shown in Equation 3.

$$T_{i,j} = \frac{MVA}{ROD} + \bar{c} \quad (3)$$

These two situations can also be applied to two consecutive departures. The minimum separation time for two departures on a single runway is determined via the Time Based Separation (TBS) minima according to RECAT-EU[Rooseleer et al., 2018], and the Departure Runway Occupancy Time (DROT) via Equation 4. This equation can also be used for a departure followed by an arrival.

$$T_{i,j} = \max [TBS_{i,j}, DROT_i] \quad (4)$$

The minimum separation time for two consecutive departures on opposite runway ends can be determined using Equation 5. Additionally, the separation time for a scenario where an arrival is succeeded by a departure on the same runway is expressed in Equation 6.

$$T_{i,j} = DROT_i \quad (5)$$

$$T_{i,j} = AROT_i \quad (6)$$

The final operational mode involves a departure followed by an arrival on opposite runway ends. The minimum separation requirement is contingent upon the rate of descent (ROD) of the arriving aircraft, the rate of climb (ROC) of the departing aircraft, and the MVA. The calculation for the minimum separation can be derived using the equation presented in Equation 7.

$$T_{i,j} = \frac{MVA}{ROD} + DROT_i + \frac{MVA}{ROC} \quad (7)$$

At airports where runways are closely situated or dependencies arise from trajectory intersections, additional separation requirements are introduced. This aspect has been investigated by [van der Klugt, 2012], and the precise equations governing the separation time for these dependencies are incorporated in this study. For a more comprehensive understanding and detailed equations, readers are referred to the research from [van der Klugt, 2012].

2.2 Fuel Burn Calculations

The fuel burn model is built upon the research performed by [Abbenhuis, 2021] and [van der Meijden, 2017], with some modifications as explained in this section. All computations are obtained from the user manual of the Base of Aircraft Data (BADA) [Nuic, 2010]. Determining the overall fuel burn for each flight and runway combination involves segmenting both departure and arrival trajectories. Each trajectory comprises three segments. Departure trajectories consist of the gate-to-runway segment, the initial climb, and the climb segment up to 10,000 feet. Arrival trajectories are divided into the Initial Approach Fix (IAF) to the Final Approach Fix (FAF), FAF to the runway, and runway to gate segments.

The total fuel burn is calculated according to Equation 8, with the fuel burn per segment obtained via Equation 9.

$$TFB = \sum_{s \in S} TFB_s \quad (8)$$

$$TFB_s = \frac{D_s \cdot \dot{m}_f}{V_{TAS}} \quad (9)$$

The fuel flow during the segments \dot{m}_f can be obtained via Equation 10 and is dependent on the thrust specific fuel consumption, C_T , and the net thrust from the engines T_{HR}

$$\dot{m}_f = C_T \cdot T_{HR} \quad (10)$$

For the jet and turboprop engines, the thrust specific fuel consumption, C_T , is obtained according to Equation 11 for jet engines, and Equation 12 for turboprop engines. C_T is a function of true airspeed, V_{TAS} , and the first C_{f1} , and second C_{f2} , max climb thrust coefficients.

$$C_T = C_{f1} \cdot \left(1 + \frac{V_{TAS}}{C_{f2}}\right) \quad (11)$$

$$C_T = C_{f1} \cdot \left(1 - \frac{V_{TAS}}{C_{f2}}\right) \cdot \left(\frac{V_{TAS}}{1000}\right) \quad (12)$$

The equation for calculating the maximum climb thrust for jet engines is provided in Equation 13, and for turboprop engines, in Equation 14. These equations are formulated to determine the maximum climb thrust under standard atmospheric conditions, and the thrust is expressed in Newtons. The thrust value is contingent on two key parameters: the geopotential altitude denoted as H_P and the true airspeed represented by V_{TAS} .

$$(T_{\max \text{ climb}})_{ISA} = C_{Tc,1} \cdot \left(1 - \frac{H_P}{C_{Tc,2}} + C_{Tc,3} \cdot H_P^2\right) \quad (13)$$

$$(T_{\max \text{ climb}})_{ISA} = \frac{C_{Tc,1} \cdot \left(1 - \frac{H_P}{C_{Tc,2}}\right)}{V_{TAS}} + C_{Tc,3} \quad (14)$$

For all types of engines, the maximum climb thrust undergoes correction for temperature deviations from the standard atmosphere, denoted as ΔT , as outlined in Equation 15. Where T_{eff} is determined via Equation 16. $C_{Tc,4}$ is the second thrust temperature coefficient.

$$T_{\max \text{ climb}} = (T_{\max \text{ climb}})_{ISA} \cdot (1 - C_{TC,5} \cdot (\Delta T)_{eff}) \quad (15)$$

$$\Delta T_{eff} = \Delta T - C_{Tc,4} \quad (16)$$

Delay is incorporated differently for arriving and departing aircraft. For inbound aircraft, the delay is assigned at the IAF. When the delay remains below 120 seconds, the delay is modeled as an extension of the approach trajectory, mirroring the flow equal at the IAF. However, if the delay exceeds 120 seconds, the aircraft will enter a holding pattern. This holding pattern, typically executed as a "race track pattern" around the IAF, consists of two straight legs plus two 180-degree turns. Due to this, the fuel burn will be higher compared to an extended approach trajectory. To incorporate this turn, a 10% increase in fuel flow is assumed [Airbus, 2004].

During taxiing for departing flights, the delay is allocated while the aircraft is on the ground. To determine this delay fuel, the fuel flow during the taxi segment is quantified in kilograms per second [kg/s] and then multiplied by the duration of the delay. The fuel flow during taxi is assumed to be 7% of the maximum thrust [Khadilkar and Balakrishnan, 2012].

2.3 Noise Annoyance Modeling

The second objective of the model is to reduce the noise annoyance in the surrounding area of the airport. As aircraft noise is a non-stationary noise signal, the duration of the noise has to be taken into account. To measure the annoyance during a noise event, the Sound Exposure Level (SEL) is used. SEL denotes a constant one-second duration, T_0 , which holds an energy level equivalent to the fluctuating level across the entire event and can be calculated using Equation 17.

$$SEL = 10 \log \left[\frac{1}{T_0} \int_0^T 10^{\frac{L_A(t)}{10}} dt \right] \quad (17)$$

A noise modeling tool is used to determine the SEL value for all the aircraft types and runway combinations. For this, the Aviation Environmental Design Tool (AEDT) developed by the FAA is used [Lee et al., 2022]. The

AEDT is a software tool that integrates established noise and emission models. The AEDT offers accurate predictions of noise impact at specific points of interest. For this research, all the different combinations of runways, Standard Instrument Departures (SIDs), and Standard Arrival Routes (STARs) are modeled according to Schiphol its Aeronautical Information Services (AIS)[LVNL, 2023].

To capture the effect of noise in airport communities due to air traffic activities the day-evening-night level L_{DEN} noise metric is used. This metric is calculated via Equation 18, where T_{ref} indicates the period. The penalty associated with a noise event in the evening or night is represented by w_i . With a 5 dB penalty for noise during the evening (19.00-23.00), and a 10 dB penalty for noise during the night (23.00-7.00)[Crocker, 2007].By adding up the number of flights and the associated SEL value, the L_{DEN} value can be computed.

$$L_{DEN} = 10 \log \left[\sum_{i=1}^F 10^{\frac{SEL_i + w_i}{10}} \right] - 10 \log \left[\frac{T_{ref}}{T} \right] \quad (18)$$

The current model lacks the incorporation of penalties for increased noise levels. To address this, a non-linear metric has been selected for this research. The metric measures the number of Highly Annoyed (HA) people and represents a dose-response relationship. It has been incorporated in the Dutch Aviation Act, which has formed the legal framework for AAS since 2003. This framework aims to restrict the environmental impact around the airport. This protection is provided by the "Criteria of equality", which restricts the number of HA people within L_{DEN} contours[Welkers et al., 2021]. The limit value for the number of HA people within the 48 dB(A) L_{DEN} contour for AAS is 166,500, and 45,000 for the number of severely sleep-disturbed people (SDP) within the 40 dB(A) L_{night} contour[Welkers et al., 2021].

To determine the number of annoyed people, three steps have been taken. Firstly, locations where the L_{DEN} value is 48 dB(A) or above have been identified. Next, using Equation 19[Heblij and Derei, 2019], the percentage of HA people has been calculated. The L_{DEN} can be calculated using Equation 18. Finally, the percentage has been multiplied by the number of people living at the grid point. The total number of HA people has been determined by adding the number of HA people per grid point.

The same procedure is used to determine the number of SDP. To obtain the percentage of SDP Equation 20 is used.

$$\%HAP = 1 - \frac{1}{[1 + e^{(-7.7130 + 0.1260 \cdot L_{DEN})}]} \quad (19)$$

$$\%SDP = 1 - \frac{1}{[1 + e^{(-6.2952 + 0.0960 \cdot L_{night})}]} \quad (20)$$

To determine the population count at specific grid points, an analysis of data obtained by the Central Bureau of Statistics (CBS) has been conducted. This dataset is structured according to the Rijksdriehoeksstelsel, comprising x and y coordinates representing the population density at those respective coordinates. Each grid point in this dataset covers an area of 500 square meters. To align the coordinates obtained from the AEDT with the Rijksdriehoeksstelsel coordinate system, a conversion process has been implemented. This conversion involved a data accumulation method wherein the corresponding CBS coordinates were matched with each AEDT grid point. This process resulted in a population file containing the number of people at each grid point as per the AEDT layout. The visual representation of this outcome can be seen in Figure 1, showcasing the distribution of populated grid points.

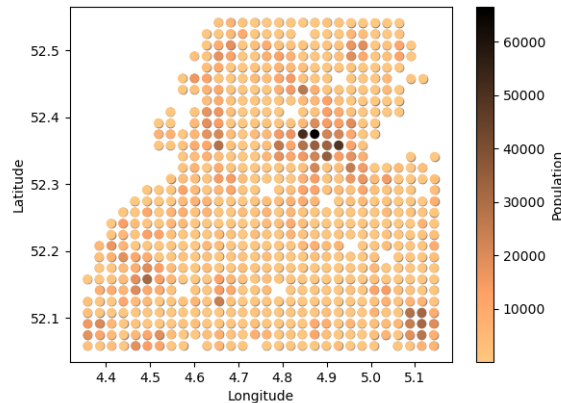


Figure 1: AEDT grid combined with population data used as input for the model.

The observed highest population density on the upper right side of AAS can be attributed to the proximity of Amsterdam in this area. Amsterdam, being a major urban center, is likely to contribute significantly to the concentration of inhabitants, resulting in the densely populated region observed on that side of AAS.

2.4 Receding Horizon Control

The concept of Receding Horizon Control (RHC) involves breaking down the original problem into smaller sub-problems within a sliding time frame, which reduces the computational burden. It relies on two key parameters, the scheduling window time interval and the receding horizon width. Figure 2 shows how RHC works. Within a designated horizon, full optimization is executed utilizing all available information. However, only scheduling decisions on the initial time interval are put into action. By ensuring that the time window for each horizon is smaller than the entire flight schedule, this approach significantly reduces the computational load, enabling real-time computations.

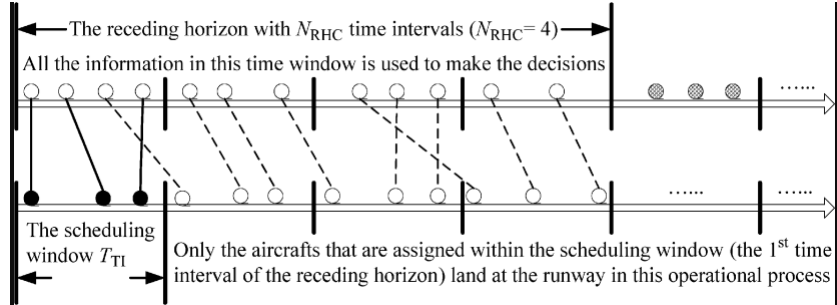


Figure 2: Graphical representation of RHC [Zhan et al., 2010]

When employing the RHC strategy in the FRSM, the problem is divided into several sub-problems by the RHC principle. The number of sub-problems is dependent on the length of the flight schedule. For each sub-problem, information is collected from the start to the end of the window size. The objective function is exclusively applied to the window currently undergoing optimization. For the research shown in this paper, a window size of 30 minutes is chosen with a window shift of 15 minutes.

It is important to know that previous window data contributes to noise and separation considerations. To maintain adequate separation in the current window, the flight schedule from the previous window is essential. Regarding noise, the noise emitted by earlier flights is taken into account. Time plays a significant role in noise calculations, as illustrated in Equation 18. Whenever the window shifts, the noise budget increases by the duration of that shift in seconds. The noise produced by flights that are already optimized guides the starting point for the new optimization at each grid point.

2.5 Mathematical Model Formulation

This section introduces the mathematical model underlying the tabu search algorithm. It begins with an overview of the sets and parameters involved in the model, followed by a fundamental Mixed Integer Programming (MIP) formulation. The basis of this formulation is derived from the model presented in [Al-Salem et al., 2012] and adapted from the earlier model introduced in [Abbenhuis, 2021] to accommodate the new objective function.

2.5.1 Sets and Parameters

Sets

- F : Number of flights
- R : Number of runway ends
- R_r : Runway ends closed for operation
- P : Number of gridpoints

Decision variables

- x_f^r : Scheduling of flight f on runway r
- T_f : Operating time of flight f
- D_f : Delay of flight f
- D_{fh} : Holding delay of flight f
- $y_{i,j}$: 1 if flight i is operating before flight j
- D_{total} : Total delay of all flights
- g_{xy} : 1 if the noise annoyance limit is reached at grid point xy

Parameters

- c_f^r : The fuel burn of flight f on runway r
- c_{df} : Delay fuel burn of flight f
- c_{dfh} : Holding delay fuel burn of flight f
- n_f : Normalization factor for fuel
- n_n : Normalization factor for noise
- HAP_{xy} : Highly annoyed people at grid point xy
- S_{ij} : Required separation between flight i and flight j
- c_{opt} : Small penalty
- α : Weighting factor fuel
- β : Weighting factor noise

2.5.2 Objective Function and Constraints

The multi-objective minimization problem is presented below.

$$\begin{aligned} \text{Min } Z = & \alpha \cdot n_f \sum_{f \in F} \left[\left(\sum_{r \in R} c_f^r x_f^r \right) + c_{df} D_f + c_{dhf} D_{fh} \right] \\ & + \beta \cdot n_n \sum_{xy \in P} g_{xy} HAP_{xy} + c_{opt} \cdot D_{total} \end{aligned} \quad (21)$$

$$\sum_{r=1}^R x_f^r = 1, \forall f \in F \quad (22)$$

$$\sum_{f=1}^F x_f^r = 0, \forall r \in R_r \quad (23)$$

$$T_f - D_f = TS_f, \forall f \in F \quad (24)$$

$$T_j \geq T_i + S_{ij} - (1 - y_{ij}), \forall i, j \in F, i \neq j \quad (25)$$

The objective function, as described in Equation 21, consists of three terms. The first term aims to minimize fuel consumption when allocating runways to flights. This factor depends on the fuel cost associated with assigning flight f to runway r and incorporates a penalty for any delay assigned to the flight. As clarified in the fuel burn modeling section, this penalty escalates when the flight enters holding mode. The second term focuses on minimizing noise disturbance. If the L_{DEN} threshold of 48 dB(A) is surpassed, the cost of annoyance is determined by the number of highly annoyed people living at that specific grid point, represented by a non-linear relationship. The final component relates to total delay minimization. To ensure the assignment of all flights without excessively delaying any single flight or disproportionately scheduling flights on the most noise-preferred runway, a small penalty is integrated into the objective function. This inclusion ensures efficient and balanced runway scheduling.

As the problem is multi-objective and the two objectives have different units, a normalization has to be applied to both, indicated by n_f and n_n . The normalization is established by considering the range between the minimal and maximal solutions for both fuel and noise outcomes per window. This chosen range enables a dimensionless trade-off. The specific normalization method for fuel is presented in Equation 26.

$$n_f = \frac{1}{\max \left(f_{fuel}^{noise_{opt}} - \min f_{fuel}^{fuel_{opt}} \right)} \quad (26)$$

Moreover, for this specific problem, the weighted sum method is adopted as the normalization technique. This method transforms a multi-objective optimization problem into a single-objective one. It involves the utilization of weighting coefficients, denoted as α and β , which are multiplied by the objective function. Through this approach, the weighting coefficients allow adjustment to entirely optimize for a single objective or any desired trade-off combination. Notably, these coefficients fall within a range from 0 to 1 and maintain a relationship where $\beta = 1 - \alpha$.

Constraint Equation 22 ensures that each flight lands on or takes off from exactly one runway. If runways are closed for operation, due to maintenance, extreme wind conditions, or other factors Equation 23 ensures that these runway ends are not used for operations. To determine the delay time of a flight regarding the operating time and original scheduled operating time of the flight, Equation 24 is used. To ensure that the separation between flights is satisfied, Equation 25 is employed. However, this constraint is only valid when flight i takes place before flight j .

2.6 Tabu Search

A tabu search algorithm has been used in this research to evaluate the effect of a different solving method. The main goal is to solve the FRSM quicker and implement non-linear elements. The tabu search algorithm is a type of search method that focuses on finding a single solution. It was first introduced by [Glover and Laguna, 1998], and can be used in a variety of optimization problems. However, it needs to be adjusted for each specific problem. In this section, a detailed explanation of the algorithm is provided, starting with the initial solution generation process.

2.6.1 Initial Solution Generation

Starting with a viable solution can enhance both the outcome's quality and reduce the computational time required. Therefore in this research, the initial solution is obtained through a greedy algorithm based on the dispatching (priority) rule. This rule, commonly used in machine scheduling, prioritizes jobs awaiting processing on a machine. This concept can be adapted to the context of FRSM, in which the runways serve as machines and the flights the jobs to be scheduled. When a runway becomes available, a dispatching rule inspects the waiting flights and selects the flight with the highest priority. These rules have proven to obtain a reasonably good solution in a relatively short time.

This approach is adapted for this research and is called the "Target Time First" greedy algorithm. In the algorithm, the flights are assigned to a runway in the order of ascending scheduled operating times. At each step, it looks for the most cost-efficient assignment for the unscheduled flight with the earliest scheduled operating time (SOT). While scheduling, it takes into account the assignment of previous flights. When all the flights are assigned to a runway the initial cost is computed and an initial feasible flight schedule is produced as the output. Algorithm 1 presents the pseudo-code for the creation of this initial solution generation.

Algorithm 1 Target Time First greedy heuristic algorithm for initial solution generation

- 1: **Input** List of flights F , list of runways R , separation matrix S , fuel burn matrix FB
 - 2: **Initialization** sort aircraft ordered in ascending scheduled operating time (SOT) (1 to F)
 - 3: **for** $f = 1$ to F **do**
 - 4: **for** $r = 1$ to R **do**
 - 5: fuel cost = FB_f^r
 - 6: Calculate E_{fr} (Earliest feasible time flight f can operate from runway r)
 - 7: **end for**
 - 8: Calculate operating time $T_f = \min\{E_{ir} \mid r \text{ in } R\}$
 - 9: **end for**
 - 10: Calculate the objective function according to Equation 21
 - 11: **return** Initial solution
 - 12: **Output** A feasible solution with runway and operating time per flight
-

2.6.2 Tabu Search Algorithm

Before explaining the functioning of the tabu search algorithm used in this research, it is essential to understand the foundational principles of this algorithm as outlined in [Lieberman and Hillier, 2021]. The tabu search algorithm is a widely employed metaheuristic method that incorporates intuitive concepts to guide the search process away from local optima. Its fundamental idea lies in maintaining a short-term memory, known as the "Tabu List". This list records recent moves or solutions, called "tabu moves", which are prohibited from being revisited in future moves. These moves are forbidden for a user-defined number of iterations. This mechanism

prevents the algorithm from becoming trapped in local cycles or repeatedly revisiting sub-optimal solutions. However, there exists one exception for a tabu move: when such a move improves the best-known solution throughout the search. This exceptional scenario is recognized as an aspiration condition.

The tabu search algorithm starts with a feasible initial trial solution and explores the solution space by making small modifications or moves to reach neighboring solutions. During the search process, the algorithm evaluates the quality of each neighbor using an objective function. It is not required that every new solution should be better than the previous solution. The algorithm continues with iterating until a stopping criteria is met, such as a fixed amount of CPU time, or a fixed number of consecutive iterations without improvement in the objective value. Furthermore, the algorithm stops when there are no feasible moves into the local neighborhood of the current trial solution.

The greedy heuristic algorithm provides a good initial solution. The flight schedule and objective function of this initial solution are used as input for the Tabu Search algorithm to perform an improving search until the termination criteria are satisfied. The best solution found during this process is returned as the final solution. The basis structure of the algorithm can be seen in Figure 3. One element of this algorithm is not explained yet, which is the neighborhood generation.

2.6.3 Neighborhood Generation

The tabu search algorithm employs a comprehensive neighborhood generation strategy centered on two key operations: swapping the order of flights and the reassignment of runways allocated to flights. This method is used to explore the solution space effectively. The swapping process allows the algorithm to explore various sequences of flights, aiming to minimize delays and optimize the scheduling of flights on the runways. Concurrently, the dynamic alteration of runway assignments for flights introduces an additional layer of exploration. This approach facilitates the discovery of optimal or near-optimal solutions.

It is important to highlight that the search space is constrained for both maneuvers. Specifically, when swapping flights, the algorithm focuses solely on flights within a Specified Window (SW) to optimize the model its performance. Similarly, in the case of runway reassignment swaps, the availability of runway ends depends on the operation type, considering that certain runways may not be accessible for either landing or takeoff.

2.6.4 Complete Overview of the Algorithm

The complete tabu search algorithm combined with the sliding time window approach can be seen in Figure 3. The first step is to initialize the parameters for the sliding time window, with window size set to 30 minutes, and window shift to 15 minutes. The starting point of the optimization is the first window, indicated by $k = 1$. Subsequently, all flights within the k -th RHC stage, operating within the window size, are selected for optimization. Upon optimization, the results of the flights within the scheduled window are stored, while those outside the current window are moved to the subsequent window for further optimization with the adjusted operating time. The final step entails verifying if all flights are scheduled. If so, the algorithm is terminated. Otherwise, the optimization progresses to the next window with k incremented by one.

The algorithm shown in Figure 3 operates on an input data set comprising a flight schedule, separation details, population statistics, noise metrics, and fuel consumption data. Pre-processing this data yields essential matrices: a separation matrix, fuel consumption matrix, and noise emission matrix. The core concept of the FRSM primarily relies on a tabu search algorithm implemented with a sliding time window.

3 Description of the Case Studies

The analysis of the FRSM utilizes Amsterdam Airport Schiphol (AAS). AAS accommodates a total of 6 runways, equating to 12 potential runway ends for operations. However, the Oostbaan, encompassing runway ends 04 and 22, is omitted from the analysis as it has a very short runway and is mostly used for General Aviation, private jets, and helicopters. The remaining five runways are strategically oriented to accommodate varying wind directions, ensuring near-constant operability. It is important to note that certain runway ends are restricted for either take-off or landing. Specifically, for departing aircraft, operations are generally limited on the following runway ends: Aalsmeerbaan 36R, Kaagbaan 06, and Polderbaan 18R. Conversely, for arriving aircraft, the following runway ends face operational restrictions: Aalsmeerbaan 18L, Kaagbaan 24, and Polderbaan 36L [Schiphol, 2023].

For the analysis, multiple flight schedules dated from 2019 are used. These schedules are formulated using authentic flight data extracted from specific days in 2019 and adjusted to function as input for the model. The adjustments involve integrating arrival or departure trajectories based on the designated sector, which relies on the origin or departure data. Additionally, every aircraft is categorized into the correct weight class according to the RECAT-EU regulations[Rooseleer et al., 2018]. The final stage involves assigning a pier to each flight to

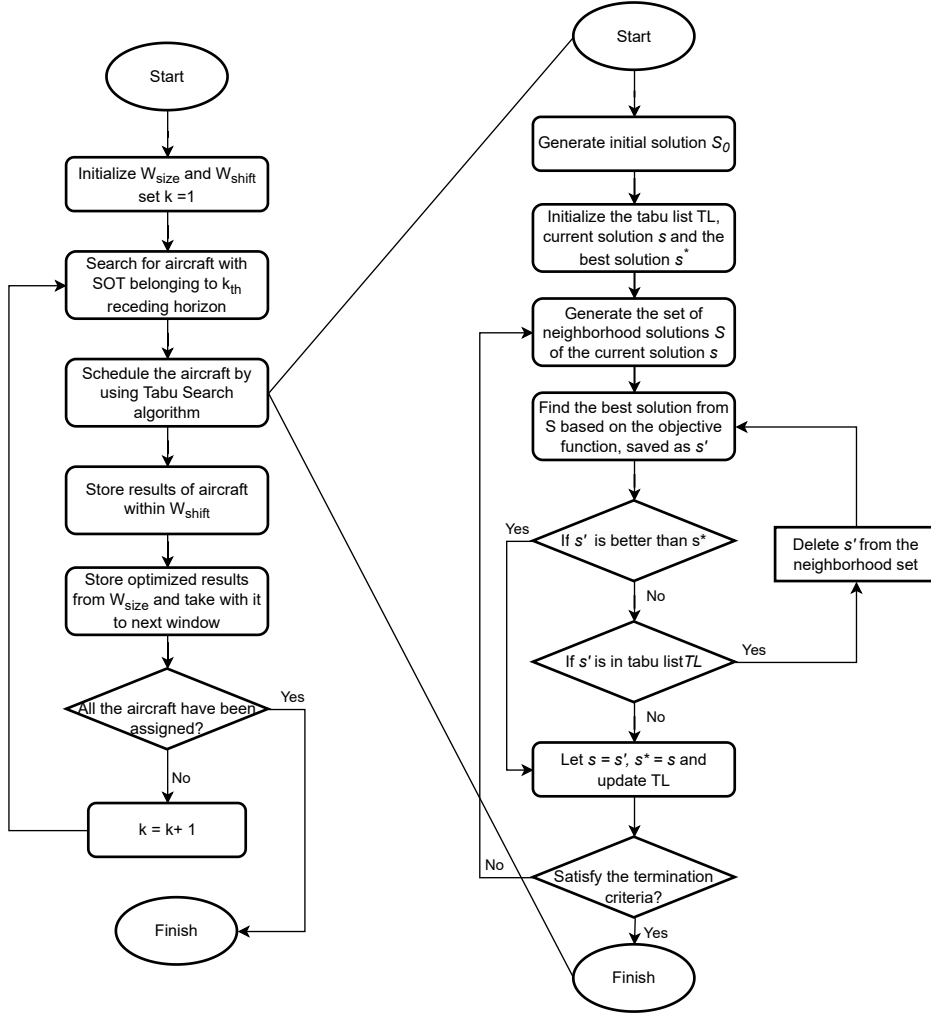


Figure 3: Flowchart of the complete algorithm including the moving horizon and tabu search

facilitate the calculation of taxi fuel consumption, achieved by considering the aircraft type and carrier. The goal of the analysis is to assess how employing an alternative-solving approach impacts the outcomes of the model in contrast to the MILP model. To conduct this comparison, the MILP model formulated by [Abbenhuis, 2021] is reconfigured and utilized for the evaluation. The optimization process is conducted using the commercial solver Gurobi. Due to the inclusion of a non-linear element for noise annoyance in the new model, direct optimization of noise objectives is unfeasible as a MILP model cannot handle non-linear elements. Consequently, the L_{DEN} limit for the noise optimization has been established at 48 dB(A). In the event of this limit being exceeded, the total population residing at the respective grid point will be considered. The metric of HA people can be calculated retrospectively.

The tabu search algorithm is implemented in Python, where multiprocessing is employed to accelerate the optimization process. Specifically, this approach involves parallel computation of the objective function for all generated neighbors in each iteration, significantly enhancing the overall speed of optimization.

Four distinct scenarios are considered in the analysis, with an outline of the schedules presented in Table 1. As the flight schedule expands in size, these scenarios reflect varying degrees of complexity. This expansion allows an analysis of both models' behaviors, enabling an observation of how they manage and adapt to the increased volume of flights. The 90-minute scenario originates from Abbenhuis his research appendix dated August 2019, whereas the six-hour scenario spans from August 23, running from 9:00 AM to 3:00 PM. The daytime scenario is drawn from August 20, covering the period from 7:00 AM to 7:00 PM. The full-day scenario originates from July 15, encompassing 24 hours from 00:00 to 23:59. Notably, the noise calculation for this scenario includes an evening penalty applied to flights between 7 PM and 11 PM and a night penalty for flights occurring between 11 PM and 7 AM.

Table 1: Flight schedules created for the analysis

Flight schedule	Total flights	Arriving flights	Departing flights	Flight schedule duration [hours]
90-minute	122	55	67	1.5
Six hour	471	180	291	6
Daytime	1,033	511	522	12
Full day	1,508	754	754	24

4 Results

This chapter reveals the findings of the enhanced FRSM. The chapter is arranged in the following manner: firstly, a comparison is made between the objective functions of both models to assess the accuracy of the improved model. Secondly, a comparison of computational times is conducted to determine the impact of the new model on computational performance. To further investigate the computational performance, a convergence analysis is carried out. Following this, the performance of both models on the trade-off is demonstrated through a Pareto Front, after which the noise annoyance and runway allocation are presented. Lastly, a sensitivity analysis is performed for the optimization horizon of the tabu search algorithm.

4.1 Objective Function Comparison

To evaluate the performance of both models concerning the main objective functions, a fuel-focused optimization ($\alpha = 1$) and a noise-focused optimization ($\beta = 1$) is conducted. For fuel optimization, this entails the total fuel burn emitted by all flights, while for noise optimization, the metric is the number of HA people. The fuel optimization results are presented in Table 2, and for noise in Table 3. The results show that, for the 90-minute and six-hour scenarios, the MILP outperforms in terms of the fuel consumption objective. Conversely, for the daytime and full-day flight schedules, the tabu search algorithm performs slightly better. Regarding noise optimization, the tabu search algorithm outperforms the MILP in all scenarios. It is essential to mention that the MILP optimization for full-day noise did not converge effectively. Consequently, the obtained solution can not be considered a genuine comparison. When the process fails to converge effectively, it means it is unable to find an optimal solution within the specified parameters. However, it has been included in the table as a reference point, acknowledging its limitations in convergence.

The variation in the number of HA people across the scenarios can be attributed to several factors. In the first scenario, a notable proportion of Lower Medium weight class aircraft is present compared to the other scenarios. The disparity between the six-hour and daytime scenarios can be allocated to the higher prevalence of aircraft in the upper heavy and lower heavy wake turbulence categories in the six-hour scenario. These aircraft emit more noise, resulting in an elevated count of HA people. Additionally, the full-day scenario contains flights during the evening and night, which incur a noise penalty. This penalty significantly influences the L_{DEN} value, leading to a higher count of HA people compared to other scenarios.

Table 2: Fuel optimized solution cost comparison

Flight schedule	Tabu search	MILP	Difference
90-minute	87,470	86,839	+0.73%
Six hours	366,422	365,712	+0.19%
Daytime	645,996	648,443	-0.38%
Full day	933,819	943,100	-0.98%

Table 3: Noise optimized solution cost comparison

Flight schedule	Tabu Search	MILP	Difference
90-minute	71,618	73,186	-2.14%
Six hours	90,469	111,580	-18.92%
Daytime	76,047	113,986	-33.29%
Full day	108,482	289,444	-62.5%

In addition to the primary objectives of minimizing fuel burn and the number of HA people, another important parameter is the delay. The FRSM incorporates the capability to delay specific flights either to meet separation requirements or to enhance the overall optimization. An analysis is conducted by comparing scenarios focused either on fuel optimization or noise optimization. The total delay is obtained and divided by the total amount of flights in the scenario. The outcomes are presented in Table 4 for fuel optimization and Table 5 for noise optimization.

Table 4: Average delay in seconds per flight fuel optimization comparison

Flight schedule	Tabu Search	MILP	Difference
90-minute	24.54	24.08	+1.09%
Six hour	8.14	15.74	-48.28%
Daytime	7.94	18.92	-58.03%
Full day	9.98	18.31	-45.49%

Table 5: Average delay in seconds per flight noise optimization comparison

Flight schedule	Tabu Search	MILP	Difference
90-minute	32.20	27.06	+18.99%
Six hour	10.61	15.27	-30.5%
Daytime	9.58	19.85	-51.74%
Full day	8.89	8.72	+1.95%

In the context of the 90-minute scenario, it is evident that the MILP model exhibits a slightly lower average delay in comparison to the tabu search approach. This pattern diverges in the other three scenarios, where the tabu search demonstrates a lower average delay. In the case of the six-hour scenario, this is accompanied by a slightly higher fuel burn. However, for the daytime and full-day scenarios, this trade-off is associated with a lower total fuel burn. Notably, substantial differences in average delay for noise optimization are observed. In the 90-minute scenario, MILP outperforms tabu search in terms of average delay, yet this does not translate into a better objective function. For both the six-hour and daytime scenarios, the tabu search exhibits not only a lower average delay but also a lower fuel burn and lower noise annoyance. This trend can be attributed to the increased complexity of the flight schedule. In contrast, for the full-day scenario, MILP yields better results in terms of average delay. This can be explained by the lower density of flights over the 24-hour duration, allowing the MILP to more effectively assign flights to runways. However, it is important to note that this solution did not converge properly, preventing definitive conclusions. Further analysis also shows the effectiveness of assigning a small penalty to the total delay as it is not desirable to delay one aircraft in favor of others. The table shows that the average delay does not exceed 32.2 seconds, a threshold considered acceptable. The information presented in this section allows to make a comparison between the accuracy of the tabu search model and the MILP model. However, it does not provide any information about the computational time required for these solutions. This aspect will be further explained in the next section.

4.2 Computational Performance

The computational performance of both models is assessed using different methods. The tabu search algorithm allows easy retrieval of computational performance by measuring the time elapsed between the algorithm’s initiation and completion. Conversely, the MILP solver continues until the solution converges within a 0% gap range, which is not observed across all the scenarios within a reasonable amount of time. However, to manage computation, a time restriction of 1200 seconds is imposed for the 90 minute flight schedule, while larger scenarios are allocated a time limit of 1800 and 5200 seconds. Additionally, a 7200-second limit is set for obtaining objective values for a comprehensive comparison between fully fuel-optimized and noise-optimized scenarios. These time constraints help regulate and ensure a standardized assessment of computational performance across varied scenarios and models. An overview of the difference in computational time for both the tabu search algorithm as the MILP is shown in Figure 4

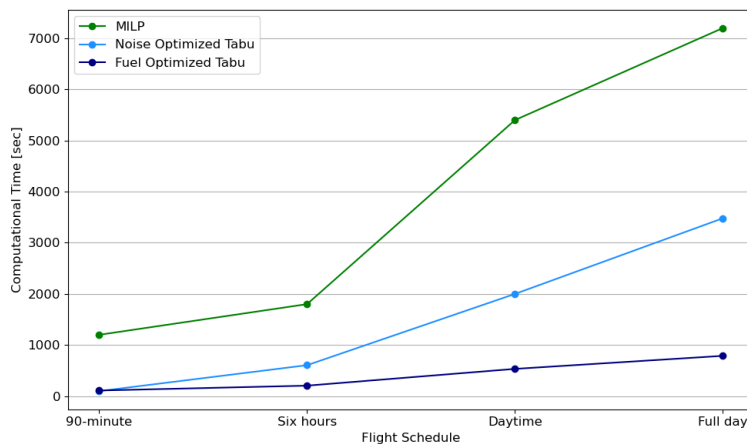


Figure 4: Computational time overview tabu search and MILP for all the scenarios

The correlation between the number of flights in the schedule and the computational time is evident from the figure and flight schedules. The greater the number of flights, the longer the computational time required. For smaller flight schedules, the computational time for noise and fuel optimization falls within a similar range. However, for longer flight schedules, noise optimization consumes significantly more time. This disparity arises

from the more extensive noise calculations, necessitating the examination of each neighbor solution across all 900 grid points, which is not required in fuel optimization.

Furthermore, the widening gap between fuel and noise optimization duration can be attributed to the employment of multiprocessing for noise calculations. Multiprocessing efficiency diminishes as data sets expand. The division of work among multiple processors takes longer with larger data sets, contributing to the increasing gap between the longer flight schedules.

Despite the differences in the optimization of both objectives, it can be seen from the figure that they are considerably faster compared to the computational time required for the MILP optimization. However, it is essential to note that these times are user-defined settings, as discussed earlier in this section. To enhance the understanding of the solution and its quality concerning computational time, an examination of convergence will be an intriguing avenue for exploration. This analysis will be conducted in the subsequent section.

4.3 Convergence Analysis

Solely evaluating the computational time of the MILP lacks context, as it might discover a promising outcome quickly and allocate the remaining time to fine-tune the solution for optimal convergence. To assess this behavior, the convergence of the MILP is graphically depicted concerning fuel burn, mirroring the objective function of the tabu search algorithm. The fuel burns objective function value from the tabu search algorithm is represented by a dashed line. Observing the intersection of both lines allows for a meaningful evaluation of the model its actual performance and convergence behavior. The convergence plot for the 90-minute scenario can be seen in Figure 5 and for the six-hour scenario in Figure 6.

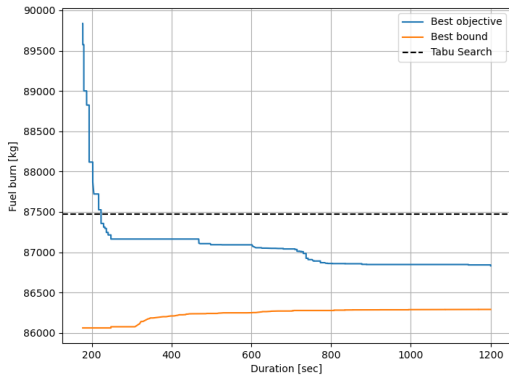


Figure 5: Convergence plot MILP fuel burn optimization 90-minute scenario

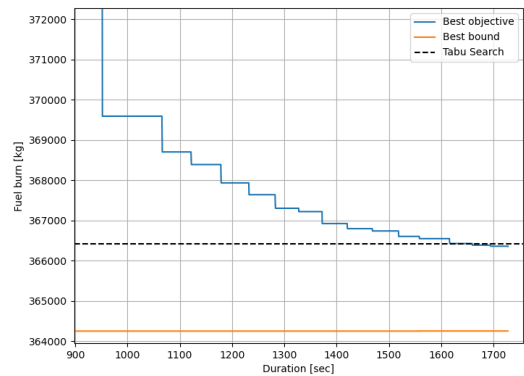


Figure 6: Convergence plot MILP fuel burn optimization six-hour scenario

In the 90-minute scenario, the optimal objective line intersects with the tabu search objective line at 220 seconds, allocating the remaining time for optimization convergence towards the best bound. Examining Figure 4, it is notable that the tabu search algorithm achieves its optimal solution within 99 seconds, marking a significant 55% reduction in computational time compared to the MILP.

In the six-hour scenario, this reduction is even more pronounced. The intersection of the best objective line with the tabu objective occurs at 1616 seconds, well within the MILP time limit of 1800 seconds. Conversely, the tabu search algorithm accomplishes the optimal solution for fuel optimization in 206 seconds, showcasing an 87.3% reduction in computational time.

Due to the non-linear nature of the noise objective function in the tabu search, direct integration into the MILP optimization is not feasible, making a convergence analysis unattainable. Despite this constraint, valuable insights emerged during the optimization phase. It became evident that the convergence of noise optimization takes longer, and this delay can be attributed to the heightened computational demands originating from the more complex calculations involved in noise optimization.

Besides optimizing one main objective, a multi-objective optimization will be performed for both models in the next section.

4.4 Pareto Front

For visualizing the impact of different weight factors, a series of scenarios were analyzed through the creation of a Pareto Front. This front has been constructed by assigning weights ranging from 0 to 1 in increments of 0.1. Each weight value was utilized to optimize the objective function, thereby enabling the exploration of the

relationship between fuel consumption and noise annoyance across various combinations.

To facilitate the selection of the most suitable solution, reference lines for noise and fuel have been plotted. The noise reference line has been derived from the Schiphol 2019 annual report [Royal Schiphol Group, 2020], specifically obtained from the recorded number of HA people amounting to 142,000. Conversely, the fuel reference case was generated by optimizing solely for fuel consumption using the original flight schedule and its runway configuration. These reference lines serve as benchmarks against which the Pareto solutions can be compared and evaluated. The Pareto front is plotted for the 90-minute scenario in Figure 7 and for the six-hour scenario in Figure 8.

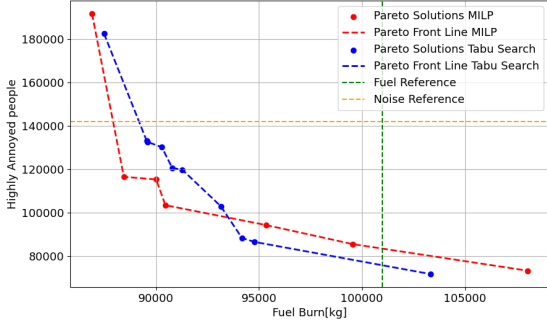


Figure 7: Tabu search and MILP Pareto Front 90-minute scenario

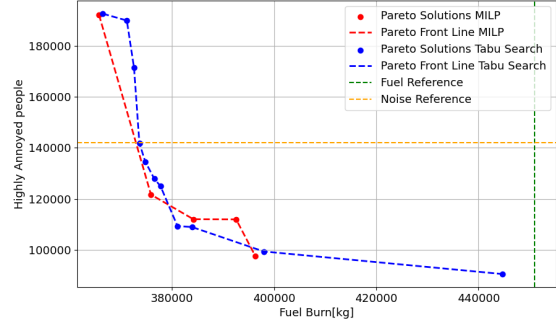


Figure 8: Tabu search and MILP Pareto Front six-hour flight schedule

Comparing both scenarios reveals similarities in the behavior exhibited by the MILP and tabu Pareto plot analyses. In the context of the 90-minute scenario, the tabu algorithm demonstrates superior performance when the focus leans towards optimizing noise. However, this trend shifts when the emphasis moves towards fuel optimization. Notably, both MILP and tabu approaches, exclusively optimizing for noise result in a solution that results in a higher fuel burn compared to the fuel reference scenario. In the case of the six-hour scenario, a more equitable performance is observed, with the tabu search yielding the most optimal solution for complete noise optimization. However, this accomplishment is accompanied by a notable increase in total fuel consumption, albeit still lower than the reference scenario. Importantly, both initial points reside within the boundaries of the fuel reference scenario.

In both scenarios, the tabu search achieves fuel savings compared to the reference scenario for multi-objective weighting. This positioning is near the left bottom of the Pareto curve, ensuring a balance between fuel efficiency and staying below the noise reference limit. The fuel saving can vary from 6.7% for the 90-minute scenario to 15.5% for the six-hour scenario. The difference between the fuel savings can be explained by the investigation of the reference runways, the operation type, and the orientation of the flights. The six-hour scenario contains more departing flights, where more savings can be accomplished compared to arriving flights. Furthermore, the departure trajectories for the 90-minute scenario are mostly located to the south, where already the most fuel-optimal runway is used, which reduces the potential for fuel saving.

In the case of the daytime and full-day scenarios, the MILP approach encountered challenges, failing to converge for various weightings in a reasonable amount of time, thereby hindering the creation of a Pareto plot to depict trade-offs. This again shows the main limitation of the MILP approach, which is the long runtime. Conversely, the tabu search method proved more adaptable to handle these large flight schedules, successfully generating a Pareto plot.

Both Pareto plots indicate that both approaches have their objectives in the same range. However, further analysis is required to determine if the modeling methods make different choices regarding runway allocation. This analysis will be carried out in the next section.

4.5 Noise Annoyance and Runway Allocation

In this section, an in-depth analysis of the behavior of both models is conducted, focusing on the aspects of noise annoyance and runway allocation. The examination is centered around the six-hour scenario, incorporating a multi-objective weighting. The selection of this scenario allows a comprehensive evaluation of model performance.

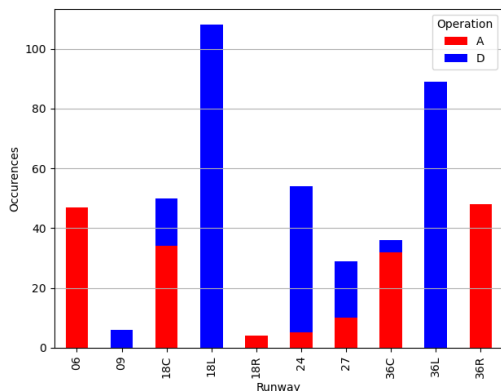
The choice of the point on the Pareto curve, as illustrated in Figure 8, is located close to the left bottom of the curve. The selected point is strategically positioned to achieve simultaneous reductions in fuel burn and noise disturbance. In Figure 9 and Figure 10 the runway allocation and noise annoyance grids of both models are shown for a combination of weights. In Figure 10 the grid points with a population that is Not Highly Annoyed

(NHA) are shown in grey.

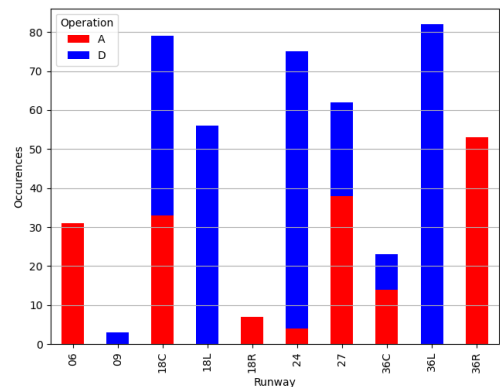
While the values for fuel burn and the number of HA people exhibit a comparable range for both solutions, several distinctions and similarities can be observed from the graphs. Notably, both solutions demonstrate minimal utilization of runways 18R and 09. The infrequent use of 18R for arrivals is attributed to the extended taxi time required from the runway to the pier, given its location furthest from the gates.

Furthermore, the limited usage of 09 for departures can be explained by geographical considerations. Departures in the eastward direction of AAS from this runway are restrained due to the potential for heightened noise annoyance, stemming from the proximity of Amsterdam in that particular area. Upon closer examination, another similarity can be observed in the utilization of runway R36L. Despite its longer taxi time, this runway experiences frequent use, attributed to the advantageous factor of a sparse population situated on its northern side, thereby minimizing noise disturbance. A contributing factor to this preference is the observation that 21% of flights are directed towards the BERGI waypoint, situated in the northern direction. This choice can also be explained by considering alternative northern heading runways. R36C traverses more densely populated areas, and R36R is unavailable for departing aircraft. Consequently, R36L emerges as the preferred runway for flights heading towards the north.

A notable difference between the two solutions can be seen in the utilization of runway 27. The MILP model exhibits a substantially higher usage of this runway compared to the tabu search approach, particularly for arrivals. This higher usage causes an increased noise annoyance over densely populated areas located east of AAS. This discrepancy is further highlighted in Figure 10b, where dark red grid points signify a high concentration of HA people. The tabu search solution, in contrast, opts for alternative runways, mitigating the impact on noise-sensitive regions.

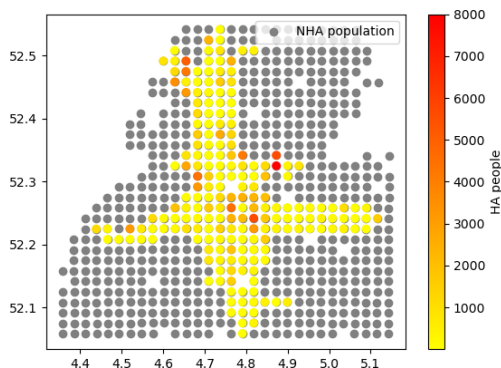


(a) Tabu: $\alpha = 0.3$ and $\beta = 0.7$

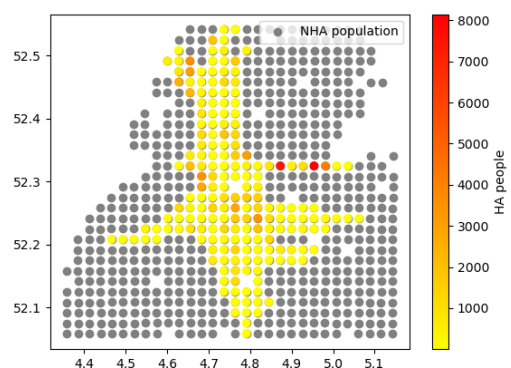


(b) MILP: $\alpha = 0.5$ and $\beta = 0.5$

Figure 9: Runway allocation comparison



(a) Tabu: $\alpha = 0.3$ and $\beta = 0.7$



(b) MILP: $\alpha = 0.5$ and $\beta = 0.5$

Figure 10: Noise annoyance grid comparison

Another interesting aspect to explore is the intensity of noise levels experienced by HA people. Given that both optimization models pursue distinct objectives in minimizing noise annoyance, the cumulative count of

HA people for each noise level is obtained from the optimization. The results can be seen in Figure 11, revealing variations in the distribution of HA people between the two models.

In both figures, a notable concentration of HA people is observed within the 48-60 dB(A) range. Nevertheless, a noteworthy distinction emerges: in the tabu search approach, the majority of HA people experience lower noise levels, while the MILP model exhibits a lower count at the lower noise levels and shows three prominent peaks at higher noise levels. This divergence can be attributed to the fact that, once the noise limit is exceeded, the MILP model no longer considers the intensity of the noise. This results in individuals being exposed to higher noise levels compared to the tabu search. The tabu search, on the other hand, accounts for noise intensity, leading to a decline in the numbers of HA people as noise levels increase. Except for two minor peaks at 63 and 64 dB(A), which can be rationalized by the strategy of avoiding exposure to densely populated areas.

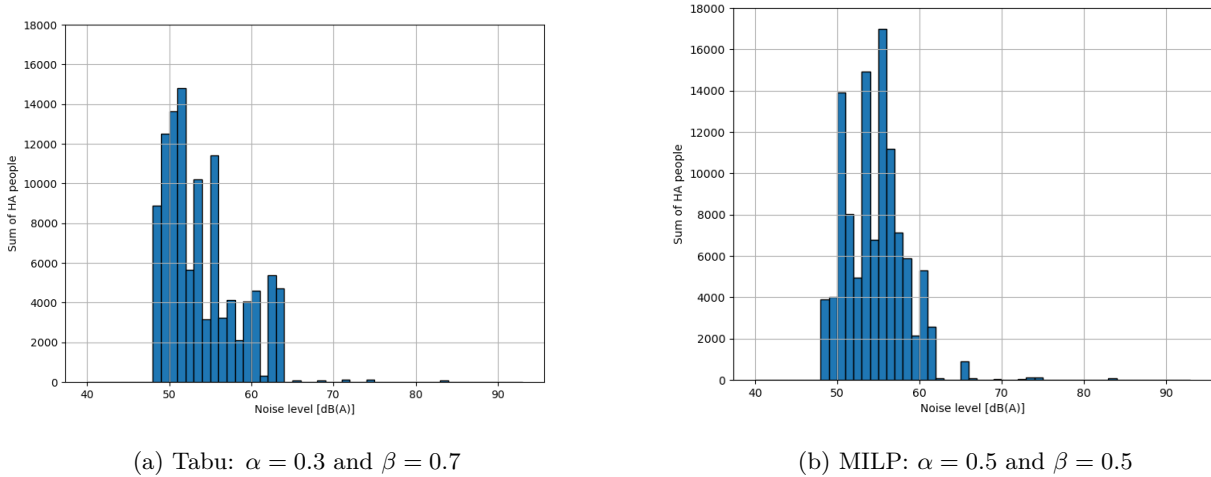


Figure 11: Highly Annoyed people distribution comparison

4.6 Sensitivity Analysis: Optimization Horizon

The performance of the model is significantly influenced by the window width of the sliding time window, which serves as a crucial parameter. This window width dictates the portion of the flight schedule optimized within each window, consequently impacting the number of flights considered. To comprehensively evaluate this impact, a sensitivity analysis is conducted on this parameter, exploring a range from 10 to 30 minutes. This means a total optimization per shift between 20 minutes and 1 hour. This analysis aims to unveil the implications of the objective functions resulting from variations in this parameter. The sensitivity analysis is performed on the six-hour scenario and the result can be seen in Figure 12 for fuel optimization and in Figure 13 for noise optimization.

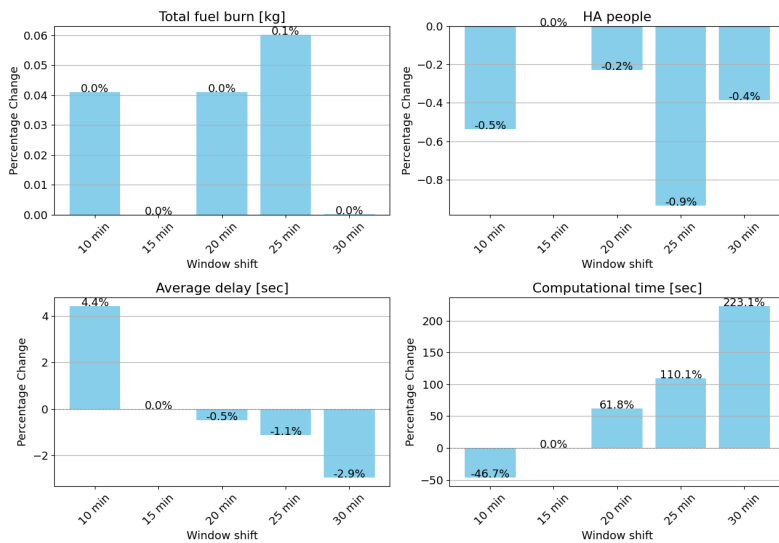


Figure 12: Fuel optimized sensitivity

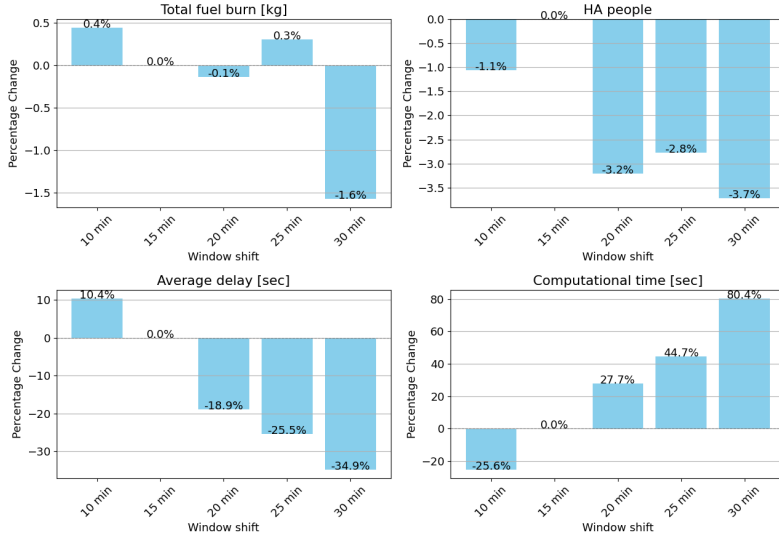


Figure 13: Noise optimized sensitivity

In the context of fuel optimization, minimal discrepancies in fuel consumption are observed across varying window sizes. This implies that the 15-minute scenario achieves an almost optimal solution, and this efficiency remains consistent regardless of the window size. Additionally, both the average delay per flight and the overall optimization duration are contingent upon the chosen window size. A notable observation is that the 10-minute window size exhibits a higher average delay, primarily attributable to the reduced opportunities for attaining an optimal solution within the narrower time frame. Conversely, larger window sizes afford the algorithm more flexibility, enabling it to sequence flights more optimally. The total optimization duration scales proportionally with the window size. This scaling effect is evident as smaller window sizes constrain the optimization scope, leading to fewer flights and a reduced number of neighbor creations and evaluations, which results in a 46.7% decrease in computational time. Conversely, larger window sizes expand the optimization possibilities, resulting in a reverse relationship with the optimization duration with an increase of 223.1% for the 30-minute time window.

In the context of noise optimization, a consistent trend can be observed in both average delay and computational time. A smaller time window size leads to a 10.4% increase in average delay, while larger window sizes show a maximum reduction of 34.9%. The differences in computational time are larger, with a substantial 25.6% decrease for the 10-minute window and a 128.7% increase for the 30-minute window. Upon closer inspection of both graphs, it becomes apparent that the 15-minute window size consistently yields the best results across fuel, noise, delay, and computational time optimization. Opting for a smaller time window results in increased delay, while selecting a larger time window leads to extended computational time with marginal gains in optimization outcomes.

5 Discussion

The existing FRSM has been modeled as a MILP, presuming linearity in all constraints. In contrast, the methodology employed in this research utilizes a tabu search algorithm within a moving horizon approach. This approach allows for the integration of non-linear elements and facilitates an analysis of the impact of a different solving method.

The results demonstrate that the tabu search algorithm model yields accurate outcomes for both objectives, fuel burn, and noise annoyance. Concerning fuel optimization, the tabu search performs less optimal for the 90-minute and six-hour scenarios. However, its objective surpasses that of the MILP model as the flight schedule expands. This improvement is primarily attributed to the MILP model and its scalability challenges. The tabu model, incorporating a moving horizon approach, effectively mitigates these issues by maintaining a more manageable scale, thereby enhancing its performance on larger flight schedules. In terms of noise optimization, the tabu search algorithm demonstrates superior performance across all scenarios concerning the number of HA people. While the improvement is marginal for the 90-minute scenario, exhibiting a 2.14% decrease, it becomes more pronounced as the flight schedule expands. Notably, the daytime scenario showcases a substantial improvement with a 33.29% decrease. It is important to acknowledge that, in the full-day scenario, the MILP model encountered convergence issues, preventing a proper comparison of results. This limitation stands out as a primary drawback of the MILP approach.

However, the tabu search approach used in this research also has its limitations. The incorporation of a moving

horizon introduces a level of complexity to the noise optimization and calculation process. Conventionally, noise is assessed over 24 hours or an entire year. However, with the moving horizon approach, the noise is segmented into budgets per horizon. This shift can impact the outcome, given that achieving the optimal noise result necessitates comprehensive information spanning the entire day. The reference scenario against which the noise results are compared originates from the noise annoyance measured over an entire year. Consequently, the comparison may not offer the most precise evaluation, as it involves a certain number of hours or one day instead of an entire year. Such a comparison might not accurately reflect the impact of external factors, such as weather conditions, which can play a crucial role over more extended time frames. Furthermore, the arrival and departure trajectories are based on the information from the AIP, using predefined routes. Specifically, for arrival trajectories, the assumption is that aircraft go from the IAF to AAS in the direction of waypoint SPL and then proceed to a runway. This simplification deviates from the more direct paths often taken in real-world operations. This limitation should be acknowledged as it affects the accuracy of the model in representing actual aircraft movements.

The improved FRSM reveals promising prospects for real-world applications. Improved computational performance makes the model more suitable for real-time operations. Additionally, the incorporation of the dose-response relationship for noise annoyance positions the model to contribute potentially to increased operations while adhering to noise regulations. This dual advantage positively impacts both the airport its operations efficiency and the well-being of residents in the vicinity.

Beyond its noise reduction capabilities, the FRSM its optimization features in fuel consumption, contribute to a positive environmental footprint. The consequential decrease in emissions in the surrounding airport area further emphasizes the holistic benefits of the model. By effectively balancing noise disturbance and minimizing fuel consumption, the improved FRSM could emerge as a useful tool with advantages for airport operations and the surrounding community.

6 Conclusions

The aim of this study was to enhance the Flexible Runway Scheduling Model (FRSM) by overcoming two primary limitations, computational performance and simplified noise annoyance modeling. Drawing on the recent model developed by [Abbenhuis, 2021], the model was redesigned by incorporating a tabu search optimization technique and integrating receding horizon control to enhance its computational performance. Moreover, the nonlinear nature of noise has been considered, and the number of Highly Annoyed (HA) people has been used as a metric to measure it.

To assess the performance of the tabu search model model, four distinct scenarios, varying in the number of flights and complexity have been compared with the MILP model. The results reveal that integrating the tabu search algorithm leads to significant computational savings, ranging from 52% for a noise-optimized full-day flight schedule to 92% for a noise-optimized 90-minute flight schedule. Furthermore, the non-linear noise objective, aimed at reducing noise annoyance, resulted in a significant enhancement, reducing the noise annoyance from 2.14% for the 90-minute schedule to 62.5% for the full-day schedule. However, it is worth noting that for shorter flight schedules, the MILP model outperforms the new model in terms of fuel optimization by 0.73% and 0.19%. This shows that linearization and simplification do affect the results regarding computational performance and noise optimization, but have limited influence on fuel optimization.

Both the MILP and tabu search algorithms demonstrated similar results concerning the Pareto front, while the MILP excelled in fuel optimization and the tabu search in noise reduction. The study reveals that reductions in both fuel and noise annoyance are achievable. For the selected 90-minute scenario fuel savings of 6.7% is achievable and for the six-hour scenario 15.5% of fuel savings. Both with a reduction in noise annoyance compared to the 2019 Schiphol reference scenario.

Additionally, the model makes divergent choices when allocating flights to runways, achieving the same results in the objective function. This discrepancy is attributed to the tabu search algorithm incorporating noise annoyance on a non-linear scale, which the MILP model does not account for. The differences between the MILP and tabu search algorithms can be attributed to their respective time horizons. The MILP optimizes the entire flight schedule in one go, while the tabu search uses a moving horizon optimization approach, optimizing smaller segments of the schedule.

To address this variability, variable noise budgets specific to each optimization window are utilized for scheduling the flights. Nevertheless, this approach has a limitation where the model is less effective in allocating flights with sudden spikes in noise levels in the upcoming windows. Despite this limitation, the results show that the majority of HA people experience lower noise levels compared to the MILP approach. This evidence supports the efficient functioning of the non-linear implementation of noise annoyance with variable noise budgets.

In summary, this research focuses on an enhanced FRSM, by addressing computational performance and noise annoyance. The research demonstrates that changing the modeling method results in faster computational

times and enhances the model its capability to handle larger flight schedules. Additionally, the study highlights the potential benefits of implementing this approach in daily operations. It also indicates positive impacts on the surrounding environment in terms of noise representation and fuel reduction.

7 Recommendations

For future research, several improvements can be made to the model to increase the performance in terms of solution accuracy and computational efficiency.

While this study employed a tabu search algorithm as a novel optimization technique, exploring alternative optimization methods and evaluating their performance could be valuable. For instance, Multi-Objective Evolutionary Algorithms (MOEAs) present themselves as promising tools adapted to tackling multi-objective functions. The exploration of MOEAs, in addition to the tabu search method, presents an opportunity to potentially improve the problem-solving capabilities of the model concerning multi-objective trade-offs.

An interesting area for future research involves integrating optimal control methodologies to effectively conserve fuel during the aircraft its trajectory. While this study considered fixed-length trajectories for both arrival and departure, existing literature has delved into optimizing either arrival or departure trajectories separately. Incorporating these trajectory optimizations, whether for arrivals or departures, in conjunction with runway scheduling optimizations could yield substantial benefits in further reducing fuel consumption and mitigating noise.

A limitation of the current model lies in the fact that it does not take into account the runway availability during the allocation of runways to flights. It assumes a best-case scenario where all the runways are available for operations. The user must manually modify the runways restricted for operations. The consideration of wind directions and maintenance of runways is crucial as it impacts aircraft operations, affecting takeoff and landing performance. Incorporating real-time or forecasted wind data into the FRSM can optimize the allocation of flights by considering wind direction and intensity. Accounting for wind conditions enables the model to make more informed decisions, such as selecting runways that align favorably with prevailing winds. This could improve aircraft efficiency, and fuel consumption, and potentially reduce noise levels during takeoffs and landings.

Additional resources can be allocated to enhance the modeling of fuel consumption. While this study has already made strides in improving accuracy, further refinement can be achieved by exploring non-linear fuel burn modeling. Incorporating non-linear fuel burn models could significantly enhance the accuracy of the model when simulating real-world data.

Lastly, the increased air traffic controller workload should be investigated. Since this model does not consider the additional attention required for constantly switching runways, further research is needed to determine its impact on Air Traffic Management (ATM) systems. The most important parameter for the air traffic controller is to limit the number of runway switching directions.

References

- [Abbenhuis, 2021] Abbenhuis, A. (2021). Flexible Runway Scheduling for Complex Runway Systems. Master's thesis, Delft University of Technology.
- [Airbus, 2004] Airbus, S. (2004). Getting to grips with fuel economy. *Flight Operations Support & Line Assistance*, (4).
- [Al-Salem et al., 2012] Al-Salem, A., Farhadi, F., Kharbeche, M., and Ghoniem, A. (2012). Multiple-runway aircraft sequencing problems using mixed-integer programming. In *IIE Annual Conference. Proceedings*, page 1. Institute of Industrial and Systems Engineers (IISE).
- [Atkin et al., 2007] Atkin, J., Burke, E. K., Greenwood, J. S., and Reeson, D. (2007). Hybrid metaheuristics to aid runway scheduling at london heathrow airport. *Transportation Science*, 41(1):90–106.
- [Crocker, 2007] Crocker, M. J. (2007). Fundamentals of acoustics, noise, and vibration. *Handbook of Noise and Vibration Control*, pages 1–16.
- [Delsen, 2016] Delsen, J. (2016). Flexible Arrival & Departure Runway Allocation. Master's thesis, Delft University of Technology.
- [Ganic et al., 2015] Ganic, E. M., Netjasov, F., and Babic, O. (2015). Analysis of noise abatement measures on european airports. *Applied Acoustics*, 92:115–123.
- [Glover and Laguna, 1998] Glover, F. and Laguna, M. (1998). *Tabu search*. Springer.
- [Heblij and Derei, 2019] Heblij, S. and Derei, J. (2019). Methodenrapport doc29. Technical report, National Aerospace Laboratory NLR.
- [IATA, 2023] IATA (2023). Global outlook for air transport: A local sweet spot.
- [Khadilkar and Balakrishnan, 2012] Khadilkar, H. and Balakrishnan, H. (2012). Estimation of aircraft taxi fuel burn using flight data recorder archives. *Transportation Research Part D: Transport and Environment*, 17(7):532–537.
- [Lee et al., 2022] Lee, C., Thrasher, T., Boeker, E., Downs, R., Gorshkov, S., Hansen, A., Hwang, S., et al. (2022). Aviation environmental design tool (aedt) version 3e technical manual. Technical report.
- [Lieberman and Hillier, 2021] Lieberman, G. J. and Hillier, F. S. (2021). *Introduction to operations research*, volume 11. McGraw-Hill New York, NY, USA.
- [LVNL, 2023] LVNL (2023). Integrated Aeronautical Information Package.
- [Nuic, 2010] Nuic, A. (2010). User manual for the base of aircraft data (bada) revision 3.10. *Atmosphere*, 2010:001.
- [Rooseleer et al., 2018] Rooseleer, F., Treve, V., and Phythian, D. (2018). "RECAT-EU" European Wake Turbulence Categorisation and Separation Minima on Approach and Departure.
- [Royal Schiphol Group, 2020] Royal Schiphol Group (2020). Annual report 2019.
- [Schiphol, 2023] Schiphol (2023). Zo gebruiken we onze banen.
- [Soykan and Rabadi, 2016] Soykan, B. and Rabadi, G. (2016). *A Tabu Search Algorithm for the Multiple Runway Aircraft Scheduling Problem*, pages 165–186. Springer International Publishing, Cham.
- [Soykan and Rabadi, 2022] Soykan, B. and Rabadi, G. (2022). A simulation-based optimization approach for multi-objective runway operations scheduling. *Simulation*, 98:991–1012.
- [van der Klugt, 2012] van der Klugt, J. (2012). Calculating capacity of dependent runway configurations. Master's thesis, Delft University of Technology.
- [van der Meijden, 2017] van der Meijden, S. (2017). Improved Flexible Runway Use Modeling. Master's thesis, Delft University of Technology.
- [Visser et al., 2008] Visser, H., Hebly, S., and Wijnen, R. (2008). Improving the management of the environmental impact of airport operations. *New Transportation Research Progress*, pages 1–65.

- [Welkers et al., 2021] Welkers, D., Sahai, A., van Kempen, E., and Helder, R. (2021). Analyse gelijkwaardigheidscriteria schiphol. Technical report, Rijksinstituut voor Volksgezondheid en Milieu RIVM.
- [Wu et al., 2019] Wu, L.-J., Zhan, Z.-H., Hu, X.-M., Guo, P., Zhang, Y., and Zhang, J. (2019). Multi-runway aircraft arrival scheduling: A receding horizon control based ant colony system approach. In *2019 IEEE Congress on Evolutionary Computation (CEC)*, pages 538–545. IEEE.
- [Zhan et al., 2010] Zhan, Z.-H., Zhang, J., Li, Y., Liu, O., Kwok, S., Ip, W., and Kaynak, O. (2010). An efficient ant colony system based on receding horizon control for the aircraft arrival sequencing and scheduling problem. *IEEE Transactions on Intelligent Transportation Systems*, 11(2):399–412.

Appendices

A Pier assignment

The assumptions concerning flight information and pier assignments are outlined in Table 6. The pier information is needed for computing taxi fuel, both for departing and arriving flights, as explained in the fuel burn calculation section 2.2 of the research paper. This information is obtained through an analysis of Schiphol data and input provided by the supervisor.

Table 6: Flight info and pier assignment

Pier	Airline	Weight Class
B	KLM	Lower Medium
C	Transavia, other	Upper Medium
D	KLM, other	Upper Medium
E	other	Lower Heavy
F	KLM	Upper Heavy
G	other	Upper Heavy
H	easyJet	All
Cargo	Cargo airlines	All

B Extract of flight schedule

Table 7 shows an extract of the flight schedule used as input for the FRSM with all the information needed.

Table 7: Example of data gathered from AAS flight schedule from August 23 2019

Scheduled operating time	Callsign	Airline	Aircraft type	Operation	SID/IAF	Weight class	O/D data	Pier
09:51:00	DAL133	DAL	A359	D	BERGI	UH	KDTW	G
09:52:00	KLM1555	KLM	E75L	D	LEKKO	LM	LIMF	B
09:52:00	KLM765	KLM	A333	A	SUGOL	UH	TNCB	F
09:53:00	KLM53W	KLM	B737	D	IVLUT	UM	EPWA	D
09:54:00	EIN603	EIN	A320	D	BERGI	UM	EIDW	D
09:54:00	AFR71DN	AFR	A320	D	LEKKO	UM	LFPG	D
09:54:00	AUA37H	AUA	A320	A	ARTIP	UM	LOWW	D
09:55:00	KLM31	KLM	B772	D	BERGI	UH	CYYZ	F
09:56:00	DAL136	DAL	A333	A	SUGOL	UH	KDTW	G

II

Literature Study
previously graded under AE4020

1

Introduction

In this chapter, the literature study focusing on runway scheduling in the context of airport operations is introduced. The efficient management of airports is essential for ensuring safe and timely aircraft movements, which are crucial for global connectivity and economic growth. A critical aspect of airport operations is the allocation and scheduling of runways, as it directly impacts an airport's capacity to handle incoming and outgoing flights. First, the background information about runway scheduling is described in [section 1.1](#). Next, the research context and the reason for the new research is explained in [section 1.2](#). Finally, [section 1.3](#) states the report structure of this literature study.

1.1. Background Runway Scheduling

Air transportation plays a crucial role in connecting the world nowadays, serving as a key driver of economic growth and facilitating global mobility. Efficient and effective management of airport operations is vital to ensure safe and punctual aircraft movements. One critical aspect of airport operations is the allocation and scheduling of runways, which directly impacts the capacity of an airport to handle incoming and outgoing flights. This allocation process, which is called the runway scheduling problem, introduces significant challenges due to the complex nature of air traffic flows, varying flight demand, and operational constraints. Besides increasing the capacity and efficiency it is crucial to consider the environmental aspects associated with runway scheduling.

Emissions from aircraft operations contribute to air pollution and climate change. Greenhouse gas emissions, such as carbon dioxide (CO₂), are a major concern due to their role in global warming. Runway scheduling can impact emissions by influencing aircraft queuing, taxiing, and idling times, which directly affect fuel consumption and, therefore, the emissions. By considering the fuel consumption with the allocation of the runway slots and minimising the taxiing distances, it is possible to reduce emissions and mitigate the environmental impact of aircraft operations.

Noise pollution is another significant environmental concern associated with airport operations. Aircraft noise can negatively affect nearby communities' well-being and quality of life. The scheduling of runway operations play a crucial role in managing noise levels. By implementing noise abatement procedures, such as preferred runway use, flight path optimisation, and time restrictions on operating hours, airports can mitigate the impact of aircraft noise on surrounding areas.

1.2. Research Context

Over the years multiple models are developed to analyse airport capacity with the accuracy of those models becoming better and better. Depending on the model's objective, they can analyse the airport capacity and, for example, environmental impacts. The first model to incorporate both fuel burn and aircraft noise in an airport capacity model has been developed by Delsen[24]. By using a flexible allocation model the runway capacity is optimised on both objectives instead of a preference list used by the airport. Further adjustments to this model have been made by Van Der Meijden [106] to incorporate pairwise flight constraints and implement aircraft-specific constraints instead of generalisation. As this model still had limitations Abbenhuis [1] changed the optimisation method to a flexible scheduling model and incorporated a method to calculate dependencies for a complex runway system. However, there are still some shortcomings to the current

model with respect to computational performance, noise limits, and fuel burn modelling during approach and therefore additional research is needed on this problem.

1.3. Report Structure

This literature study is structured as follows. In [chapter 2](#) the airport capacity is described and all the relevant theories and calculations are discussed. [chapter 3](#) discusses the fuel burn modelling techniques available and discusses the important factor that fuel consumption has on airline economics. The aircraft noise modelling is described in [chapter 4](#), including all the calculations related to aircraft noise and the annoyance of noise. Furthermore, noise mitigation strategies and regulations are presented. The different mathematical models and solving methods for the runway scheduling problem are stated and explained in detail in [chapter 5](#). Finally, [chapter 6](#) presents the research proposal resulting from this literature study.

2

Airport Capacity

This chapter will discuss the subject of airport capacity and the factors influencing this capacity. With some background information on the topic of airport capacity in [section 2.1](#). [section 2.2](#) starts by explaining the different definitions of runway capacity and the concept of delay. The different factors influencing the runway capacity with explanation are described in [section 2.3](#). The sequencing of aircraft plays an important role in the runway capacity. The techniques to hold the aircraft during sequencing are discussed in [section 2.4](#). Another important parameter is the separation, the new separation standards according to RECAT-EU are explained in [section 2.5](#). [section 2.6](#) describes the way runway capacity is calculated. To help ATC in the runway scheduling several decision-support tools are developed. These are stated and explained in [section 2.7](#). Finally, [section 2.8](#) discusses the available literature on airfield capacity modelling.

2.1. Background Information

Understanding and analysing the airport capacity and the factors influencing this capacity is crucial for airport planning and design, as the airfield's capacity, especially the runway system, is often the primary factor that determines the total airport capacity. The airport capacity problem started in the early 1990s, at that time the U.S. transport system was not able to handle the total air traffic demand anymore[7]. This resulted in the problem becoming a national issue that required collaboration between air transport industry partners and the government. However, the problem is not easy to solve as capacity expansions are expensive and require a long lead time. Furthermore, capacity was not well understood and is a very complex issue technically and operationally. The increase in air travel had led to a situation where the airport capacity could not keep up with the rising demand, causing congestion and delay. This has resulted in significant inconvenience, declining quality of service, and safety concerns for both the air transport industry and the travelling public.

The runway complex is often the primary bottleneck of the Air Traffic Management (ATM) system. This is because air traffic transitions from three-dimensional flows in the airspace to a single-file regime on the runway. Increasing runway capacity is often a capital-intensive and time-consuming process because building a new runway involves many external factors.

2.2. Runway Capacity Measures and Delay

Numerous methods exist to determine runway capacity, each designed to estimate the number of aircraft movements, including arrivals and/or departures, that an airport's runway system can handle during a particular time unit, usually an hour. It is crucial to comprehend the definitions of these alternative measures to utilise them accurately and prevent misunderstandings. Below four different measures of runway capacity are stated and explained, all of them coming from Neufville and Odoni [22]

- **Maximum Throughput Capacity (MTC)**

The MTC is defined as the expected number of aircraft movements that can be carried out within an hour on a runway system, while complying with ATM regulations and in the presence of continuous aircraft demand. The MTC depends on the specific conditions under which the runway operations are

conducted. Level of service (LOS) requirements are neglected in the MTC measure, this means a delay per movement of a few minutes or several hours is trivial.

- **Practical Hourly Capacity (PHCAP)**

The PHCAP is defined as the anticipated number of aircraft movements that can be executed within one hour on a runway system, with an average delay of 4 minutes per movement. The FAA originally proposed this method in the early 1960s [29]. This definition takes LOS into account and indicates when the runway system is approaching its capacity when the LOS threshold is exceeded.

- **Sustained Capacity**

The sustained capacity refers to the number of aircraft movements per hour that can be reasonably sustained over several hours. The term "sustained" primarily refers to the workload of the ATM system and the air traffic controllers. The ATM system must operate at full potential to achieve MTC, but this is not practical for more than a couple of consecutive hours. Therefore, it is suggested that a more realistic target be established for sustained capacity during periods of several hours or entire days of air traffic activity. The sustained capacity is around 90 percent of MTC with high maximum throughput capacity and up to almost 100 percent of MTC with configurations with low maximum throughput capacity [22]

- **Declared Capacity**

Declared capacity is a similar measure to sustained capacity, based on the same concept. It is defined as the number of aircraft movements per hour that an airport can handle while maintaining a reasonable LOS, with the delay being the main indicator of LOS. It forms the basis for the worldwide practice of "schedule coordination" and "slot allocation". This means that airports affected by congestion 'declaring' a capacity, which is then employed to establish a cap on the number of movements that can be scheduled per hour. For example, Schiphol's declared capacity for the summer of 2023 during day time is between 106 and 110 movements per hour [36], depending on the ratio of arrivals to departures. The declared capacity is typically 85-90 percent of the MTC [89].

In the aviation sector, when demand exceeds the capacity at a given component of an airport or airspace this will result in system delays. Delay can be defined as the increase in time to operate compared to a "normal" nondelayed operation. This increase in time can manifest in different ways, such as waiting in queues or delays in executing operations, or a reduction in speed due to congestion. At an airport, an operation can be defined as a takeoff or landing on the airfield, or the processing of a passenger through the terminal. In the airspace, an operation can be defined as an aircraft travelling through a specific sector or airspace [44]. Following Neufville and Odonno [22] two types of delays can occur, overload delays and stochastic delay. Overload delays occur when the demand rate exceeds the capacity for a significant time. Delays can also occur when the demand rate is less than but reasonably close to the service rate. Even if the demand rate is less than the capacity for the entire day, "spikes" in the demand or variability in the inter-arrival or inter-departure times end in delays. This can form clusters and result in queues of aircraft on the ground or in the air. When the demand rate is smaller than the capacity but in the proximity, it may take a while for the queues to disappear.

The airport runway system can be seen as a queuing system. A queuing system consists of a user source, a queue, and service facility with 1+ parallel servers [90]. The server in the case of the runway system is the ANSP providing the ATC within the region of a specific airport.

The utilisation ratio, ρ , is defined as the demand rate, λ , divided by the service rate, μ , as shown in Equation 2.1. An equilibrium only exists when ρ is smaller than 1.

$$\rho = \frac{\lambda}{\mu} \quad (2.1)$$

In a steady state system the delay, D , is proportional to the relationship shown in Equation 2.2. When ρ is bigger than 1 the delay of the system will increase rapidly.

$$D \sim \frac{1}{1 - \rho} \quad (2.2)$$

Figure 2.1 gives a graphical representation of the delay as a function of capacity and demand. Both the PHCAP and the MTC can be seen in the figure, with the 4 minutes acceptable delay as proposed by the FAA.

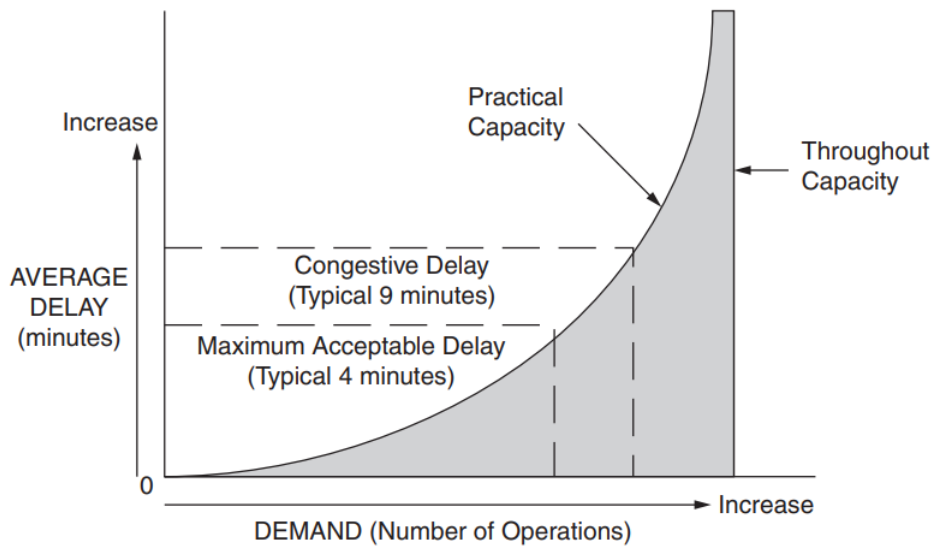


Figure 2.1: Delay as a function of capacity and demand [44]

The figure indicates the difference between the PHCAP and the MTC, as the practical capacity is defined in terms of delay, and the throughput capacity is not.

To calculate the expected time a user spends in the queue, the Pollaczek-Khinchin formula can be used, which is given in Equation 2.3. Where the user is in this case the arriving or departing aircraft. A Poisson distributed demand is assumed, meaning independent inter-arrival times between the users. W_q is the expected time in queue per aircraft, and the arrival rate of aircraft is defined by λ . Furthermore, the equation is dependent on the variance of service time, σ_T^2 , the expected service time, $E(T)$, and the rate of service, μ .

$$W_q = \frac{\rho \left[1 + \frac{\sigma_T^2}{E^2(T)} \right]}{2\mu(1 - \rho)} \tag{2.3}$$

2.3. Runway Capacity Factors

Runway capacity can vary as a result of a wide range of causative factors. To have a clear overview of the different factors related to runway capacity, they are classified into five different categories. The categories are based on the research performed by Zhao et al. [113] on dynamic capacity-demand balance research and are shown in Table 2.1.

Table 2.1: Classification of Runway Capacity Factors[92]

Category	Description
Operation/procedures	Factors related to anything that makes activities function as addressed
The geometry of airside facilities	Factors related to physical characteristics of airside facilities
Aircraft performance	Factors related to aircraft characteristics of airside facilities
Human factors	Factors related to pilot, ATC officer and human-related
External	Factors excluding 4 categories above and unmanageable factors

In the following subsections, the main runway capacity factors will be discussed, starting with the runway configuration

2.3.1. Runway Dependencies

When the airport consists of multiple runways the layout of the runways is an important factor influencing the runway capacity. Dependencies between those runways could occur and separation regulations are dependent on the runway operations. Research done by van der Klugt[105] shows five different categories of dependencies. All of them are discussed in this subsection, starting with converging and diverging runways.

Converging and Diverging Runways

Runways that do not intersect, but converge or diverge towards each other are known as converging and diverging runways. During certain operation modes, such as departing-arriving or arriving-arriving, the missed approach paths may intersect, while some runway layouts can cause issues with jet blasts or wake turbulence on the ground. These dependencies are shown in Figure 2.2.

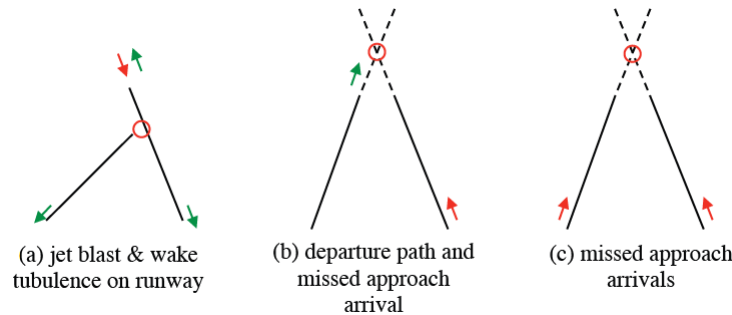


Figure 2.2: Operations on converging and diverging runways [105].

The wake turbulence and jet blast cause the operation of one runway to interfere with the operation on the other runway shown in Figure 2.2 a. The countermeasure depends on the exact layout of the runways, the type of operation, and the aircraft type.

The missed approach is shown in Figure 2.2 b and c. The first case of missed approach is when the departure path crosses the missed approach path of arrival. To avoid this from happening a departure is only allowed when the arriving aircraft has a specific distance from the runway. The second case is when the missed approach track of two arriving aircraft intersects. The countermeasure is applying a separation between two arrivals on different runways, which is called "staggering".

Intersecting Runways

The runway dependencies with intersecting runways are coming from the jet blast and wake turbulence combined with the point of the runway intersection. Intersecting runways can be used for multiple operations, shown in Figure 2.3. To minimise runway dependencies and optimise the use of intersecting runways, airports often employ several strategies. These can include using staggered runway approaches and creating designated holding areas for aircraft waiting to take off or land. The highest capacity of runways that intersect is usually achieved when the intersection is at the very beginning of both runways in the direction of operation [22].

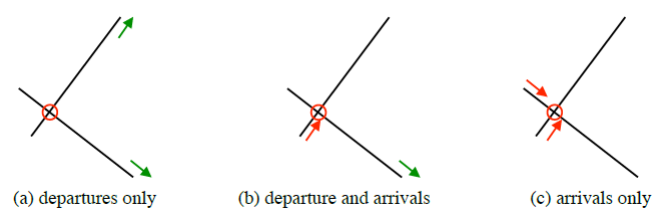


Figure 2.3: Operations on intersecting runways [105].

Mixed Mode

Mixed-mode operations refer to the use of a single runway for both departures and arrivals. In alternating mixed mode operation, which is used when the arrival/departure ratio is around 1, each arrival is followed by a departure (A-D-A-D-...). Other patterns are used when the ratio is not equal to one, such as increasing gaps between arrivals to fit more departures (A-D-D-A-...) or fitting departures into some arrival gaps (e.g. A-A-D-A-A-...).

To ensure safe operations, separation regulations exist for both combinations. For a take-off roll to commence, three conditions must be met: the preceding aircraft must have left the runway, the next arrival must be at a specified distance from the runway threshold when the departure is released, and the next arrival

must be at or before the latest point before the threshold where a missed approach can be initiated when the departure lifts off.

Parallel Runways

Parallel runways are runways whose centerlines are aligned and may be used simultaneously for takeoffs and landings. These runways are typically found at large airports where there is a high volume of air traffic. To ensure safe operations on parallel runways, some specific rules and procedures must be followed. The separation regulations are dependent on the distance between the centerlines of the runways and the operational mode and direction of the runway. Four different operating modes for parallel runways are known [82].

[noitemsep]Independent parallel approaches Dependent parallel approaches Independent parallel departures Segregated parallel operations

To allow parallel operations the minimum distance between the runway centerlines has to be 760 m [82]. The runways are considered as one single runway when this distance is smaller.

The first two modes mentioned above are approaches, for the first one no special separation conditions apply. However, for the second mode, there are some dependencies. One form of segregated operation is semi-mixed parallel operations. This means that one runway is only used for either approaches or departures.

2.3.2. Runway Occupancy Time

The Runway Occupancy Time (ROT) affects the time interval between successive takeoffs or landings on a runway. A longer ROT can result in a greater time gap between the departure of the arrival of aircraft, which reduces the overall number of operations that can be accommodated on the runway in a given period. The influence on the runway capacity may seem small, but the saving of a few seconds per movement can result in a big increase in the capacity. Saving 5 seconds per movement has the potential to increase capacity by 1. to 1.5 movements per hour [27].

The ROT is defined differently for arriving and departing aircraft. The Runway Occupancy Time of Arrival (ROTA) is defined as the time interval between crossing the beginning of the portion of the runway usable for landing and the aircraft tail vacating the runway [83]. The Runway Occupancy Time of Departure (ROTD) is the time interval between crossing the holding stop bar and the main gear lifting off the runway [83]. The ROT of an aircraft is influenced by many factors, such as the aircraft type, speed, and weather conditions.

2.3.3. Separation

Separation has a significant impact on runway capacity. The separation requirements between aircraft are established to ensure safe operations and prevent collisions, which are critical to maintaining high safety standards.

Wake turbulence is created behind an aircraft in flight, particularly in the wake of the wings. The wake turbulence is turbulent air and can be hazardous to other aircraft flying nearby. The ICAO has established standard wake turbulence separation regulations. These regulations prescribe minimum separation distances that aircraft must maintain. The wake turbulence is dependent on the aircraft size, therefore the ICAO has created categories, called "Wake Turbulence Categories" (WTC), which are based on the Maximum Take Off Weight (MTOW) of the aircraft. The different categories and their corresponding MTOW are shown in Table 2.2. Originally, only three categories were introduced. However, with the introduction of the Airbus A380, the Super Heavy (J) category was added.

Table 2.2: ICAO Wake Turbulence Categories [82]

Code	Class	MTOW [kg]	Example Aircraft
J	SUPER	MTOW \approx 560,0000	Airbus A380
H	HEAVY	MTOW \geq 136,000	B763, A346
M	MEDIUM	7,000 < MTOW < 136,000	AT45, B738
L	LIGHT	MTOW \leq 7,000	General Aviation

There are two types of separation, namely Time-Based separation (TBS) and Distance-based separation (DBS). The wake turbulence is the main factor influencing the separation values. Table 2.3 shows the DBS and Table 2.4 the TBS according to the ICAO. The values shown in parentheses are not based on the wake vortex separation, but on the minimum radar separation, which is common 3 nmi

Table 2.3: Distance-based separation minima [82]

Lead	Following	Super	Heavy	Medium	Light
Super		-	6	7	8
Heavy		-	4	5	6
Medium		(3)	(3)	(3)	5
Light		(3)	(3)	(3)	(3)

Table 2.4: Time-based separation minima [82]

Lead	Following	Super	Heavy	Medium	Light
Super		-	120	180	180
Heavy		60	90	120	120
Medium		60	60	60	120
Light		60	60	60	60

2.3.4. Aircraft Mix and Sequencing

The sequencing of aircraft plays a crucial role in determining the capacity of a runway. Sequencing is the process of determining the order in which aircraft will take off or land on the runway. Different sequencing techniques can have a significant impact on runway capacity. The most common sequencing technique is based on the First-Come First-Served (FCFS) rule. This rule is based on the Estimated Time of Arrival (ETA) and the Estimated Take-off Time (ETT) of each aircraft. For arriving aircraft the sequencer computes the Scheduled Landing Time (SLT) based on the ETA obtained when an aircraft enters the airport's radar taking into account the separation requirements [75]. The FCFS heuristic is widely used due to its easy implementation, low controller workload and it provides fairness among aircraft. However, the technique may not provide optimal sequences regarding runway throughput or average delay due to the presence of WV separations. This is especially the case in congested airports.

To address this issue other sequencing techniques are developed, for example, CPS (Constrained Position Shifting), which was introduced by Dear [23]. CPS involves shifting the position of an aircraft in the landing sequence, while maintaining a safe distance from other aircraft, to reduce delays and increase runway capacity. With CPS the aircraft is not allowed to shift more than a given number of positions from its FCFS position. It has the benefit of treating equitably and reducing the solution time of exact scheduling techniques. The improvement of CPS compared to FCFS can be seen in Figure 2.4.

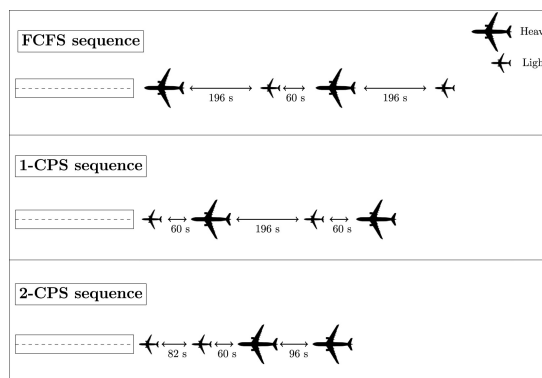


Figure 2.4: Comparison of FCFS and CPS [52]

The FCFS requires a total of 452 s to land the four aircraft in the sequence, whereas the CPS methods require 316 s and 238 s, depending on the number of position shifts. One could argue that a possible downside of the CPS could be the degradation of fairness among the aircraft. However, as aircraft are only able to shift a given number of positions from its FCFS position this remains limited. Furthermore, the time improvement gained due to CPS will decrease delays, and this benefits airlines.

2.3.5. Weather and Wind Conditions

Weather and wind can play a crucial role in runway capacity. ATC needs to consider various meteorological factors when determining which runways to use and in which direction to operate the aircraft.

Visibility, Ceiling, and Precipitation

Cloud ceiling and visibility are the two parameters that determine the weather category. Under conditions of poor visibility, ATC becomes more cautious. This results in longer aircraft separations and greater runway occupancy times. When the visibility or cloud ceiling falls below certain prescribed values, Instrument Flight Rules (IFR) are employed. If the visibility is very poor and the clouds are extremely low, the Low Visibility Procedures (LVP) take effect. This applies several safety precautions, such as runway protection with stop bar lights and increased aircraft separation. There are four categories of LVP, ranging from A to D, with D applying to the poorest conditions[68].

Precipitation and icing have the negative potential of affecting the runway capacity, because of poor visibility, braking action, and deicing. In case of extreme weather events, such as snowstorms and thunderstorms, the airport can be temporarily closed.

Wind Direction and Strength

Wind strength and direction can have a significant impact on runway capacity. The wind strength can affect the take-off and landing performance of an aircraft, with stronger winds potentially requiring larger separation distances between takeoffs and landings. Crosswinds can also impact the safe operation of aircraft and may require runway closures or restrictions. A runway can be used only when crosswinds are within prescribed limits and tailwinds do not exceed 5 or 6 knots [22]. The wind direction can impact runway configuration and availability. Airports typically have designated runways for specific wind directions, and if the wind direction is different than the usual direction, it may require a change in runway configuration and limit the runway capacity.

ATC has a significant degree of flexibility in deciding which runways to use and the direction of operation when the wind speed is below 5 knots, which are called "calm" conditions. To determine the active runways and direction of operation during these situations, multiple factors such as maximizing runway capacity or reducing environmental impacts may be considered.

2.4. Holding Techniques

As discussed in [subsection 2.3.4](#) sequencing influences the capacity of the runway. However, the techniques covered typically assume that the aircraft is "waiting" in the air or on the ground and can land or take off at any time. Sometimes unpredictable delays can make it difficult to follow the original schedule, leading to some aircraft holding before landing or taking off. For aircraft taking off this can easily be solved by creating "holding positions" on the ground. Landing aircraft can be redirected via trombone arrival routes, these routes are pre-defined cycling tracks in the arrival route that some aircraft follow until they receive clearance from ATC[9].

The literature discusses also other techniques used for holding aircraft, such as Vector For Space (VFS), which stretches the path of an aircraft instead of letting it fly the direct path between two points[14] or Holding Patterns (HP), which are waiting loops on the different flight levels. These loops have a constant delay associated with them, typically 4 minutes. For short delays, the VFS is an efficient solution to implement a delay in the model. Nevertheless, in instances where delays exceed a certain threshold, HP actions will be the superior choice. Consequently, within the framework of the proposed model, an integration of these two approaches can be employed to achieve optimal management of delay.

2.5. RECAT-EU

The introduction of the Airbus A380 created a new development in the ATM world, as it required a new approach to the designing of wake turbulence separations. This led to a revision of the traditional ICAO provisions as explained in [subsection 2.3.3](#) because the A380 overtook the largest passenger aircraft generating greater vortices than those from the "Heavy" category [91]. The RECAT-EU aims to safely increase arrival and/or departure capacity at airports by redefining wake turbulence categories and their corresponding separation minimums. The ICAO separations are dependent on the MTOW of the aircraft and defined on the worst case in each scenario. This causes over-separation in many instances, each category may include a wide range of different-sized aircraft with high deviation in the MTOW. The over-separation means a loss

of runway throughput and therefore a sub-optimal airport capacity. The RECAT-EU divides the Heavy and Medium categories into two different categories, furthermore a new Super Heavy category was created for the A380. This process can also be seen in [Figure 2.5](#).

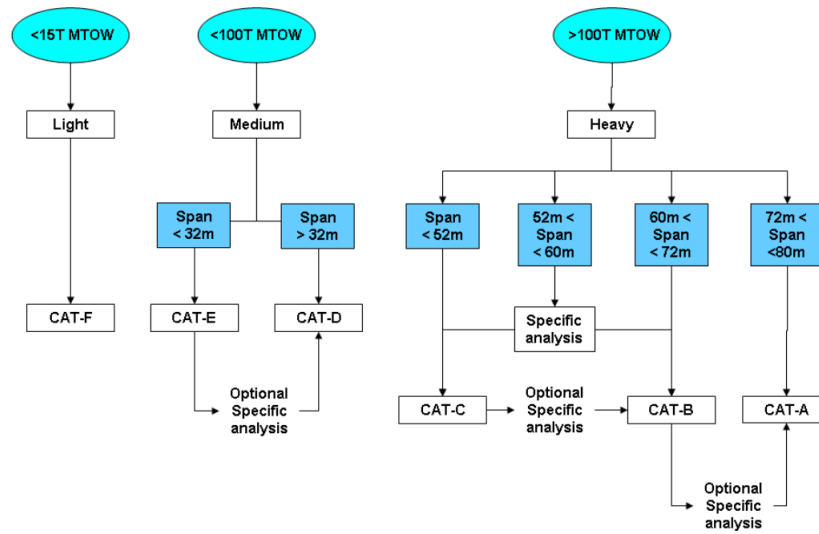


Figure 2.5: Categorisation process and criteria for assigning an existing aircraft into RECAT-EU scheme[91]

By introducing the new categories new separation minima were introduced. The same approaches are used compared to the ICAO WTC separation minima, resulting in new DBS minima and new TBS minima. The separation minima used for the RECAT-EU wake turbulence categories are shown in [Table 2.5](#). The first value in the table indicates the distance-based separation between aircraft in Nautical Miles (NM), and the second value represents the time-based separation in seconds between aircraft.

Table 2.5: RECAT-EU separation in NM / seconds [91]

	Lead	Follower	Super Heavy	Upper Heavy	Lower Heavy	Upper Medium	Lower Medium	Light
			A	B	C	D	E	F
Super Heavy	A		3/80	6/100	6/120	7/140	7/160	8/180
Upper Heavy	B		3/80	3/80	3/80	4/100	5/120	6/140
Lower Heavy	C		3/80	3/80	3/80	3/80	4/100	6/120
Upper Medium	D		3/80	3/80	3/80	3/80	3/80	5/120
Lower Medium	E		3/80	3/80	3/80	3/80	3/80	4/100
Light	F		3/80	3/80	3/80	3/80	3/80	3/80

Besides the wake turbulence separation minima, the ROT was also adjusted. The ROT is dependent on several factors, such as landing weight, brake setting, flap setting, approach speed, etc. The Departure Runway Occupancy Time (DROT) and the Arriving Runway Occupancy Time (AROT) for the different RECAT-EU categories can be seen in [Table 2.6](#).

Table 2.6: Runway Occupancy Times for the RECAT-EU categories [57]

RECAT- EU Category	DROT [s]	AROT [s]
Super Heavy	51.7	47
Upper Heavy	50	47
Lower Heavy	50	45
Upper Medium	40	45
Lower Medium	35.3	45

2.6. Runway Operation Modelling

Besides understanding the definitions and factors influencing the runway capacity, it is essential to estimate the actual capacity of the runway system. The first model developed to estimate the capacity of a single runway was done by Blumstein [16]. It is only applicable for arrivals, but with the same approach it can extend to departures or mixed operations. This section will discuss the theory behind runway operating modelling and explain the arrival mode, departure mode, and maximum throughput capacity calculations.

2.6.1. Arrival Mode

The arrival mode is shown in Figure 2.6, with a single runway system. Aircraft will descend towards the merge point, indicated as a gate in the figure until they touch down on the runway. The final approach is typically between 5 and 8 nmi and during the approach the aircraft should follow the separation regulations as explained in subsection 2.3.3. Furthermore, the runway has to be clear before the next aircraft can arrive.

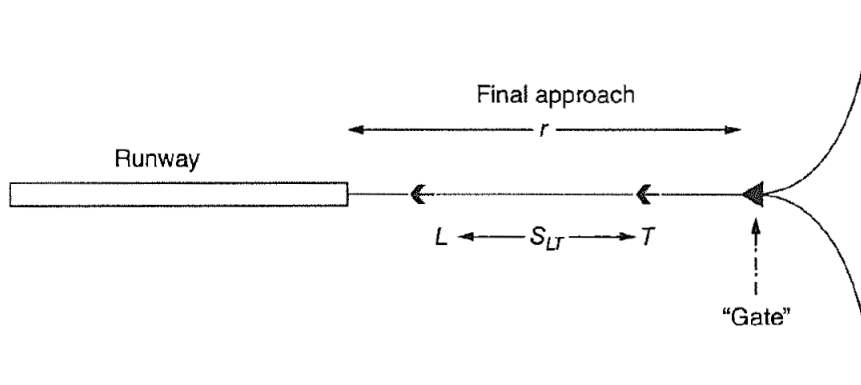


Figure 2.6: Runway capacity modelling for arrival mode [22]

To calculate the minimum separation time between two arriving aircraft Figure 2.6 can be used as a reference. With n being the length of the common final approach path. Consider the case in which an aircraft of type i is landing, followed immediately by another aircraft of type j . Both aircraft have their speed, indicated by V_i and V_j . The ROT of the leading aircraft is indicated by ROT_i . The minimum longitudinal separation while they are both airborne, according to the ICAO or RECAT-EU regulations, is included with s_{ij} . The minimum possible time interval between the leading and following aircraft, T_{ij} , is the minimum time separation between the two landing aircraft that can be achieved without violating any ATM separation regulations. Upon approach two different cases can occur:

Closing case

In the closing case, $v_i \leq v_j$ occurs when the trailing aircraft has a higher or equal speed than the leading aircraft. This means that the separation between the successive aircraft decreases during the approach. The separation is at the lowest point when the leading aircraft is at the runway threshold. The minimum required arrival time is calculated via Equation 2.4.

$$T_{ij} = \max \left[\frac{s_{ij}}{v_j}, ROT_i \right] \quad (2.4)$$

Opening case

The situation when $v_i > v_j$ is called the "opening case", because the separation distance between both aircraft increases due to the higher approach speed of the leading aircraft. The difference in approach speed is incorporated in the calculation of the minimum required arrival time interval shown in Equation 2.5.

$$T_{ij} = \max \left[\frac{n + s_{ij}}{v_j} - \frac{n}{v_i}, ROT_i \right] \quad (2.5)$$

2.6.2. Departure Mode

The Inter-Departure Time (IDT) is used for the minimum separation times for departing aircraft. The IDT is defined as the maximum of the TBS minimum according to the ICAO or RECAT-EU regulations and the DROT of the leading aircraft. The IDT can be calculated via Equation 2.6.

$$T_{i,j} = \max [TBS_{i,j}, DROT_i] \quad (2.6)$$

2.6.3. Maximum Throughput Capacity

In reality, achieving the exact separation as proposed by the separation matrix T is extremely difficult. As the operation involves human factors, it is expected that deviations from T_{ij} occur. In general pilots and air traffic controllers have a natural tendency to be very cautious and conservative with decisions resulting in separations that are larger than the theoretical values for T_{ij} . The separation model explained in this section can be adapted to include a Buffer Time (BT). This BT can be added to the separation time from the model which results in a new T_{ij} . With this new T_{ij} and the probability for all class pairs p_{ij} the expected value of T_{ij} between consecutive landings can be calculated via Equation 2.7.

$$E(t) = \sum_i \sum_j p_{ij} T_{ij} \quad (2.7)$$

With the expected amount of time between consecutive operations known, the MTC μ can be calculated with Equation 2.8.

$$\mu = \frac{1}{E(t)} \quad (2.8)$$

2.7. Decision-support Tools

Whereas the calculation described in the previous section are easy to solve for one or a pair of aircraft, it quickly becomes more difficult and impossible to solve as a human. Therefore decision-support tools are created to support air traffic operators at the airport.

There is a various amount of decision-support tools to help manage the flow of arriving and departing aircraft. One of them is the Center-TRACON Automation System (CTAS) developed by NASA and the FAA[52], which has three different functions. The traffic management advisor for runway assignment and scheduled landings, the descent advisor for guiding aircraft to metering fixes, metering fixes are specific points along an established air route over which aircraft will be metered before entering the terminal airspace surrounding airports, and the final approach sequencing tool for providing speed and heading recommendations. Furthermore, the CTAS has an additional function that aids in managing departing aircraft [26].

In Europe, the Arrival MANager (AMAN) tool serves a similar purpose to the CTAS, assisting controllers with guiding arrival flows in terminal areas to the runway or metering fixes. There are different versions of the AMAN tool, the basic one can provide a landing sequence, a timeline with a view of the runway threshold, and a target landing time for each aircraft. Advanced versions can offer additional control actions such as radar vectoring for altitude, speed, and heading. However, unlike CTAS, AMAN tools cannot detect or resolve conflicts, which can increase the workload on controllers in busy airspace [64]. A new version of AMAN, called Extended AMAN (E-AMAN), includes the airspace up to 500 nm around the airport, whereas the normal version covers around 100 to 200 nm. This extension aims to reduce congestion, noise, and fuel burn in the airspace near airports by sequencing aircraft earlier [74].

The European tool for departure operations is called Departure MANager (DMAN). It is used for managing and merging departure flows in en-route traffic.

2.8. Airfield Capacity Models

This section will discuss the information found on existing capacity models. Airfield capacity models can be classified according to three aspects: level of detail, methodology, and coverage.

The level of detail can be divided into macroscopic, mesoscopic, and microscopic. Macroscopic models in general focus more on providing approximate answers mainly for planning and design purposes. They are less detailed and can therefore explore a wide range of possible scenarios. Mesoscopic models are more detailed than macroscopic, but still focused on strategic planning. It uses simulation modelling but can generalise parameters, depending on the level of detail needed, which reduces the computational time. Micro-

scopic models provide information with a high level of detail. They are mainly used for tactical issues and aim at an exact representation of the various processes that take place at the airport.

The models can be divided into analytical and simulation models. The level of detail and the methodology are dependent on each other in most cases. Microscopic models are always simulations, whereas macroscopic models are mostly analytical and can sometimes be converted to simulations.

Lastly, the airfield models can be divided into three scopes, the taxiway system and apron area, the runway system, and integrated models.

A complete overview of the available airfield models sorted by the level of detail, methodology, and coverage can be seen in Table 2.7. All the models stated are explained in more detail in the upcoming subsections.

Table 2.7: Overview of airport capacity models [72], [79]

Level of detail	Coverage/Scope		
	Aprons and taxiways	Runway and final approach	Integrated model
Macroscopic	Horonjeff model and extensions	Blumstein model and extensions FAA Airfield Capacity Model DELAYS LMI Capacity and Delays Model AND	MACAD
Mesoscopic		runwaySimulator ACATS	
Microscopic		STROBOSCOPE	SIMMOD TAAM The Airport Machine HERMES RAMS Plus Total AirportSim AirTOP CAST

2.8.1. Macroscopic Models

Blumstein [16] developed the first analytical model to estimate the runway capacity. The model is set up for calculating the capacity with a single runway system for arrivals only while taking ATM separation into account. It assumes continuous demand of operation. The mean time interval between landings depends on the length of the common final approach path, separation requirements, and fleet mix. The model formed the basis for runway capacity modelling and over the years several extensions to the model have been made. The first extension was made by Harris [40]. He included departures and mixed operations in the model and introduced stochastic parameters. Hockaday and Kanafani [43] made improvements to the model developed by Harris. They introduced the effect of wake turbulence in the separation, and the derivation of optimal operating strategies of arrivals and departures. Furthermore, the model includes the runway capacity for a runway system with different configurations of multiple runways.

The Blumstein model and its extensions served as the basis for the FAA Airfield Capacity model. This model uses the same method, but is transformed into computer language, which has the advantage of faster calculations. The first version of the FACM was released during the 1970s by Peat, Marwick, Mitchell and Company, and McDonnell Douglas Automation. It calculates the MTC of the runway system for 15 different runway configurations. 4 main configurations are used to make the combinations, single runway, closely-spaced parallel, medium-spaced parallel, and crossed runways.

The model was updated in a later stadium by the MITRE Corporation [103]. Several new features were implemented in the upgraded versions. Such as the capability to compute the runway capacity for more complex runway systems, the model logic was changed, which resulted in reduced running time and/or improved accuracy. Furthermore, it could compute multiple different operations in one single run.

To overcome the limitations encountered by the Blumstein model, the LMI Capacity and Delays model was developed with the NASA Terminal Area Productivity (TAP) program [60]. One of the main features of the

model is that it tries to include the operational side of the airport itself. Variables such as approach speeds, ROTs, and delay in communication between airport controllers and pilots are incorporated in the model as random variables. The basis is a model that computes the capacity of a single runway for one kind of operation only, arrivals, departures, or for mixed operations. The output of the LMI Capacity model is a runway capacity curve, which is a boundary that defines the limits of the maximum throughput capacities that can be attained at the runway, taking into account all arrival and departure mixes that can occur [35]. If a point lies inside the runway capacity envelope this means the runway has sufficient capacity to serve x arrivals and y departures per hour.

A different model, not directly related to estimating the runway capacity, is the AND (Approximate Network Delays) model. AND is a network queuing model developed at MIT Operations Research Center [79]. It was first conceptualised by Malone [69] and developed further by Pyrgiotis et al. [87]. The model is not directly related to estimating the runway capacity, but it has the goal to analyse the impact of airline schedules, traffic volume, and airport capacity on flight delays. DELAYS is used as a software in the AND model to solve the equations related to delay, with AND being the analytical tool.

All the models mentioned previously focus on the runway and final approach operations. However, the Mantea Airfield Capacity and Delay (MACAD) model is an integrated airfield model [101]. It is developed by the Athens University of Economics and Business and integrates macroscopic airside models to provide approximate estimates of the capacity and delays related to every element of the airfield. As the model is fast, flexible, and easy to use it is used for strategic decision making. MACAD consists of five different models: airside, weather, detailed schedule generation, coordination, and running the model. The methodology of the model is based on the LMI Capacity and Delays model, but the main difference is the single-runway model has been extended to two-runway configurations.

To calculate the delays at the runways MACAD uses an analytical queuing model, not a simulation. DELAYS, a queuing model that computes delays numerically, is used in MACAD. It is a slightly modified version compared to the original version of DELAYS, where the robustness is increased.

2.8.2. Mesoscopic Models

Mesoscopic models are classified between macroscopic and microscopic models. The main mesoscopic model known for airfield capacity is the runwaySimulator model. It was first developed under the name of Airport Capacity Analysis Through Simulation (ACATS) in 2005 by Barrer and Kuzminski [12]. Barrer improved this model in 2007 under the name of runwaySimulator [11]. The models were developed by the MITRE Corporation and are used for runway system capacity estimation. In 2011 MITRE began to improve the model regarding its capabilities and maintainability, which resulted in an improved runwaySimulator model [56]. The goal of the model is to provide the speed and simplicity of an analytical model without the limitations regarding complex runway sets. Furthermore, the model has to be efficient, flexible, and ready to be applied to any airport in the world while keeping the computational time low. The runwaySimulator model is ranked between an analytical and a simulation model. The accuracy regarding complex runway systems is much higher compared to analytical models, with the computation time being much faster than simulation-based models. The input parameters of the model consist of the runway configuration, traffic demand characteristics, and the ATC separation rules. A detailed air traffic schedule is not needed for the model, which decreases the complexity compared to microscopic models.

In a study performed by Kim and Hanssen [55] the FAA Airfield Capacity Model is compared with the runwaySimulator model. The study showed that both models predict a higher capacity compared to the empirical capacity. Especially the Visual Meteorological Conditions (VMC) capacities are overestimated. The runwaySimulator estimates are typically better than the FAA model, which was expected.

2.8.3. Microscopic Models

In microscopic models, the aircraft are simulated as individuals, and the model creates and records their interactions with each other and their environment. The most well known microscopic models, as shown in Table 2.7, are explained in this subsection, starting with STROBOSCOPE.

STROBOSCOPE is a capacity and delay estimation activity-based simulation system developed by Martinez, Trani, and Ioannou [70]. The model is different compared to classical runway capacity and delay simulation tools, which use objects moving through the model's network. STROBOSCOPE makes use of network nodes that represent activities or tasks performed by various resources.

The Airport and Airspace Simulation Model (SIMMOD), developed by the ATAC corporation can be used to simulate various amount of operations. Ranging from a full individual airfield to a regional volume of airspace. The main outputs of the model are aircraft travel times, flows and throughput capacity per unit of time, delays, and fuel consumption [79]. SIMMOD is based on a node-link model, with each link and node being able to accommodate one single aircraft at a time. The model solves for converging aircraft and the aircraft paths can be set up by the user or via a shortest path (Dijkstra) algorithm. The setup of the model is a time-consuming process, as the complete network structure of the airfield and/or airspace simulated has to be mostly done by hand. The average set-up time for a typical major airport is approximately 2 days. The main drawback of the model is that SIMMOD makes use of a 1-dimensional model, only checking for conflicts along the aircraft's longitudinal path.

The main competitor of the SIMMOD is TAAM (Total Airspace & Airport Modeller), developed by the Preston Group (TPG) in corporation with the Australian Civil Aviation Authority (CAA). It is a large scale detailed fast-time simulation package for modelling entire air traffic systems [17]. TAAM can be used both for planning and for analysis of ATM concepts and takes as input air traffic schedules, environment descriptions, aircraft flight plans, air traffic control, and output control rules. The main outputs of the model are delays, conflicts, airport capacity, noise, fuel burn, and costs. TAAM is a 4D flight path simulation tool and is therefore more realistic than SIMMOD, which is 1-D.

One of the new generation gate-to-gate fast-simulation tools is AirTop [5]. It is a modular software that allows users to assess and improve airport and airspace capacity by modelling various kinds of airport operations. There is no big difference in modelling the airfield itself, but the major advantage is the possibility of quickly integrating future or customer-specific ATC concepts. The interface of AirTOP is easy to use, leading to faster results and better cost efficiency.

The HEuristic Runway Movement Event Simulation (HERMES) tool is a fast-time simulation developed by the British Civil Aviation Authority/ National Air Traffic Services (CAA/NATS) [79]. The runway capacity can be estimated with both current and future demand, as well as for potential technological advancements. Additionally, it can be utilised to assess infrastructure modifications such as adjustments to runway length. The main emphasis is put on runway operations. With the input being traffic recordings and the output delays to all flights simulated. HERMES is only designed for Heathrow and Gatwick airport and cannot model runway crossings. The tool is suitable for cases where minor changes in demand have a significant impact on delays.

The Airport Machine is developed by Airport Simulation International (ASI) and is a tool for simulating in detail all aspects of airfield operations [79]. A similar node-link structure as SIMMOD is used and includes the complete operation from a few minutes before landing until a few minutes after takeoff. It has a good graphical interface and outputs the flows and delays at specific locations. The model is not easy to use and users have to follow extensive training. However, the user interface is remarkably better compared to that of SIMMOD.

Total AirportSim is a model developed by LeTech in corporation with IATA in 2001 [58]. The model originates from improvements made to the SIMMOD model by LeTech, slowly increasing towards a model capable of simulating a total airport. Total AirportSim consists of 3 modules; the airport/runway module, gate module, and terminal module. The airport/runway module is an improved alternative to FAA's SIMMOD. It supports SIMMOD data format with enhanced GUI using fast-time engines. Total AirportSim can simulate the relationship between airspace, runway, gate, and terminal and is a cost-effective solution for all planning designs. Finally, CAST is a scalable and modular aviation simulation tool and is developed by Airport Research Center (ARC) [4]. It comprises simulation-, allocation-, and optimisation systems for pedestrian, vehicle, and aircraft traffic as well as process models of landside, terminal, airside, and airspace. CAST is used by many airports around the world, such as Abu Dhabi Airport, Prague Airport, Düsseldorf Airport, Toronto Pearson, etc. CAST solutions offer numerous benefits that result in cost reduction for investments and operations, accelerated decision-making and planning processes, and support for smooth, safe, and punctual operations. With CAST, organisations can seamlessly integrate strategic and tactical planning, as well as operational and real-time optimisation, into their workflows.

3

Fuel Burn Modelling

The aviation industry relies on accurate fuel burn modelling to optimise efficiency, reduce costs, and mitigate environmental impacts. In the process of runway scheduling, the fuel burn is dependent on the routes flown by the aircraft. For example, when a noise-optimised track is flown this can lead to additional fuel usage. This fuel burn increase is not favoured by the airlines.

This chapter will explain the influence of fuel cost in aviation, fuel economics, and the cost structure of an airline in [section 3.1](#). [section 3.2](#) states the current state-of-the-practice fuel burn models and explains the methods used in those models to calculate the fuel burn. Finally, [section 3.3](#) discusses the influence of optimal control theory on fuel consumption during the approach phase.

3.1. Airline Fuel Economics

Fuel costs play an important role in the economic dynamics of the airline industry. With jet fuel being a primary expense for airlines, understanding the relationship between fuel economics, the airline cost structure, and the influence of fuel cost is crucial. This section dives into the different aspects of fuel economics, exploring how fuel costs influence an airline's overall cost structure and examining strategies employed by airlines to manage this significant expenditure.

3.1.1. Airline Cost Structure

Before diving into the actual fuel burn modelling itself, it is important to understand the impact of fuel price on aircraft cost and airline economics. The focus is on the airline operating costs, as the fuel price is part of this division. The Total Operating Cost (TOC) can be divided into the Indirect Operating Cost (IOC) and the Direct Operating Cost (DOC). The DOC is directly related to the aircraft type itself, while the IOC is more dependent on the strategy of the airline [62]. Flight crew allowance, aircraft fuel, and oil, aircraft maintenance, and ground handling are examples of DOC. The DOC can be subdivided into Fixed Direct Operating Cost (FDOC) and Variable Direct Operating Cost (VDOC). The fuel costs are part of the VDOC as well as maintenance and crew cost. A breakdown of the TOC can be seen in [Figure 3.1](#)

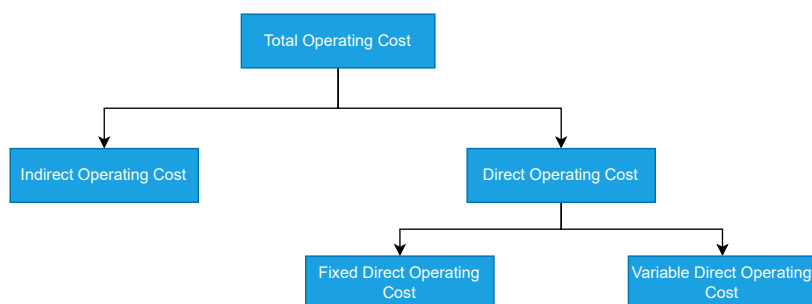


Figure 3.1: Total Operating Cost breakdown

3.1.2. Aviation Fuel Cost

The fuel cost for an airline is dependent on two factors. Namely, the actual fuel price and the fuel consumption. The key factors that affect the price of jet fuel are crude oil prices, refining and distribution costs, seasonal demand, taxes and regulations, and currency exchange rates. Fluctuations in global oil supply and demand, geopolitical events, and economic factors can all contribute to changes in crude oil prices.

The price of jet fuel has a significant influence on the total costs of an airline. The fuel cost form almost 18% of the total operating cost of an airline as seen in Figure 3.2. Together with the labor cost it forms half of the total airline costs. When the price of jet fuel increases, it directly affects the fuel costs of the airline. This can put pressure on profitability, especially if the airline is not able to transfer these increased costs to the passengers.

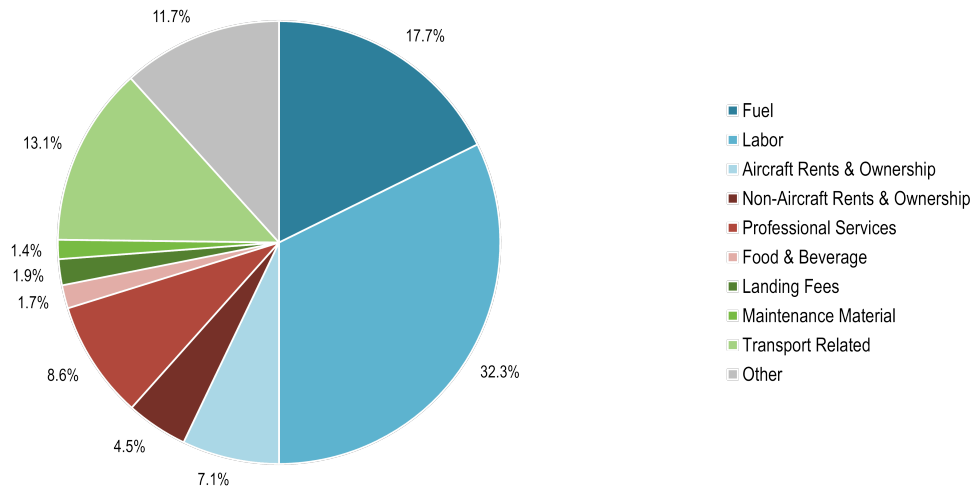


Figure 3.2: Passenger airlines operating costs United States 2019 [3]

Figure 3.3 shows that the fuel prices have been fluctuating substantially over the past 7 years. The red line indicates the jet fuel price and the blue line is the crude oil price. As can be seen from the figure these two are heavily correlated. The peak of both the crude oil price and the jet fuel price at the beginning of 2023, is due to sudden loss of supply from Russia as a result of Russia's invasion of Ukraine. The spread between the jet fuel price and the crude oil price is lifted by the strong post-Covid recovery in demand for air transportation[47].

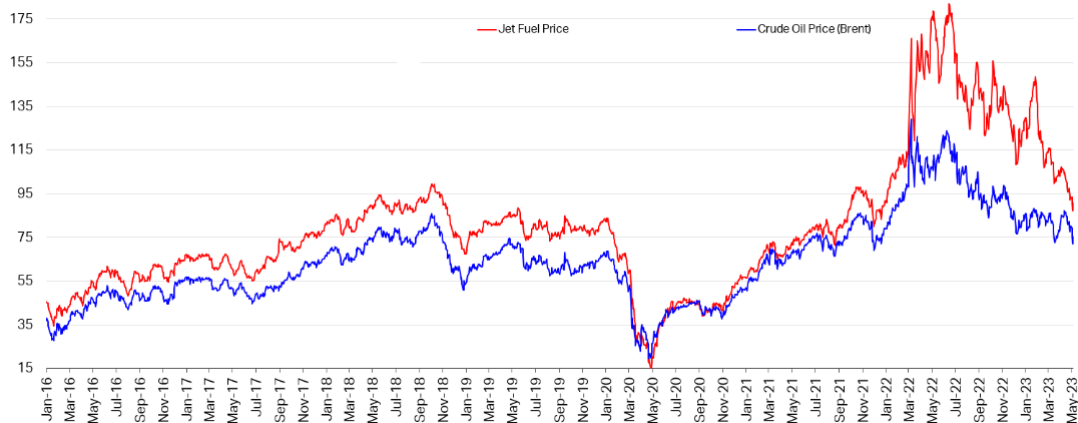


Figure 3.3: Jet fuel price developments, Jet Fuel & Crude Oil price (\$/barrel)[47]

To mitigate the impact of fuel price fluctuations, airlines participate in fuel hedging strategies. With fuel hedging airlines sign a financial contract to secure fuel at pre-determined prices for longer periods. If an airline has hedged a portion of its fuel consumption at a lower price, it can provide a measure of protection against sudden price spikes. On the other hand, when the fuel price decreases, the airline does not fully benefit from

the lower fuel prices due to its hedging contract.

Rising fuel prices will make airlines look for ways to reduce fuel consumption. This can include measures such as optimising flight routes, improving airline maintenance to ensure optimal fuel efficiency, and investing in newer and more fuel-efficient aircraft. By minimising the fuel consumption, airlines can mitigate the effect of high fuel prices on their total costs.

3.2. Existing Fuel Burn Models

As fuel has a big impact on the operating cost of the airline much research is done in the field of fuel burn and fuel consumption. Especially in times of rising fuel costs, improved algorithms have been developed for modelling fuel consumption. This section will discuss the existing fuel burn models and explain the theory behind the fuel consumption for each of the models.

3.2.1. Base of Aircraft Data

The base of Aircraft Data (BADA) is an Aircraft Performance Model (APM) developed and maintained by EUROCONTROL [78] and it consists of two models: the APM and the Airline Procedure Model (ARPM). Each aircraft model is described by coefficients that serve as input for the APM and ARPM.

Currently, two versions of BADA are being developed, BADA v.3 and BADA v.4. Both are based on the same modelling approach with the same structure and elements. In the early 90s, BADA 3 was created to provide realistic modelling of aircraft performance within a nominal flight envelope. With the introduction of BADA applications dependent on APM increased significantly with the need for more advanced features to support ATM modelling and simulation requirements. These requirements include increased accuracy, complete coverage of the operation envelope, better representation of different flight phases, and support of different types of operations. Studies have been performed to investigate whether BADA would be suitable to achieve the levels of accuracy that are needed and comply with the new requirements. The results show that BADA 3 cannot provide the needed level of accuracy over the entire flight envelope. This has been a driving force for the development of BADA 4, to provide accurate modelling of aircraft performance across the entire flight envelope.

The further development of BADA 3 was complicated due to the lack of high-quality reference data, and the requirement that the model should be kept simple due to limited computing capabilities. The BADA 4 model has been developed on the improved high-quality aircraft performance reference data and computing capabilities. Dimensionless variables are used in BADA 4, which prevents mistakes, and allows the discovery of physical similarity relationships.

The BADA model is based on the total energy model (TEM) of an aircraft, which equates the work done by forces acting on the aircraft to the rate of increase in potential and kinetic energy [19]. This leads to [Equation 3.1](#).

$$(T - D)V_{TAS} = mg \frac{dh}{dt} + mV_{TAS} \frac{dV_{TAS}}{dt} \quad (3.1)$$

Whereas both BADA models are based on the same TED of an aircraft, the fuel consumption modelling is different. The fuel consumption calculations are shown in more detail in the following subsections, starting with BADA 3.

Fuel Consumption BADA 3

For jets and engines the TSFC, C_T (kg/min*(kN)), is specified as a function of true airspeed, V_{TAS} (knots). The TSFC can be calculated via [Equation 3.2](#). C_{f1} and C_{f2} indicate aircraft-specific fuel consumption coefficients that are obtained by BADA.

$$C_T = \left(1 + \frac{V_{TAS}}{C_{f2}}\right) C_{f1} \quad (3.2)$$

The nominal fuel flow f_{nom} (kg/minute) can then be calculated via [Equation 3.3](#), with T being the aircraft's total net thrust from the engines (kN).

$$f_{nom} = C_T \cdot T \quad (3.3)$$

These expressions are used for all flight phases except during cruise and for descent/idle operations. For the runway capacity model, the cruise operations are not important, as only aircraft in departing and arriving

operations are considered. For idle thrust or descent operations the minimal fuel flow f_{min} is used. The minimal fuel flow is dependent on the altitude of the aircraft above sea level, h . The relationship is shown in Equation 3.4.

$$f_{min} = \left(1 - \frac{h}{C_{f_4}}\right) C_{f_3} \quad (3.4)$$

Fuel Consumption BADA 4

The BADA 4 model uses a different approach compared to BADA to calculate the fuel consumption. Each type of engine has a separate fuel consumption model, all part of the Propulsive Forces Model (PFM). The model includes the contribution from all engines and provides the fuel consumption as a function of air-speed, throttle parameter, and atmospheric conditions. The general formulation of the fuel consumption F [kg/s] is shown in Equation 3.5 [77].

$$F = \delta \cdot \theta^{\frac{1}{2}} \cdot W_{mref} \cdot a_0 \cdot L_{HV}^{-1} \cdot C_F \quad (3.5)$$

The fuel flow is calculated with the pressure ratio δ , temperature ratio θ , the reference mass, m_{ref} [kg] from the PFM, the weight force, W_{mref} [N], at m_{ref} , the speed of sound, a_0 [m/s], at MSL in standard atmosphere, the fuel lower heating value from the PFM L_{HV} [m^2/s^2] and the fuel coefficient C_F , which is dependent on the type of engine. The fuel coefficient C_F is determined by Equation 3.6.

$$C_F = \begin{cases} C_{F, idle} & \text{when idle rating is used} \\ \max(C_{F, gen}, C_{F, idle}) & \text{when a non-idle rating or no rating is used} \end{cases} \quad (3.6)$$

The idle fuel coefficient for the turbofan engine is calculated via Equation 3.7 as a function of Mach number and the atmospheric conditions.

$$C_{F, idle} = \left(\begin{array}{l} \hat{f}_1 + \hat{f}_2 \delta + \hat{f}_3 \delta^2 \\ + (\hat{f}_4 + \hat{f}_5 \delta + \hat{f}_6 \delta^2) \cdot M \\ + (\hat{f}_7 + \hat{f}_8 \delta + \hat{f}_9 \delta^2) \cdot M^2 \end{array} \right) \cdot \delta^{-1} \theta^{-\frac{1}{2}} \quad (3.7)$$

The general fuel coefficient $C_{F, gen}$ is calculated as a fourth-order polynomial of M with coefficients that are fourth-order polynomials of C_T as shown in Equation 3.8.

$$\begin{aligned} C_{F, gen} = & f_1 + f_2 C_T + f_3 C_T^2 + f_4 C_T^3 + f_5 C_T^4 \\ & + (f_6 + f_7 C_T + f_8 C_T^2 + f_9 C_T^3 + f_{10} C_T^4) \cdot M \\ & + (f_{11} + f_{12} C_T + f_{13} C_T^2 + f_{14} C_T^3 + f_{15} C_T^4) \cdot M^2 \\ & + (f_{16} + f_{17} C_T + f_{18} C_T^2 + f_{19} C_T^3 + f_{20} C_T^4) \cdot M^3 \\ & + (f_{21} + f_{22} C_T + f_{23} C_T^2 + f_{24} C_T^3 + f_{25} C_T^4) \cdot M^4 \end{aligned} \quad (3.8)$$

Where C_T is the thrust coefficient and M is the Mach number.

It should be noted that the equation takes up to 25 non-idle rating fuel coefficients, f_i , to calculate $C_{F, gen}$, but the number of coefficients is not fixed and depends on the quantity and quality of available data. This results in simpler expressions most of the time where some of the f_i coefficients are equal to zero.

3.2.2. Aviation Environmental Design Tool

The Federal Aviation Administration (FAA) has developed the Aviation Environmental Design Tool (AEDT). This tool is a software system designed to model aircraft performance in both space and time, providing estimates for fuel consumption, emissions, noise, and the resulting air quality impact.

AEDT employs two different methods to calculate the fuel consumption for fixed-wing aircraft on various flight path segments[59]. The first method, available in both terminal and en-route areas, utilises Section 3.9 of the BADA 3 user manual[19] and is discussed in Equation 3.2.1. It is used to determine the fuel consumption for each flight segment. The second method, exclusive to the terminal area, employs the Senzig-Fleming-Iovinelli (SFI) method as described in subsection 3.2.4 to calculate the fuel consumption for each segment. Beyond the terminal area, AEDT relies on the BADA 3 method. In cases where fixed-wing aircraft lack thrust data in their performance calculations, AEDT utilises the Boeing Fuel Flow Method 2 (BFFM2)

subsection 3.2.3 to determine the fuel flow. While the majority of aircraft using the BFFM2 method are military, some civil aircraft that do not include the thrust data in their profile definitions also utilise this method. The BADA 4 analysis of the profiles use the BADA 4 fuel model to calculate the fuel flow through the engines. When BADA 4 thrust data is available, the BADA 4 fuel data is also used by the AEDT. However, when this data is not available, AEDT switches automatically to, sequentially, either the SFI, BADA 3, or BFFM2 fuel consumption methods. This depends on the first available source of data.

It is important to note that all these methods specify the fuel flow rate. In the case of the SFI and BFFM2 methods, AEDT calculates the fuel consumption in a segment by multiplying the fuel flow rate per engine by the duration of the segment and the number of engines on the aircraft. For the BADA 3 method, AEDT calculates the fuel consumption in a segment by multiplying the fuel flow rate for all engines by the segment duration.

3.2.3. Boeing Fuel Flow Method 2

The Fuel Flow Method 2 is developed by DuBois and Paynter from The Boeing Company [25]. The reason behind the method was to come up with a method to model fuel flow in a less rigorous way than the P3T3 method. This is a model for calculating aircraft engine emissions of NO_x, HC, and CO. The method relies on proprietary data from aircraft and engine manufacturers. To provide a transparent method for calculating the aircraft engine emissions several nonproprietary fuel flow-based methods have been developed. The "Fuel Flow Method 2" is one of them and can be used for emissions certification, and fuel flow methods and can give approximations on emissions on the order of around 10 to 15 % for NO_x compared to the P3T3 method. The BFFM2 method to calculate the fuel flow is shown in Equation 3.9. The equation calculates the fuel flow at non-reference conditions, W_f (kg/s), and is dependent on the Modal-specific adjustment factors, B_m , fuel flow at reference conditions, RW_f [kg/s], Mach number, M , Static Temperature ratio, δ , and the Static Pressure ratio θ .

$$W_f = \frac{B_m RW_f \delta}{\theta^{3.8} e^{0.2M^2}} \quad (3.9)$$

The fuel flow at reference conditions used in the BFFM2 is the fuel flow data retrieved from the ICAO Aircraft Engine Emissions Databank.

3.2.4. Senzig-Fleming-Iovinelli (SFI) Model

The BADA fuel consumption model uses an energy-balance thrust model with the Thrust Specific Fuel Consumption (TSFC) as a function of airspeed. Research shows that the BADA performs well in cruise conditions, with differences of 3% compared to reported fuel burn data [61]. However, it is observed that BADA has shortcomings in the Terminal Manoeuvring Area (TMA) concerning airline fuel consumption.

A new method to model the fuel consumption in the TMA has been proposed by Senzig and Flemming [96]. The objective was to make it more accurate, take into account the proprietary interest of manufacturers, be suitable for existing and planned environmental models, and have a proposed target accuracy of 5% to make it interesting enough for decision-makers. The major consideration for the new TSFC algorithm for the TMA area is the type of thrust model used.

All major engine manufacturers use a function of Mach, thrust, and altitude to present the TSFC of their engines. For the departure TSFC algorithm a linear relationship between those parameters is used, extended with a dependence on the square root of the temperature ratio θ from Hill and Petersen[42]. This results in a departure TSFC given in Equation 3.10.

$$\text{TSFC}/\sqrt{\theta} = K_1 + K_2 M + K_3 h_{\text{MSL}} + K_4 F/\delta \quad (3.10)$$

The arrival TSFC algorithm is also based on Hill and Petersen [42], with the implementation of modifications proposed by Yoder [108]. Equation 3.11 shows the arrival TSFC algorithm for fuel consumption in the TMA.

$$\text{TSFC}/\sqrt{\theta} = \alpha + \beta_1 M + \beta_2 e^{-\beta_3 (F/8/F_0)} \quad (3.11)$$

The determination of fuel consumption coefficients for a specific airframe/engine combination involves the generation of airplane performance data for the TMA area. This data is collected and organised into a unified structure, which is then subjected to statistical analysis.

The results are implemented in the aviation environmental impact model of the FAA, the AEDT.

3.3. Optimal Control and Fuel Consumption

Besides modelling the fuel consumption itself with aircraft performance models another factor that can influence the fuel consumption during flight is the trajectory of the aircraft. Research has been performed on the Aircraft Trajectory Optimization Problem (ATOP), which aims to determine the optimal trajectory for an aircraft within a given set of dynamic constraints [95]. These constraints define the feasible motion of the aircraft. The ATOP system takes into account the initial and expected final state of the aircraft, which includes its position, altitude, speed, and climb angle in a specific TMA.

The objective of the ATOP system is to find the best aircraft trajectory based on a specific performance indicator, which is typically chosen to minimise travel time, fuel consumption, or noise emissions. To achieve this the ATOP is formulated as an optimal control problem. By solving this problem, the reference trajectory for each aircraft flying through a specific part of the TMA can be obtained, ensuring efficient flight operations while maintaining safety standards.

This section will describe the mathematical formulation of the optimal control problem, the possibilities for solving the ATOP, and discuss ways to incorporate the ATOP in the RSP.

3.3.1. Aircraft Trajectory Optimisation Problem

The ATOP is a simplified optimal control problem that models the dynamics of an aircraft as a two-dimensional point mass. It involves the state variables z, h, V , and γ , which represent the aircraft's position, altitude, speed, and climb angle.

The control variables in the ATOP are α and T , which represent the angle of attack and the thrust of the aircraft. An example of the mathematical formulation of the ATOP with the variables as described above is described in Equation 3.12 and is obtained from Samà et al. [95]. The parameter ω is responsible for the optimisation of either the minimum travel time ($\omega = 1$), the minimum fuel consumption ($\omega = 0$), or a combination of the two when ω has a value between 0 and 1. The constraints are responsible for establishing the initial and final states of the problem and setting boundaries for the state variables.

$$\begin{aligned}
 \min \quad & \omega \cdot \tau_i + (1 - \omega) \cdot \left[\int_0^{\tau_i} T(t) / T_{\max} dt \right] \\
 \text{s.t.} \quad & \\
 \dot{z}(t) = & V(t) \cos \gamma(t) & \text{for a.e. } t \in (0, \tau_i) \\
 \dot{h}(t) = & V(t) \sin \gamma(t) & \text{for a.e. } t \in (0, \tau_i) \\
 \dot{V}(t) = & \frac{T(t) - D(t)}{m} - g \cdot \sin \gamma(t) & \text{for a.e. } t \in (0, \tau_i) \\
 \dot{\gamma}(t) = & \frac{L(t) - m \cdot g \cdot \cos \gamma(t)}{m \cdot V(t)} & \text{for a.e. } t \in (0, \tau_i) \\
 0 \leq T(t) \leq & T_{\max} & \text{for a.e. } t \in (0, \tau_i) \\
 0 \leq \alpha(t) \leq & \alpha_{\max} & \text{for a.e. } t \in (0, \tau_i) \\
 V_{\min} \leq V(t) \leq & V_{\max} & \forall t \in (0, \tau_i) \\
 LOAD_{\min} \leq \frac{L(t)}{m \cdot g} \leq & LOAD_{\max} & \forall t \in (0, \tau_i) \\
 V(t) \cdot \sin \gamma(t) \leq & 0 & \forall t \in (0, \tau_i) \\
 (z, h, V, \gamma)(0) = & (z_0, h_0, V_0, \gamma_0) \\
 (z, h, V, \gamma)(\tau_i) = & (z_i, h_i, V_i, \gamma_i) \\
 \tau_i \in & [0, +\infty) \\
 (z, h, V, \gamma) \in & W^{1,\infty}([0, \tau_i], \mathbb{R}^4) \\
 (T, \alpha) \in & L^\infty([0, \tau_i], \mathbb{R}^2).
 \end{aligned} \tag{3.12}$$

3.3.2. Solving the ATOP

To solve the ATOP the most used technique in optimal control theory is the discretize-then-optimize technique. It approximates the original infinite-dimension problem with a suitable finite-dimensional one. The approximation is solved and the final solution is interpreted as an approximation of the solution of the original problem. Several tools exist to solve the ATOP, the software used by Samà et al [95] from the previous section is OCPID-DAE1, which is produced at the Munich University of the Federal Armed Forces. Furthermore, there are packages for MATLAB and Python to solve optimal control problems. For MATLAB Gauss Pseudospectral Optimization Software (GPOPS) is a suitable tool for solving non-sequential multiple-phase optimal control problems. The most used package for Python is Gekko, which is an optimisation framework capable of handling differential-algebraic equations. For this research Python will be used for all the coding, so if the optimal control problem will be incorporated Gekko is going to be used as the software.

3.3.3. Implementation of the ATOP in The Runway Scheduling Model

It is important to consider how the ATOP can be implemented in the runway scheduling model as both problems are heavily dependent on each other. However, in literature, the two problems are usually studied and solved separately. Still, some literature was found on the combination of the ATOP and the RSP.

One of the first combinations of the ASP and ATOP was developed by Hansen[39], he used genetic algorithms for the routing and sequencing of arriving aircraft in a multiple runway system. The major limitation of the model was that the approach routing was modelled as a choice of approach routes. The algorithm would choose the best fit instead of optimising the approach trajectory.

A hybrid optimisation algorithm has been developed by Toratani et al. [104]. The objective was to minimise fuel consumption during the approach trajectory while simultaneously optimising the TMA entry point and place in the landing queue.

Finally, Sama et al. [95] develop a framework for the lexicographic optimisation of both based on the order of importance of the performance indicators. The primary indicator establishes the initial issue to be optimised. Subsequently, the problem solutions are examined to address certain constraints in optimising the secondary problem, which is related to the less important performance indicator. The results of this approach can be seen in Figure 3.4

First Problem	Second Problem	Maximum Delay	Travel Time	Fuel Consumption
TCA-ASP	ATOP-tt	59	10582	2174
TCA-ASP	ATOP-fc	59	11962	1288
ATOP-tt	TCA-ASP	262	10177	2433
ATOP-fc	TCA-ASP	501	13637	276

Figure 3.4: Results of the lexicographic approach[95]

4

Noise Modelling

Aircraft noise generated during takeoff and landing operations has a significant impact on nearby communities surrounding airports. In this chapter, the subject of noise modelling is treated. Starting with the different noise sources generated by an aircraft, including airframe noise and engine noise, are discussed in [section 4.1](#). The calculations needed to measure aircraft noise and the different metrics used to define the perception of noise are explained in [section 4.2](#). [section 4.3](#) touches upon the measurement of noise annoyance and the mitigation strategies used to reduce the noise annoyance. Finally, [section 4.4](#) mentions and explains the most used noise modelling tools.

4.1. Sources of Aircraft Noise

Aircraft noise arises from various sources within an aircraft. Two primary contributors to this noise are the airframe and the engines[97]. Understanding the noise generated by these components is essential for developing effective noise reduction strategies. This section explains in more detail what causes the airframe and engine noise and the improvements made to reduce the noise generated. Starting with airframe noise.

4.1.1. Airframe Noise

With the increasing bypass ratios of aircraft engines since the 1970s, airframe components have emerged as a significant source of aircraft noise[15]. During the approach, airframe noise has the potential to surpass other sources and become the dominant contributor to the overall noise experienced on the ground. On commercial aircraft, the main sources of aircraft noise are the wing systems including the High Lift Devices (HLD), the airbrakes, the landing gear, and all the imperfections on the airframe [73].

4.1.2. Engine Noise

The combustion engines have consistently been one of the primary sources of noise on aircraft, regardless of the flight situation. For conventional combustion engines, the overall engine noise is mainly determined by the noise generated by the fan and the jet. While these two sources have dominated noise generation for decades, recent advancements in engine design, such as increased engine bypass ratios and improved fan design, have started to decrease their presence and contribute to noise reduction. Although the main objective of the modifications has been to improve the engine performance, they have also led to a decrease in noise generation from the fan and the jet[15].

The introduction of higher bypass ratios in engines has resulted in reduced jet exhaust velocities, leading to a significant decrease in jet noise. Furthermore, advancements in fan blade design and the arrangement of rotor-stator components have also led to noise reduction. Another innovation that has reduced fan noise emission is the implementation of specially designed acoustical lining concepts. As the jet and fan noise is so dominant, other noise sources of the engine are still less relevant in the context of overall engine noise. However, if the jet and fan noise is further reduced through advanced design or specific operating conditions like flight idle, the engine core can have a noticeable impact on the overall engine noise.

[Figure 4.1](#) gives an overview of the main aircraft noise sources for both the airframe and the engine. Where the airframe noise sources are in black and the engine noise sources are in red.

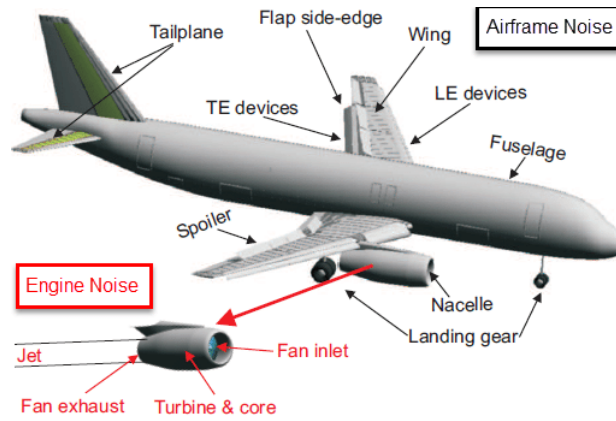


Figure 4.1: Overview of main aircraft noise sources[32]

4.2. Aircraft Noise Calculation

Aircraft noise relies on a level of "annoyance". To model aircraft noise it is of great importance to explain what annoyance means and how subjective perceptions can be quantified to provide meaningful engineering metrics. Unlike physical measures such as acoustic pressure (Sound Pressure Level), which can be directly measured, annoyance is a subjective experience that can only be interpreted. Aircraft noise presents unique challenges in measurement due to its complex nature, which requires numerical operations, tone corrections, weighting, and integration for accurate assessment[33].

A human perceives noise not only based on the Sound Pressure Level (SPL), as shown in Equation 4.1, but also on frequency, duration, regularity, and time of the day[97]. This section will explain those factors and the calculations behind them based on the noise reader of Simons [97].

$$SPL = 10 \log \left(\frac{p_e^2(t)}{p_{e0}^2(t)} \right) \quad (4.1)$$

4.2.1. Weighted Sound Pressure Level

Noise can have different frequencies, which influences the observed loudness. The SPL does not include this loudness. To determine the loudness of a signal, the sound pressure levels in various frequency bands are determined. After that, the SPL values are weighted according to one of the weighting functions. The most used weighting function is called A-weighting and is based on the equal loudness contour at 40 phon. To calculate the A-weighting function ΔL_A Equation 4.2 is used.

$$\Delta L_A = -145.528 + 98.262 \log f - 19.509 (\log f)^2 + 0.975 (\log f)^3 \quad (4.2)$$

By using Equation 4.2 the overall A-weighting sound pressure level L_A can be determined with a summation over the frequency bands, i , as shown in Equation 4.3

$$L_A = 10 \log \sum_i 10^{\frac{SPL(i) + \Delta L_A(i)}{10}} \quad (4.3)$$

4.2.2. Sound Exposure Level

The calculations shown so far are only for stationary noise signals. However, as aircraft noise is non-stationary, the duration of the noise has to be incorporated. As the human ear is not only sensitive to the maximum noise level but also to the duration of the noise event it is not possible to simply take the maximum value of L_A . To measure the annoyance during a noise event Sound Exposure Level (SEL) is used. SEL refers to a constant level of one-second duration T_0 that encompasses the same amount of energy as the fluctuating level throughout the entire occurrence and can be calculated via Equation 4.4.

$$SEL = 10 \log \left[\frac{1}{T_0} \int_0^T 10^{\frac{L_A(t)}{10}} dt \right] \quad (4.4)$$

4.2.3. Day-Evening-Night Average Level

To capture the effect of noise in airport communities due to air traffic activities the day-evening-night level (DENL) is used. This evaluates the noise at different times of the day and puts different penalties on noise events in the evening or night. Equation 4.5 shows how the L_{DEN} is calculated, where the time span is indicated with T_{ref} . This variable is often equal to 24 hours or a year. The w_i term represents the penalty associated with a noise event in the evening or at night. The definitions of the time and the corresponding penalty can be seen in Table 4.1. All the noise events, F , that take place in the specified time are accumulated and the L_{DEN} is calculated in dBA.

$$L_{DEN} = 10 \log \left[\frac{1}{T_{ref}} \sum_{i=1}^F 10^{\frac{SEL_i + w_i}{10}} \right] \quad (4.5)$$

Table 4.1: Day-evening-night average level penalties[21]

	Day	Evening	Night
Time [hrs]	07.00-19.00	19.00-22.00	22.00-07.00
Penalty [dB(A)]	0	5	10

As the metric used to calculate L_{DEN} is based on a logarithmic scale, it is not directly usable for linear optimisation. It is still unsure which exact solving method is going to be used in the final model. However, to keep all the options open, the method to convert the estimated noise data towards a linear function will be explained. The first step is to convert the SEL into the Acoustic Energy Level (AEL) via Equation 4.6. Here E_0 is the reference sound exposure.

$$AEL = \frac{E_i}{E_0} = 10^{\frac{SEL_i}{10}} \quad (4.6)$$

By combing Equation 4.5 and Equation 4.6 a new function for L_{DEN} is retrieved as shown in Equation 4.7. This equation can be used in a linear optimisation model, eventually.

$$L_{DEN} = 10 \log \left[\sum_{i=1}^F w_i \frac{E_i}{E_0} \right] - 10 \log \left[\frac{T_{ref}}{T_0} \right] \quad (4.7)$$

4.3. Noise Annoyance and Mitigation

Aircraft noise has emerged as a prominent source of noise annoyance in many communities. The increasing volume of air traffic and the expansion of airports have led to concerns regarding the impact of aircraft noise on the quality of life. This chapter will discuss the measurement of annoyance and how this influences communities. Furthermore, the mitigation strategy developed by the ICAO to reduce aircraft noise, the Balanced Approach, is explained.

4.3.1. Measurement of Annoyance

The L_{DEN} has a good correlation with community annoyance. This is illustrated in Figure 4.2, which shows the percentage of highly annoyed people as a function of L_{DEN} . The figure is constructed with surveys among communities and it can be seen that around 30% of the population is highly annoyed by a noise level of 55 dBA. However, it is important to note that considerable variations can exist among different airports. Furthermore, noise annoyance is not only dependent on the noise acoustics itself but also on demographic, social, and personal factors.

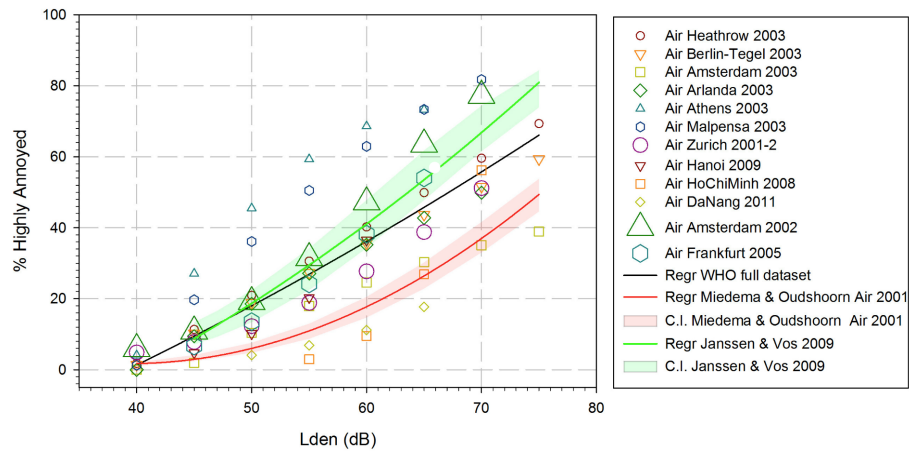


Figure 4.2: Percentage of highly annoyed people versus L_{DEN} for various airports[37]

In a research performed by Miedema and Oudshoorn [71] the relationship between the percentage of highly annoyed (HA) people and the DENL exposure metrics was investigated. They performed research on noise caused by road traffic, railway traffic, and aircraft. The relationship for aircraft is shown in Equation 4.8 and indicates the percentage of people that get highly annoyed by the noise caused by aircraft. The level of annoyance is determined by a combination of emotional as well as physical factors that contribute to the perception of noise.

$$\%HA = -9.199 \cdot 10^{-5} (L_{DEN} - 42)^3 + 3.932 \cdot 10^{-2} (L_{DEN} - 42)^2 + 0.2939(L_{DEN} - 42) \quad (4.8)$$

4.3.2. Balanced Approach

As explained in the previous section aircraft noise is the most significant cause of adverse community reactions. This trend is projected to persist across most regions worldwide in the foreseeable future. Therefore, the ICAO developed the Balanced Approach to Aircraft Noise Management and this policy was adopted in 2001[50]. In this section, a comprehensive overview of the Balanced Approach will be given and the four key elements will be explained. The full explanation can be found in Guidance on the Balanced Approach to Aircraft Noise Management [81].

The Balanced Approach involves a systematic process for addressing noise concerns at specific airports. It consists of a comprehensive analysis of available measures aimed at reducing noise. These measures can be divided into four key elements, as illustrated in Figure 4.3. The primary objective is to tackle noise issues at each airport individually and determine the most cost-effective and environmentally beneficial measures. The four principal elements are explained in more detail in the upcoming sub-subsections.

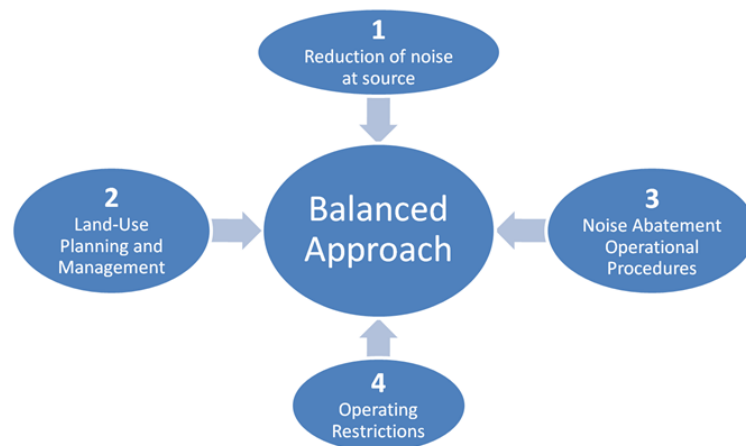


Figure 4.3: The four principal elements of the Balanced Approach to Aircraft Noise Management[50]

Reduction of Noise at Source

The first element of the Balanced Approach is the reduction of noise at the source. Since the 1970s, aircraft noise has been regulated through the establishment of noise limits for aircraft. These limits are defined in the form of Standards and Recommended Practices (SARPs) and are still in use today.

The noise regulations on aircraft are outlined in Annex 16, Volume 1 to the Convention on International Civil Aviation (the "Chicago Convention") [80]. The primary objective of noise certification is to guarantee the incorporation of the latest available noise reduction technology into aircraft design. This certification process includes procedures that are relevant to daily operations, with the ultimate goal being to ensure that the noise reduction offered by the technology is translated into reduced noise levels around airports.

The SARPs define three reference measurement points for noise certification: approach reference points, sideline references, and flyover reference points. The Standards also determine noise limits as a function of MTOW to incorporate the effect that heavier aircraft, produce more noise than lighter aircraft. This set the standard for the Chapter 2 Noise Standard. After the introduction of Chapter 2, aircraft became quieter due to the introduction of high bypass ratio jet engines. This resulted in a new, more strict noise standard introduced by the ICAO in 1977, called Chapter 3 Noise Standard. Even more noise reduction technologies were incorporated in the following years and this improved aircraft noise performance towards a higher level, resulting in the introduction of the Chapter 4 Noise Standard in 2001.

In 2014, a new increase in stringency of 7 Effective Perceived Noise (EPNdB) was adopted by the ICAO. The Chapter 14 Noise Standard for jet and propeller-driven aircraft. An overview of all the chapters and the relationship between EPNdB and MTOW is illustrated in Figure 4.4. The Chapter 14 Noise Standard will be the ICAO standard for the coming years and is applicable for aircraft types submitted on or after 31 December 2017.

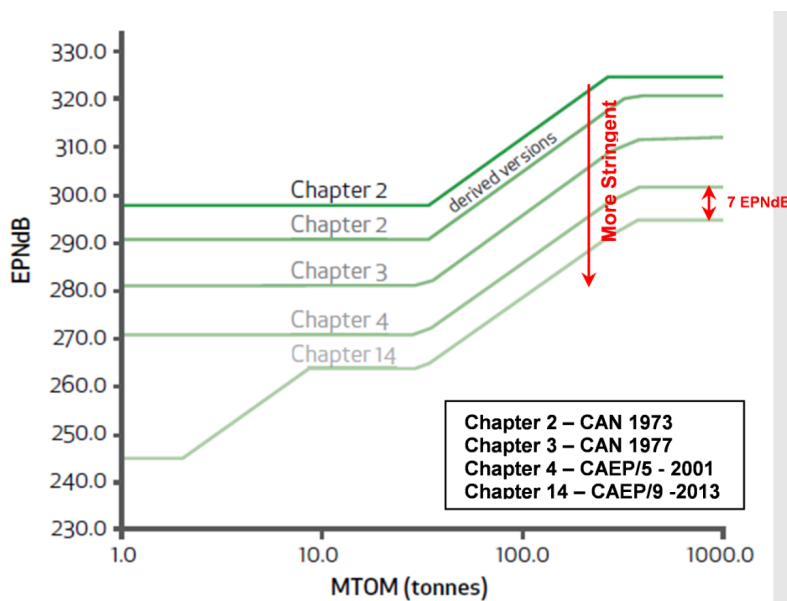


Figure 4.4: The ICAO Noise Standards for aeroplanes [51]

It is expected that, due to the implementation of the new Chapter 14 Noise Standard, over one million individuals that are affected by DENL of 55 dB could be removed between 2020 and 2036. This results in a significant reduction in the number of people affected by significant aircraft noise.

Land-use Planning and Management

Land-use planning and management are crucial for ensuring the compatibility of activities around airports. The primary objective is to minimise the impact of aircraft noise on nearby residents by implementing specific land-use zoning and compatible land usage within airport areas[110].

The ICAO is continuously developing a policy on land use planning and management, outlined in the Assembly Resolution A40-17, Appendix F. Its goal is to minimise the aircraft noise impact through various measures. These measures include locating new airports away from noise-sensitive areas, considering protective measures for existing and planned land use from the earliest stages of airport development, defining protection

zones around airports with varying noise limits based on the population size and air traffic forecasts, enacting legislation and providing guidance to ensure compliance with land use criteria, and informing communities near airports about aircraft operations and their environmental effects.

The ICAO guidance on this subject is contained in the ICAO Doc 9184 manual[49].

Another noise management tool is the introduction of noise charges. Although efforts are being made in reducing aircraft noise at the source, airports still require noise mitigation or prevention measures. Those noise related should be designed to recover only the costs associated with alleviating or preventing noise, and should not discriminate among users for the operation of certain aircraft.

Noise Abatement Operational Procedures

Airport operations also present impacts in terms of the noise that reaches the ground. ICAO plays a role in supporting the development standardisation of safe and cost-effective low-noise operations procedures for aircraft. These procedures contain various options such as noise preferential runways and routes, as well as noise abatement procedures during take-off and landing.

Departure Procedures

The ICAO PANS-OPS, Volume 1, contains general guidance on the development of two Noise Abatement Departure Procedures (NADPs). These procedures consist of two main types: NADP1, which focuses on minimising noise close to the airport, and NADP2, which aims to reduce noise further along the departure path. Both procedures end at an altitude of 1000 meters, but it is important to consider the potential noise reduction benefits or deterioration above this altitude in specific areas[110]. The differences between NADP 1 and 2 are the thrust or power reduction altitudes and the high-lift device retraction-acceleration segments.

Today, the operational opportunities for reducing the departure noise also include Continuous Climb Operations (CCO), Noise Preferential Routes (NPR), Noise Preferred Runway operations, alternation and respite, and usage of Performance Based Navigation (PBN).

Arrival Procedures

Continuous Descent Arrival (CDA) is a concept that has been developed to reduce or minimise constant altitude segments during aircraft approach flights and focus on flying along descent segments. By employing this concept, aircraft can descend with reduced thrust, at or near idle thrust, resulting in lower noise levels compared to level flight segments. Furthermore, CDAs consider environmental factors such as emissions and fuel burn, while ensuring safe and efficient ATM.

To address community noise concerns and optimise operational efficiency, airports may designate a specific landing runway for noise abatement purposes. Safety remains the top priority when considering such measures, but community noise considerations can be taken into account.

The deployment of PBN procedures has become more common at airports. It has the benefits of enhanced airport capacity, emissions reduction, and reduced noise exposure. However, it is important to note that PBN may lead to more predictable and precise flight paths, resulting in a concentration of air traffic along designated routes. Therefore, it is crucial to consider the impact on the surrounding population and take appropriate measures to mitigate potential noise effects.

Operating Restrictions

The Balanced Approach guidance recommends avoiding applying operating restrictions as a first measure to reduce noise. However, if the combined effectiveness of the first three elements is insufficient to reduce noise levels, operating restrictions may be considered.

In response to noise concerns, some countries have considered banning certain noisy aircraft from operating at airports sensitive to noise. From 1980, the focus was on Non-Noise Certificated (NNC) aircraft to Chapter 2 aircraft in the 1990s, and currently to the noisiest Chapter 3 aircraft. However, implementing such operating restrictions can have significant economic implications for both domestic and international airlines operating at affected airports.

Currently, many ICAO member states have already phased out NNC and Chapter 2 aircraft. Regarding Chapter 3 aircraft, the ICAO urged states to refrain from imposing operating restrictions on such aircraft at airports without thoroughly assessing available measures to address the specific noise issue in line with the balanced approach.

Apart from phasing out aircraft, other potential operating restrictions can be employed, including curfews,

nighttime limitations, noise quotas/budgets, cap rules, non-addition rules, and restrictions related to the nature of the flight.

4.3.3. Noise Regulations at Schiphol Airport

As Amsterdam Airport Schiphol (AAS) will be used as input for the model it is interesting to have an overview of the noise regulations present at the the airport.

The Dutch Aviation Act has formed the legal framework for Schiphol Airport since 2003. The Dutch Aviation Act is stated that the airport decree contains rules and limits that limit the environmental impact around the airport. This protection is provided by "criteria of equality", which limit the number of houses, highly annoyed people, and severely sleep-disturbed people within L_{den} and L_{night} contours. Table 4.2 shows the criteria of equality corrected for the use of the European Doc29-model.

Table 4.2: Criteria of equality[107]

Criteria of equality	Limit value
Number of houses within the 58 dB(A) L_{den} contour	13,600
Number of highly annoyed people within the 48 dB(A) L_{den} contour	166,500
Number of houses within the 48 dB(A) L_{night} contour	14,600
Number of severely sleep disturbed people within the 40 dB(A) L_{night} contour	45,000

Due to the conversion from the NRM to the Doc29 method, a new function with respect to the number dose-response relationship was needed. Based on research performed by the NLR[41] a new relationship has been established for the number of highly annoyed people as seen in Equation 4.9.

$$EGH = 1 - \frac{1}{[1 + e^{(-7.7130 + 0.1260 * L_{den})}]} \quad (4.9)$$

The same has been done for the number of severely sleep-disturbed people, which resulted in Equation 4.10.

$$ESV = 1 - \frac{1}{[1 + e^{(-6.2952 + 0.0960 * L_{night})}]} \quad (4.10)$$

4.4. Noise Modelling Tools

Aircraft noise modelling in airport environments serves various purposes, including estimating cumulative noise exposure and identifying the affected population in specific areas. These models play a crucial role in establishing dose-response relationships. The ICAO offers guidance on the use of these models and provides methods for assessing the acoustic characteristics of different sources related to aircraft noise events[109]. This section will give an overview of the major noise modelling tools and they will be explained in more detail.

4.4.1. Integrated Noise Model

The Integrated Noise Model (INM) is a computer model designed by the FAA to assess the effects of aircraft noise near airports[30]. It was based on the algorithm and framework from the SAE AIR 1845 standard to estimate noise levels, taking into account factors such as operation mode, thrust setting, source-receiver geometry, acoustic directivity, and environmental conditions. By using Noise-Power-Distance (NPD) data, the INM provided estimates of noise contours for specific areas or noise levels at predetermined locations. The model output for noise could be exposure-based, maximum-level-based, or time-based.

The INM had many analytical uses, such as:

- Assessing current aircraft noise impacts: The model could evaluate the existing noise effect in the vicinity of an airport or heliport, providing a quantitative understanding of the noise levels experienced by the surrounding community
- Analysing changes in noise impact due to runway modifications: By inputting new information related to new or extended runways or runway configurations the INM could estimate and compare the resulting noise impacts.

- Evaluating changes in noise impact resulting from traffic demand and fleet mix: This analysis was useful in forecasting and managing future noise levels
- Assessing noise impacts of new operational procedures: The information provided by INM regarding altered flight paths, modified approach/departure procedures or changes in airspace management was valuable in designing noise abatement strategies.

The INM has been replaced by the AEDT as of May 2015. The AEDT will be discussed in the following subsection.

4.4.2. AEDT

As stated above the AEDT is the replacement of the INM and are both developed by the FAA. The AEDT is a new software tool that integrates established noise and emissions models. Its purpose is to analyse the impact of noise and emissions on one another.

The AEDT tool set combines and replaces five legacy noise and emissions models. The models, namely the Emissions and Dispersion Modeling System (EDMS), Integrated Noise Model (INM), Noise Integrated Routing System (NIRS), System for Assessing Aviation's Global Emissions (SAGE), and Model for Assessing Global Exposure to the Noise of Transport Aircraft (MAGENTA), have been integrated into the AEDT to facilitate a more streamlined and efficient assessment of inter-dependencies.

The AEDT offers accurate predictions of noise impact at specific points of interest or within defined noise contours. Furthermore, the output of the AEDT has a broad range of noise metrics. Such as, SEL, DENL, L_{Aeq} , and L_{Amax} [76]

4.4.3. Dutch Aircraft Noise Model (NRM)

Another model developed for predicting aircraft noise in The Netherlands, and particularly at Schiphol Airport is called "Nederlands Rekenmodel (NRM)" and it comprises the following steps[98]:

1. A system of aircraft classes is established that represents groups of aircraft types with similar weight and noise characteristics. The classification is based on the MTOW of the aircraft, which is divided into nine weight categories. Each weight category is further associated with four noise classes, determined by aircraft noise certification data. This results in a total of 36 aircraft classes, with each class represented by a single aircraft.
2. Flight profiles for different aircraft are established based on the specific procedure and flight distance. A flight profile table outlines the altitude, flight speed, and corresponding thrust settings for various segments of the flight distance. These profiles are designed for optimal conditions. However, the actual flight profile may deviate due to factors such as pilot input and specific aircraft configurations. There are nine procedures for take-off and three procedures for landing. For each of these procedures, extra class numbers include information about the distance to the destination or additional information about the landing procedure. Fixed flight profiles have been determined for each procedure/class combination.
3. The noise characteristics of a representative aircraft are documented in an NPD table, which contains information on the overall A-weighted SPL (in dB(A)). This data is provided for specific combinations of source-receiver distances (m) and engine settings (kN or rpm). For combinations that are not in the NPD table, linear interpolation is used. It is important to note that the NPD data assumes that the aircraft is an omnidirectional point source.
4. The overall A-weighted SPL retrieved from the NPD tables correct for the lateral attenuation effect using simple empirical formulas. These corrections account for factors such as ground attenuation, meteorological effects, and the directionality of the aircraft sound.
5. Finally, to analyse the noise levels of a specific flight movement, a grid is defined on the ground. The grid coordinates consist of an x-coordinate parallel to the flight path and a y-coordinate perpendicular to it. For a given fixed grid point, the distance and thrust setting are determined based on the flight profile, which provides information about the flight as a function of time. By using the ground velocity data in the flight profile table, the corresponding time values are calculated. The L_A is computed over time by linearly interpolating the relevant data from the NPD table. Using the L_A values versus the time

curve, the SEL metric is evaluated using [Equation 4.4](#). These steps are repeated for each defined grid point, resulting in a noise contour that represents the SEL metric for the specific flight movement.

While there are similarities in the modelling tools for aircraft noise, there are also notable differences that can lead to varying results. Both the INM and the NRM utilise NPD look-up tables for their calculations. However, one key difference between both models lies in the treatment of lateral sound attenuation. This difference in calculations results in the INM predicting higher noise levels in close proximity to the airport and a lower noise load at greater distances from the airport[20]. Furthermore, the NRM is a point-based model, and the INM is a segment-based calculation model.

4.4.4. ECAC Noise Model

Where the United States developed the AEDT, the European Union developed its own noise modelling tool, namely the Doc29 model. The European Civil Aviation Conference (ECAC) Doc.29 (Doc29) operates as a segmentation model, designed to assess aircraft noise generated by individual flight instances[85]. It achieves this by combining the sound emissions of distinct sound-producing elements known as flight path segments. Each flight path segment represents a specific section of the aircraft's trajectory, encompassing all the relevant flight geometric and operational variables at its starting and ending points. By combining multiple flight path segments, a segmented flight path is constructed, providing a comprehensive depiction of the aircraft's motion throughout the flight event.

Once the flight path has been determined, the relevant parameters such as aircraft position, speed, engine power, and bank angle are inputted into suitable equations at the endpoints of each segment. These equations then yield the corresponding noise levels at specific receiver positions, resulting in a comprehensive assessment of the noise generated by the aircraft.

The Doc29 model provides the noise levels of a single flight event by performing the following operations:

1. Calculate the ground track via flight data analysis
2. Calculate the flight profile by synthesis from ANP procedural steps
3. Merge ground track and flight profile to obtain a segmented flight path
4. Calculate the sound levels generated by each segment as specified ground locations
5. Superpose the effect of all segments to obtain the final noise levels at those locations

As of August 2016, the government of the Netherlands decided to replace the NRM with a calculation method based on Doc29.

5

Mathematical Problems and Solving Methods

The main problem related to airport capacity is the Runway Scheduling Problem (RSP) which can be split into two types of problems. The Aircraft Landing Problem (ALP) and the Aircraft Take-off Problem (ATP). In general, the ALP and ATP involve two main steps. First, an available runway is assigned to each aircraft that is ready to land or take off. Then, a scheduled landing or take-off time is allocated to each aircraft. When both problems are combined, it is called the Aircraft Scheduling Problem (ASP), which is more realistic, because ATC has to handle both arriving and departing traffic [52]. The first known publication about the RSP was written by Dear in 1976[23]. Nevertheless, the solution approaches employed for the ALP, ATP, or ASP can prove to be valuable in addressing the RSP. Hence, this chapter also encompasses a discussion of these problems along with their relevant literature. It begins with an explanation of the existing mathematical models in [section 5.1](#), followed by an exploration of the various solution methods and illustrative examples from literature in [section 5.2](#). Finally, the receding horizon theory is examined in detail in [section 5.3](#).

5.1. Mathematical Models

In the mathematical formulation of the RSP, several operational constraints have to be taken into consideration. The most important constraint is the safety separation between consecutive aircraft, followed by the time window in which the aircraft has to land, taking into account fuel consumption. The objective function is dependent on the decision maker, which can be the airport, the airline, the government, ATC, etc. An example of the main objective of the airport is to maximise the punctuality relative to the operating schedule. More examples of other decision-making objectives can be found in a review performed by Bennell et al. [14].

The input for the RSP is a set of runways, and a set of aircraft ready to land or take off. A pre-defined time window, with a possible preferred time for the landing or take-off is known for each aircraft. In its simplest form, the RSP involves initially assigning an available runway and a scheduled time of operation, all while considering the relevant constraints.

Mathematical formulations of the RSP can be classified according to several parameters:

- The availability of the input data: When all the parameters of the model are known in advance, the model is static. The model is dynamic when some input parameters are unknown or subject to change within the considered time horizon.
- The uncertainty of the parameter value: The model can be categorised as either deterministic or under uncertainty based on the level of uncertainty associated with the parameter values. The parameter values are known in a deterministic model. However, in an uncertain model, certain parameter values are not precisely known, and they exhibit variability within a specific range or distribution.
- The number of runways and their configuration: The complexity of the model can vary based on the number of runways and its configuration. It can be a single-runway system or a multi-runway system with various configurations. Different runway systems may require specific constraints and optimisation techniques.

- The objective function: The objective of the model plays an important role in the optimisation of the model. The choice of the objective function depends on the specific goals and priorities of the runway scheduling process.
- The constraints taken into account: With the separation constraint being the most fundamental one.

5.2. Solving Methods

There are several methods proposed in the literature to solve the RSP, from exact approaches, such as dynamic programming and mixed-integer programming, to metaheuristic approaches. Those include genetic algorithms, simulated annealing, tabu search, and ant colony optimisation. Figure 5.1 shows an overview of the different solving methods that were found in the literature.

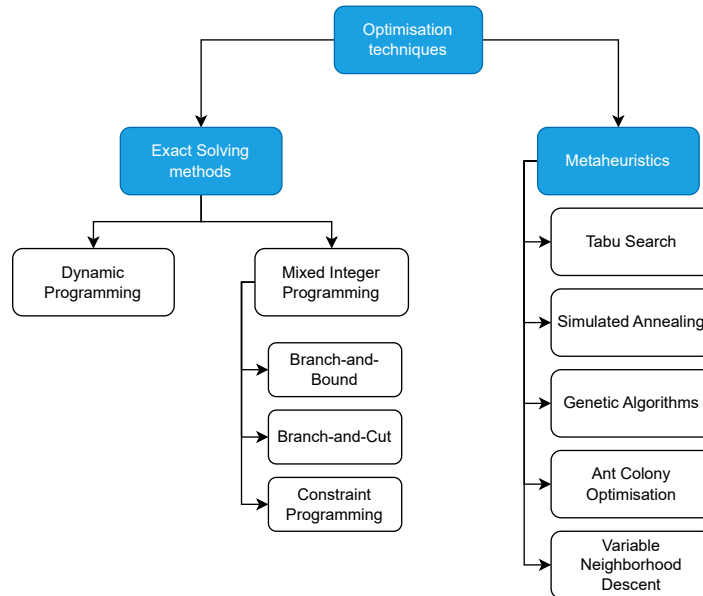


Figure 5.1: Overview of Optimisation Techniques

In the subsequent subsections, the solving methods will be elaborated upon in greater detail, accompanied by examples of research conducted in relation to these solving methods. The discussion commences with an explanation of the exact solving methods.

5.2.1. Exact Solving Methods

The literature discusses several methods to solve the RSP with an exact method. The most common methods are MIP programming methods and dynamic programming methods. A few studies use a different approach with constraint programming as the main method. This is done by Van Leeuwen and Van Hanxleden Houwert [63] to solve the ATP. It is also used by Artiouchine et al.[6] to solve the ALP with an analogy with the K-king problem. This subsection provides an explanation of the distinct exact-solving methods, alongside an overview of the relevant research studies regarding these methods.

Dynamic Programming

Dynamic Programming (DP) is a useful mathematical technique for making a sequence of interrelated decisions. A specific mathematical formulation for "the" dynamic programming problem does not exist. Dynamic programming is a broad approach to problem-solving, and the equations used must be tailored to each specific situation. Consequently, solving a problem using dynamic programming requires creativity and an understanding of the problem's overall structure. It is essential to recognise when and how dynamic programming techniques can be applied to effectively solve a problem[65]. A basic feature of a DP problem is that it can be divided into stages, with a policy decision required at each stage.

One of the first researches using DP to address the ALP has been performed by Psaraftis [86], initially focusing on a single runway and subsequently expanding it to encompass two runways. The model was extended by

Briskorn and Stolletz[18] to multiple independent runways. They proved that, within each class, it is optimal to schedule aircraft according to the FCFS rule. Lieder and Stolletz[66] improved the model made by Briskorn to incorporate interdependent and heterogeneous runways. Furthermore, they introduced a rolling planning horizon heuristic.

Mixed Integer Programming

Mixed Integer Programming (MIP) is a mathematical programming technique used to solve optimisation problems that involve a combination of discrete (integer) and continuous variables. MIP problems involve optimising an objective function subject to a set of constraints, where some variables can only take on integer values. The process of solving a MIP problem typically involves algorithms that explore different combinations of feasible solutions to determine the optimal solution. Branch and bound, branch and cut, and advanced heuristics are commonly used techniques in MIP solvers. Examples of online solvers are CPLEX and Gurobi.

The MIP is often used in literature to solve the RSP. As mentioned earlier, Beasley et al. developed the first MIP model to solve the ALP. The model is extended to incorporate multiple interdependent runways and solved with CPLEX.

An adaptation was made by Briskorn and Stolletz [18] regarding the objective function. They changed it to account for different aircraft classes and solved it via CPLEX. This resulted in better computational times compared to the model of Beasley et al. Ghoniem and Farhadi[34] added the ASP to the model of Beasley et al. Furthermore, they introduced a set-partitioning model with a column-generation approach to solve the problem. This results in better computational times and the ability to solve for larger instances.

The same model as Beasley et al. has been used by Salehipour et al.[94]. Both models are the same regarding the decision variables. However, Salehipour et al. simplify some redundant constraints. Furthermore, they designed a hybrid meta-heuristic applying a simulated annealing framework resulting in a very high-quality solution in reasonable computation times.

A time-discretization approach has been used by Faye[31], where the planning horizon is divided into time slots, ensuring that no events occur between consecutive slots. To solve the problem a dynamic constraints generation algorithm is used, consisting of two main blocks. The first block solves a relaxed version of the problem by estimating the separation matrices using rank-2 matrices. The second block of the algorithm looks for pairs of aircraft that may violate the separation constraints and corrects them.

Avella et al.[10] use a time-indexed formulation for the ASP. This is motivated by the fact that time-index formulations offer a good compromise between the compactness of the formulation and the quality of the LP bounds.

As explained in subsection 2.3.4 sequencing can be changed from FCFS to CPS. CPS is used in the research performed by Prakesh et al.[84] for the scheduling of both landings and takeoffs on a single runway. The MIP formulation is split into pairs and solved by using GuRoBi.

All the research mentioned above focuses on mainly one objective; minimising the total weighted delay. However, other objectives are also researched, including multi-objective problems.

A flexible runway allocation model method was developed by Delsen[24]. The objective function tries to minimise both fuel and noise exposure to the environment, while taking a variety of constraints into account. Examples are runway dependencies and noise exposure. A Weighted Sum normalisation is used for the normalisation of fuel and noise. The outcome is evaluated via a Pareto optimisation, which is validated by applying the model to several case study scenarios.

Van der Meijden[106] made improvements to the model developed by Delsen. These proposed improvements led to a more accurate representation of the aircraft in the model by introducing pair-wise separation and using more than two types of aircraft. However, a discrete representation of flight scheduling is used due to the time steps of 20 seconds. This affects the runway capacity negatively. Moreover, the dependencies between runway systems are not incorporated in the separation modelling, which limits the model. New research performed by Abbenhuis[1] has changed the model to a scheduling model instead of an allocation model. By changing the decision and auxiliary decision variables, the scheduling model is more suitable for complex runway systems. Furthermore, assigning continuous delays to the scheduled flights prevents the model from becoming infeasible. For the noise modelling, the Aviation Environmental Design Tool (AEDT) is used to estimate the noise more accurately.

5.2.2. Metaheuristics

Exact solutions create a feasible and optimal solution for the objective function. However, due to its large computational time, this approach does not always work. For certain problems, achieving an optimal solution may prove excessively complex or require excessive computational time. In such scenarios, it remains crucial to obtain a feasible solution that is reasonably close to optimal. Heuristic methods are commonly used to search for such a solution. The downside of a heuristic solution method is that heuristics tend to be ad hoc in nature, which means that each method is designed to fit a specific problem type rather than a variety of applications. This problem was resolved with the introduction of metaheuristics. A metaheuristic is an overarching approach that offers a general framework and strategic principles for creating a tailored heuristic method to address a specific type of problem [65].

As the RSP can be dynamic and an update of solutions is needed when a new event occurs heuristic approaches and metaheuristics are also researched. This section will discuss three different metaheuristic solving methods for solving the RSP, based on the most-used techniques in literature, which are Genetic Algorithms (GA), Tabu Search (TS), and Simulated Annealing (SA). Other metaheuristics that are used in literature are Ant Colony Optimisation (ACO)[112] [13] [54], and Variable Neighborhood Descent (VND) [94] [93].

Tabu Search

Tabu search is a popular metaheuristic algorithm that incorporates intuitive concepts to help the search process break free from local optima[65]. The algorithm's core idea is to maintain a short-term memory, known as the "tabu list", which keeps track of recent moves or solutions that are prohibited from being revisited in future moves. This prevents the algorithm from getting stuck in cycles or repeatedly visiting suboptimal problems.

The Tabu Search algorithm starts with a feasible initial trial solution and explores the solution space by making small modifications or moves to reach neighbouring solutions. During the search process, the algorithm evaluates the quality of each candidate solution using an objective function. The algorithm continues iterating until a stopping criterion is met, such as a fixed amount of CPU time, or a fixed number of consecutive iterations without an improvement in the best objective value. Furthermore, the algorithm stops when there are no feasible moves into the local neighbourhood of the current trial solution.

To commence the discussion of research conducted on the RSP, Atkin et al.[8] introduced a hybrid metaheuristic system taking into account a larger number of aircraft that can be managed by a human controller. Their model puts forward schedules that proactively address potential future challenges.

Research performed by Soykan and Rabadi[99] uses a TS approach for scheduling airport operations on multiple independent runways. The approach can be divided into two main steps. The first step follows an FCFS sequence and utilises a greedy algorithm called the Target Time First Greedy Algorithm (TTFGA), which prioritises aircraft landing/take-off by looking at their target times. This minimises the delay of the operation. The aircraft are assigned to runways accordingly. The initial solution is improved in a second step that makes use of a TS. Potential solutions are created by changing the order of aircraft landing on the same or different runways, or by deleting/inserting aircraft off/in sequences. During the search, if a new best value of the objective is found, an aspiration mechanism is employed to bypass tabu restrictions. The algorithm terminates when no further improvement is achieved after a specific number of iterations.

New research performed by Soyak and Rabadi[100] focuses on multi-objective runways operations scheduling. A simulation-based optimisation approach is used with a discrete-event simulation component to account for uncertain conditions and an optimisation component to find a Pareto set of solutions. The problem is solved with a hybrid Tabu/Scatter Search algorithm due to its large, complex, and unstructured search space. The main objective of the problem is to maximise runway utilisation and fairness. Results show that the proposed model is effective and the computational times are suitable for practical applications.

Simulated Annealing

Simulated Annealing, a commonly utilised metaheuristic, is designed to facilitate the exploration beyond local optima during the search process. In tabu search, a common approach involves initially ascending the current hill in the steepest direction until reaching its peak, followed by a gradual descent while simultaneously searching for a new hill to ascend. However, this method has a drawback: it consumes a significant number of iterations to climb each individual hill instead of prioritising the search for the highest hill available [65]. The approach used in simulated annealing is to focus mainly on searching for the tallest hill.

The simulated algorithm starts with a feasible initial trial solution and uses the move selection rule to select the next trial solution. When the desired number of iterations has been reached at a certain level of T , T is decreased to the next value in the temperature schedule and continues performing iterations at the next value.

When the desired number of iterations have been performed at the smallest value of T in the temperature schedule the algorithm is stopped. The best trial solution found in any of the iterations is selected as the final solution.

The SA framework is used in research performed by [38] by using three types of greedy algorithms. To generate candidate solutions for Simulated Annealing (SA), the process involves randomly selecting two aircraft and swapping their positions. The model used improves the computational time and initial solutions. The same principle of swapping aircraft to generate candidate solutions has been done in the research of Rodriguez-Diaz et al.[88]. The model takes WV separation and CPS constraints into account for the problem of scheduling aircraft operations on a single runway. The model outperforms the model of Salehipour et al.[94] in terms of computational time, but not in terms of percentage improvement. In recent work, performed by Su et al.[102], SA is used in combination with a large neighbourhood search algorithm and the receding horizon control strategy to solve the ARSP. The proposed model and algorithm are evaluated by comparing them to existing algorithms known for their excellent performance in solving large-scale ARSP. The evaluation demonstrates that the proposed model and algorithm are both accurate and efficient. Moreover, the algorithm outperforms other methods in terms of optimisation results when tackling large-scale ARSPs.

Genetic Algorithms

Genetic Algorithms offer a distinct approach as a metaheuristic, differing from the previously mentioned methods. GAs are known for their ability to effectively explore different areas within the feasible region and progressively evolve towards the optimal feasible solution[65]. They are used to solve optimisation problems by iterative evolving a population of candidate solutions to find the optimal or near-optimal solution. The algorithm's name comes from the analogy to biological evolution and genetics. GAs mimic the process of natural selection by applying genetic operators such as selection, crossover, and mutation to candidate solutions.

The algorithm initiates by generating an initial population consisting of feasible trial solutions. The fitness, which represents the value of the objective function, is then evaluated for each individual within the current population. The fittest individuals of the current population are selected to become parents. These parents are paired up randomly and give birth to two children, new feasible trial solutions, whose features are a random mixture of the features of the parents. The children are retained and again the best members of the current population are selected to form a new population of the same size for the next iterations. The fitness of each new member in the new population is evaluated. The algorithm is terminated when a fixed number of iterations, a fixed amount of CPU time, or a fixed number of consecutive iterations without any improvement in the best trial solution is found. The best trial solution found on any iteration is used as the final solution.

In literature GAs were the mostly-used metaheuristic before the use of Tabu Search and Simulated Annealing. However, still, research is performed with GAs. An example is the research performed by Hu and Paolo [46] who considered the problem of scheduling aircraft landings on a single runway. They introduced a novel GA framework based on the ripple spreading on a liquid surface. Furthermore, Sholel et al.[2] solved the ASP with GAs, with the novelty of finding the best-fit runway configuration that maximises runway throughput. The selected solution approach employs a GA that involves the co-evolution of a population consisting of candidate aircraft sequences and candidate runway configurations. A multi-objective optimisation model was developed by Zhou and Jiang[114]. The genetic algorithm combined with a sliding time window algorithm was used to solve the model. The sliding time window algorithm is explained in more detail in [section 5.3](#). The same method is used to solve the traffic scheduling in airport terminal areas and this has been researched by Liu et al.[67].

5.3. Receding Horizon Control

The research discussed in this chapter is mainly based on offline optimisation. This refers to the process of improving a system or process without actively running it in real time or making changes during the process. For solving dynamic optimisation problems the Receding Horizon Control (RHC) is a very effective tool. The concept of RHC involves breaking down the original problem into smaller sub-problems within a sliding time frame. This approach reduces the computational burden and allows for real-time adaption to uncertainties and disturbances in a dynamic environment[45]. When there are uncertainties or disturbances, the RHC can detect and solve these in the current or subsequent time frames.

RHC relies on two parameters, the time interval of a scheduling window, and the width of the receding horizon. Figure 5.2 provides an illustration of RHC where the width of the horizon is 4 times the time interval. The optimisation is done for all the information available in the width of the receding horizon. However, only the scheduling decisions for the first time interval are actually implemented, i.e., optimisation is globally made within the horizon of interest while scheduling decisions are implemented locally in the first interval.

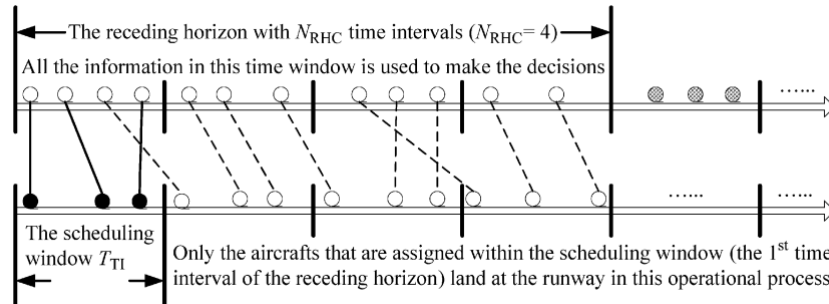


Figure 5.2: Example of RHC for the RSP [111]

The RHC strategy in optimisation problems, and thus the RSP, involves dividing the problem into subproblems using the receding horizon technique. Each subproblem considers environmental information collected from the beginning of the time interval to the end of the time interval. The objective is focused solely on the specific time interval and the process is repeated for subsequent receding horizons until the entire problem is solved.

6

Research Proposal

In this chapter, the essential background and contextual information that sets the stage for our research proposal is discussed. The overarching problem, its significance, and the rationale behind our literature study is explored. By providing a comprehensive overview, the aim is to establish a solid foundation upon which the research questions can be formulated. First, the literature is discussed in [section 6.1](#) to have a clear idea of what the potential research could be. Taking into consideration the aforementioned information, the research objective is formulated in [section 6.2](#), while the research questions are outlined in [section 6.3](#).

6.1. Discussion Literature

Before the research question is formulated, an overview of the literature found and the potential future work is stated and discussed. The main objective of this literature review was to identify areas of improvement for the existing flexible runway scheduling model proposed by Abbenhuis [1], and to explore potential solutions for these limitations. A comprehensive overview of the findings of the literature can be seen in [Table 6.1](#). The table shows an overview of the different subjects treated in this literature review and the methods and assumptions used in previous work. With the findings of the literature study on each of the subjects, potential research has been formulated, which can serve as a basis for the MSc thesis on the topic of flexible runway scheduling.

Table 6.1: Overview of potential research for the Thesis

Subject	Previous Model	Potential research
Optimisation method	MILP	Tabu Search / Sliding Time Window
Fuel	BADA 3 with 3 segments for arrival and 2 segments for departure	AEDT / more segments / optimal control
Noise and the dose-response relationship	AEDT with 1 general noise limit	More detailed noise limits, as the regulations around Schiphol
Optimal Control	N/A	Implementation of optimal Control in the approach trajectory

The subjects indicated in the table represent each chapter in the literature study. In the following subsections, a concise overview of the topics is provided, followed by a more comprehensive explanation of potential research aspects.

6.1.1. Fuel

One of the objectives of the runway scheduling model will be the fuel consumption of the aircraft. During the literature study, several fuel burn models were found. All the models discussed are based on BADA, which provides the aircraft performance parameters related to thrust and fuel consumption. Two versions of BADA exist, namely BADA 3 and BADA 4. BADA 4 provides more accurate modelling of aircraft performance across the entire flight envelope. However, as the TU Delft does not have access to the newest version of BADA and not all aircraft types are present in BADA 4, only BADA 3 can be used. The preceding model also relies on BADA 3, and a simplification was implemented by dividing the arrival trajectory into three segments: Initial Approach Fix (IAF) to Final Approach Fix (FAF), FAF to Runway, and Runway to Gate. As for the departure trajectory, two segments were selected: Gate to runway, and Runway to the initial waypoint of the Standard Instrument Departure (SID). This limits the accuracy of the fuel burn in the runway scheduling model.

This literature study also discussed the AEDT and the fuel burn modelling method used. It showed that the AEDT incorporates the SFI model, which increases the accuracy of the fuel burn in the terminal area. Also, a completely new topic is covered compared to the previous model, the implementation of ATOP during the approach phase. This can lead to the reduction of fuel consumption while scheduling aircraft to runways.

6.1.2. Noise

The second objective of the model will be to limit the noise exposure during the scheduling of runways to aircraft. In this literature study, the major noise modelling tools were stated and explained. The main tools are INM, AEDT, NRM, and ECAC Noise Model. The INM has been replaced by the AEDT and the NRM has been replaced by the ECAC noise model. Therefore, for the purpose of this research, the noise modelling will be conducted using either the AEDT model or the ECAC noise model. Given that the AEDT model utilises the methodologies outlined in the ECAC Doc29 to calculate noise levels, the decision has been made to employ the AEDT model for generating the noise profiles in the forthcoming study.

Furthermore, it became clear that in the current model, a generalised noise limit is used for the environment around the airport. This is not realistic, as the noise limit is dependent on the distance from the airport. The noise regulations regarding Schiphol Airport have been investigated and this has led to an overview of the current noise regulations and the corresponding noise limits. Consequently, it is interesting for this research to explore the feasibility of integrating variable noise limits into the model, with the aim of reducing its simplification.

6.1.3. Optimal Control and Trajectory

The implementation of optimal control in the arrival trajectory can be a new addition to the current runway scheduling model, which can lead to a reduction in fuel consumption. The decision is made to focus on fuel consumption first and it can potentially be expanded to incorporate noise. It is important to consider how the ATOP can be implemented in the runway scheduling model. Research has been performed on the Aircraft Sequencing Problem, but this did not include the allocation of runways to the flights.

Another important subject to consider related to optimal control is the trajectory. For both the fuel burn and the noise the trajectory flown by the aircraft is an important input parameter. The Aircraft Performance Data is retrieved from BADA. However, when it comes to the profile and track data, there exist two options for retrieving the specific information. The tracks can be acquired either through actual track data or by performing calculations on the map. As for the profile, radar data can be utilised or a predefined profile for speed versus altitude can be employed. The main question concerning the trajectory lies in the conversion of this information into thrust, with the mass of the aircraft being the most uncertain variable. Given that this literature study primarily focuses on the theoretical aspect, the decision regarding which approach to adopt will be made after gaining familiarity with the software, which will occur during the course of the research itself. Consequently, this subject will be explored in greater depth within the thesis itself.

6.1.4. Optimisation Method

With the objectives and the potential improvements of the model known, the last topic to cover in the literature study is the optimisation method. The current model is built as a MILP, and together with the constraint on pairwise separation, this results in a model with a large computational time. This can be solved by using a different optimisation method, which is discussed in this literature study. Where MILP is an exact solving method, metaheuristics can also be used as an optimisation method. These include Tabu Search, Simulated Annealing, Genetic Algorithms, Ant Colony Optimisation, and Variable Neighbourhood Descent. The literature study shows that most of the works use heuristic approaches to solve the runway scheduling problem. Researchers often opt for stochastic approaches due to the intricate nature of the problem at hand. These methods offer high-quality solutions within shorter computation times compared to exact methods, which can be computationally demanding. Another reason is the dynamic nature of the problem. In practice, aircraft dynamically enter the scheduling horizon, which means that an optimal solution for the RSP within a specific scheduling horizon may not remain optimal when new aircraft are introduced. Consequently, computing new optimal solutions using exact methods can be time-consuming and computationally intensive. Literature shows that GAs were the mostly-used metaheuristic in the past. However, the Tabu Search and Simulated Annealing gained much more attention and became the most used metaheuristics. Tabu Search efficiently explores large solution spaces, is effective in overcoming local optima, and can provide near-optimal and high-quality solutions. The algorithm will perform at its best with a well-defined initial solution. This can be solved by combining a Tabu search algorithm with a MILP, which leads to an efficient algorithm that

can compute the solution in parallel. For example, the runway allocation is done by the tabu search and the MILP solves the sequence of the aircraft landing on the specific runway.

To decide which metaheuristic to use in the research a trade-off table is used with important Key Performance Indicators (KPI). The trade-off is made on four parameters: How easy it is to implement/set up the algorithm, the ability to overcome local optima and reach the global optimum, the time required by the technique to converge or reach an acceptable solution, and the ability of the technique to handle larger problem sizes. The result of the trade-off is presented in Table 6.2.

Table 6.2: Trade-off between selected metaheuristic algorithms

Optimisation Technique	Implementation	Overcoming local optima	Computational Time	Scalability
Genetic Algorithms	+	-	--	+
Tabu Search	++	+	+	++
Simulated Annealing	+	-	+	+

As can be seen from the table, Tabu Search scores the best overall on the KPIs, followed by SA. As the RSP involves complex constraints and potentially non-linear constraints, Tabu Search may be more suitable.

Finally, to increase the computational performance of the current model, a sliding time window called Receding Horizon Control can be incorporated into the model. By implementing a sliding time window, the model assigns flights for example, for the next 30 minutes accurately according to all regulations and for the subsequent 30 minutes only determines a rough runway allocation. One factor to take into account is to convert the yearly noise budget into an hourly noise budget to have a better representation of the aircraft noise.

6.2. Research Objective and Context

Having examined the literature and established a clear difference between the existing flexible runway scheduling model and the desired future model, the research objective can now be formulated.

The objective of this thesis research is to remodel the existing flexible runway scheduling model. By changing the modelling method, it will be possible to evaluate the effects of a different solving method on the current model. Furthermore, non-linear and/or more detailed constraints can be incorporated with respect to noise disturbance and fuel savings.

In accordance with the research objective as described above, the model should be able to assign flights to a certain optimal runway end. This should be done by taking into account aircraft-specific noise and fuel burn, the separation between aircraft for both arrival and departure operations, implementation of delay, and optimal control in the approach trajectory.

6.3. Research Questions

Following the research objective that defines the boundaries of the future model, the research question can be formulated. The potential research question of this research could be:

"How can the performance of the flexible runway scheduling model be further improved by introducing a different optimisation technique and by implementing a sliding time window to make the model more operational to use in day-to-day airport operations, while considering separation, noise annoyance, fuel burn, and runway capacity?"

After establishing the primary research question, the subsequent sub-questions have been formulated and are provided below.

1. What is the best alternative optimisation technique to remodel the flexible runway model with a sliding time window?
2. To what extent does the trade-off between model linearisation and simplification affect the model performance?
3. Which fuel burn models are available and how can they be implemented in the runway model?
4. How can optimal control be incorporated to further reduce fuel consumption during the approach?
5. How can a variable noise limit be incorporated into the model?

III

Supporting work

Previous Work

The recently created Flexible Runway Scheduling Model (FRSM) represents an advancement over previous studies conducted by Abbenhuis [1], Delsen [24], and Van Der Meijden [106]. This chapter aims to provide an outline of the model established by Abbenhuis, serving as the basis for comparing outcomes between the tabu model and the MILP model.

1.1. Flexible Runway Scheduling Model

This section delves into the most recent iteration of the FRSM crafted by Abbenhuis [1]. The model is structured as a Mixed Integer Linear Programming (MILP) system, diverging from the approach utilizing a meta-heuristic tabu search algorithm in the update model.

Firstly, this section starts with the introduction of the objective function. Following this, a detailed presentation of the constraints is provided and evaluated.

1.1.1. Objective Function

The objective function is given in Equation 1.1 and consists of three parts and is a minimization problem.

$$\min Z = \alpha \cdot n_f \sum_{f \in F} \left[\left(\sum_{r \in R} c_f^r x_f^r \right) + c_d D_f \right] + \beta \cdot n_n \sum_{xy \in P} c_{xy} g_{xy} + c_{opt} (OR + D_{max} + T_{max}) \quad (1.1)$$

The fuel consumption objective aims to minimize the combined cost of fuel for assigning flight f to runway r , denoted by the variable c_f^r , along with the cost associated with the assigned delay in seconds, indicated by c_d in [kg/s]. Whenever the noise threshold is exceeded, the disturbance cost is determined by the population count c_{xy} residing in that area.

The third component of the objective function comprises parameters designed to enhance the optimization process, incurring a minor penalty denoted by c_{opt} . These parameters include Order Changes (OR), the maximum allowable delay D_{max} , and the final parameter T_{max} , which ensures the expedient handling of all flights.

1.1.2. Constraints

The constraints are presented in Equation 1.2 to Equation 1.7. To determine the operating time and assigned delay, Equation 1.2 is applied, where TS_f is the scheduled time of flight f .

$$T_f - D_f = TS_f \quad , \forall f \in F \quad (1.2)$$

To ensure that each flight is only assigned to one runway Equation 1.3 is used. If a runway or multiple runways are closed for operation Equation 1.4 is employed.

$$\sum_{r=1}^R x_f^r = 1 \quad , \forall f \in F \quad (1.3)$$

$$\sum_{f=1}^F x_f^r = 0, \forall r \in R_r \quad (1.4)$$

Flights are allowed to switch order if they are within a specified window (SW) of each other, which on the first line of Equation 1.5. To ensure that order changes outside this window are prohibited two extra constraints are necessary. The second line determines the value of the auxiliary decision variable $x_{i,j}$ which can be used for separation. The third line determines the time between operations and ensures outside the SW a First-Come, First-Serve principle is used.

$$\begin{aligned} x_{i,j} + x_{j,i} &= 1, \forall j \neq i \wedge |TS_i - TS_j| \leq SW \\ x_{i,j} &= 1, \forall j > i \wedge |TS_i - TS_j| > SW \\ T_j - T_i &\geq 0, \forall j \neq i \wedge TS_j - TS_i > SW \end{aligned} \quad (1.5)$$

Flight separation is guaranteed through Equation 1.6. This constraint is formulated using the big-M method, allowing activation solely when all decision variables are active; otherwise, the constraint remains inactive. The separation time $T_{i,j}^{r,q}$ hinges on flight operations, considering aircraft types, their respective weight classes, and the runways they utilize. To improve model efficiency, emphasis is placed on considering separation requirements solely for flights within 2SW.

$$\begin{aligned} -Mx_{i,j} - Mx_i^r - Mx_j^q + T_j - T_i &\geq -3M + T_{i,j}^{r,q} \\ , \forall i \in F, \quad \forall j \in |TS_i - TS_j| \leq 2SW \\ &, \forall r, q \in R \end{aligned} \quad (1.6)$$

An indicator constraint is employed to address noise disturbance, switching the decision variable to 1 when the noise threshold is surpassed and retaining a value of 0 otherwise. This constraint is depicted in Equation 1.7. It's important to highlight that the cost coefficient $c_{xy}^{f,r}$ represents the Acoustic Energy Level (AEL) rather than the Sound Exposure Level (SEL) utilized in the tabu model. The AEL value is derived from the linearization process applied to the SEL value.

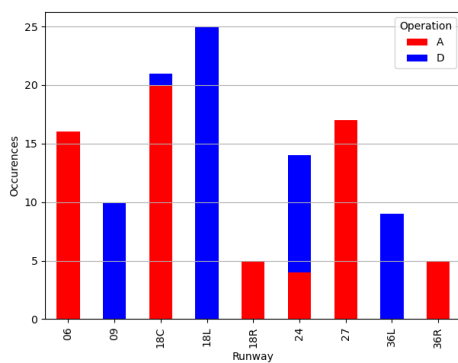
$$\begin{aligned} g_{xy} &= 1 \leftarrow \sum_{f=1}^F \sum_{r=1}^R c_{xy}^{f,r} x_f^r > L_{\text{limit}} \quad \forall xy \in P \\ g_{xy} &= 0 \leftarrow \sum_{f=1}^F \sum_{r=1}^R c_{xy}^{f,r} x_f^r \leq L_{\text{limit}} \quad \forall xy \in P \end{aligned} \quad (1.7)$$

2

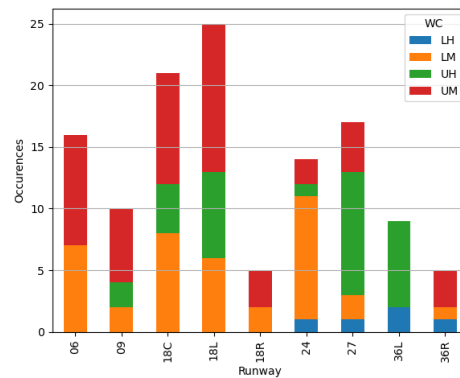
Additional Results

This chapter provides additional results to support the research outlined in the scientific paper discussed in Part I. The results are presented for each scenario, including visualizations of runway allocation, noise grids, and noise intensity. Moreover, for scenarios where a comparison with the MILP method was impossible, a Pareto Front is presented.

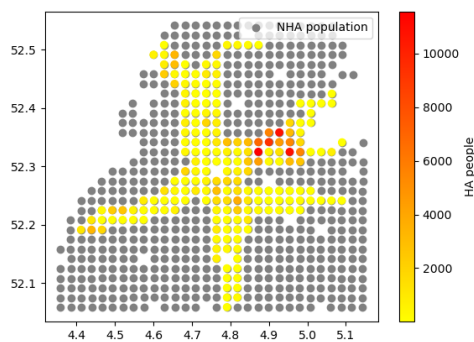
2.1. 90-minute flight schedule



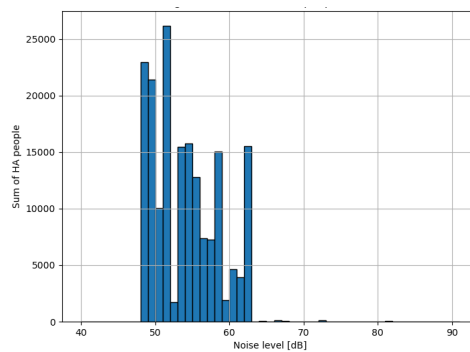
(a) Runway allocation



(b) Runway allocation per weight class

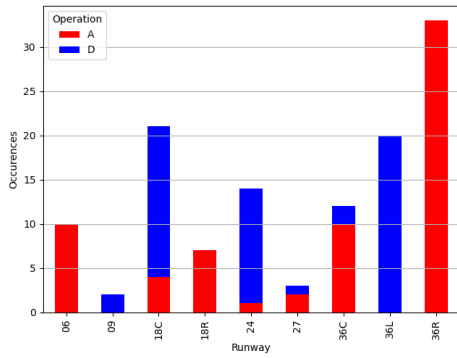


(c) Highly annoyed people heat map

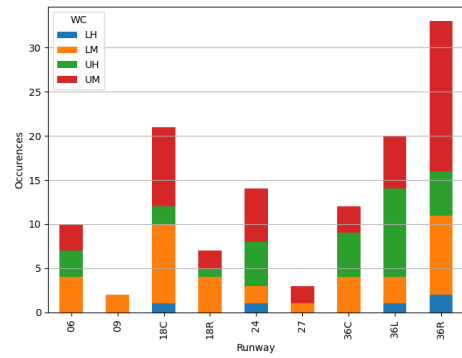


(d) Highly annoyed people noise level distribution

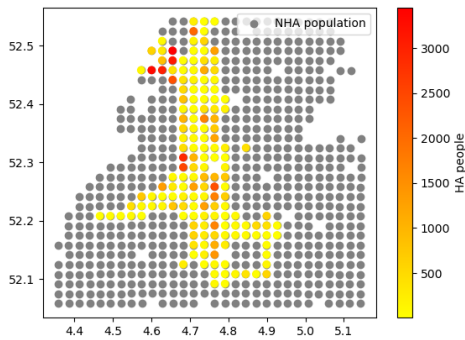
Figure 2.1: Additional results fuel optimization 90-minute flight schedule



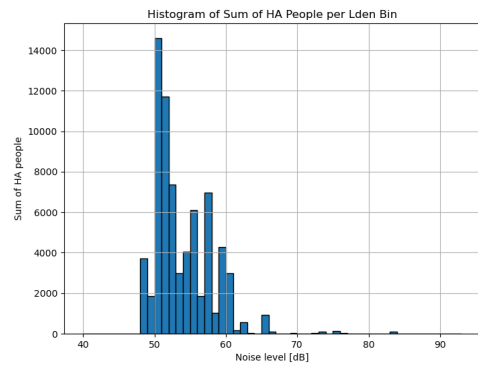
(a) Runway allocation



(b) Runway allocation per weight class



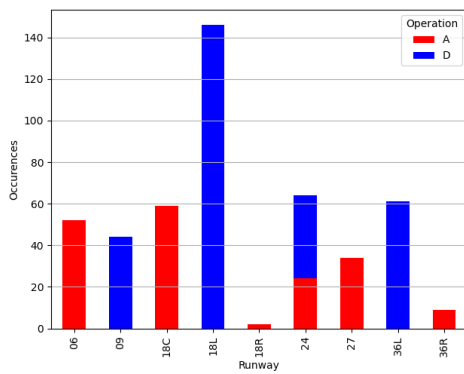
(c) Highly annoyed people heat map



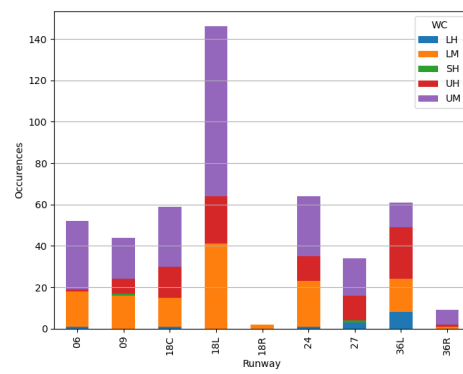
(d) Highly annoyed people noise level distribution

Figure 2.2: Additional results noise optimization 90-minute flight schedule

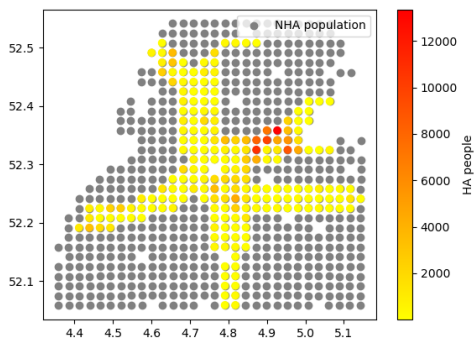
2.2. Six-hour flight schedule



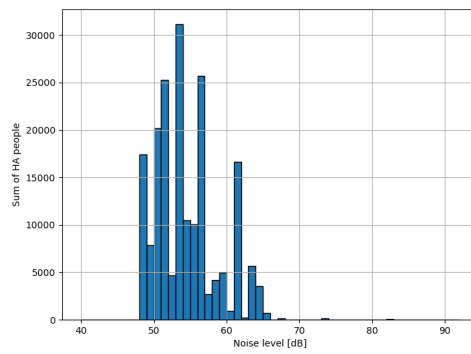
(a) Runway allocation



(b) Runway allocation per weight class



(c) Highly annoyed people heat map



(d) Highly annoyed people noise level distribution

Figure 2.3: Additional results fuel optimization six-hour flight schedule

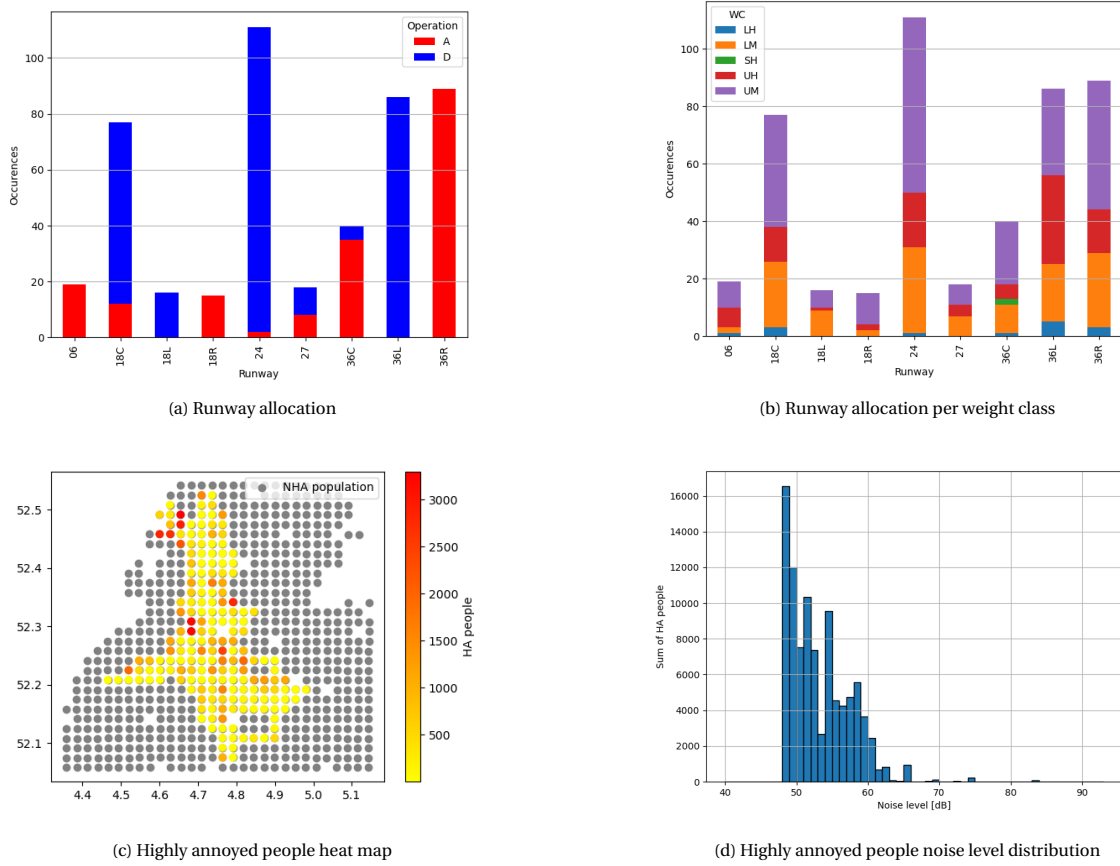


Figure 2.4: Additional results noise optimization six-hour flight schedule

2.3. Daytime flight schedule

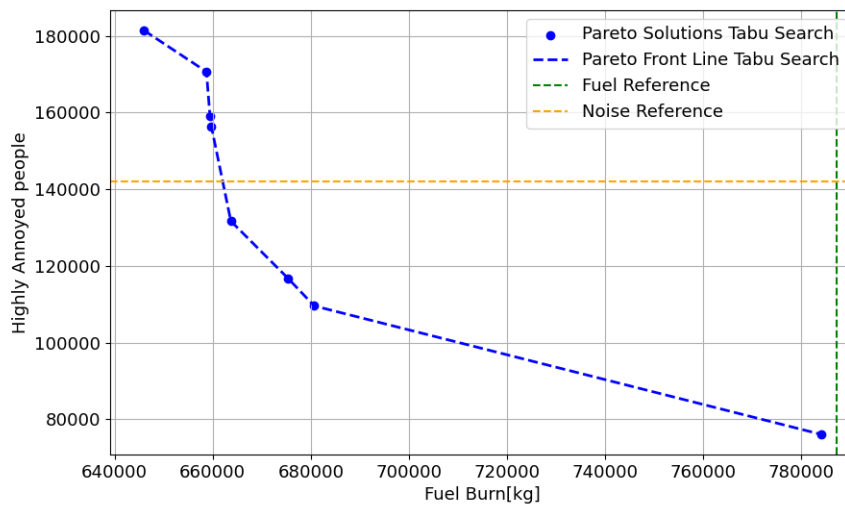
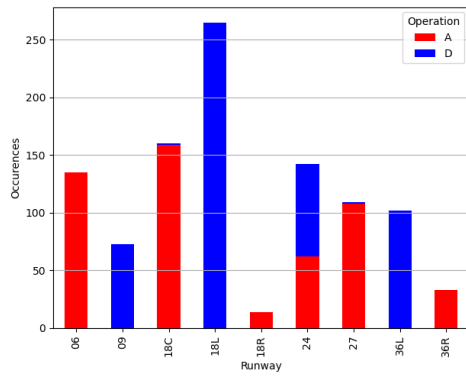
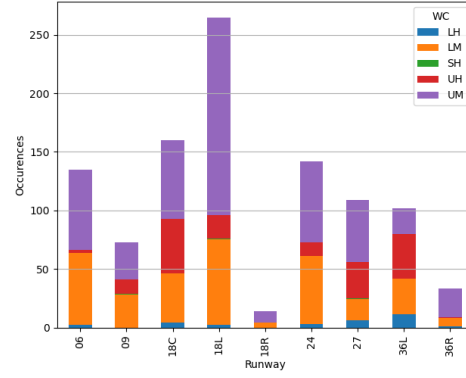


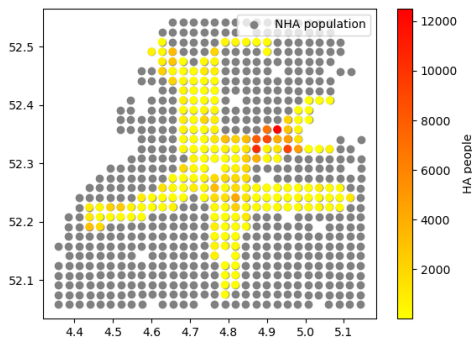
Figure 2.5: Pareto Front daytime flight schedule



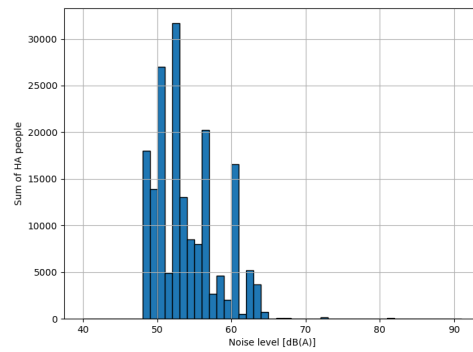
(a) Runway allocation



(b) Runway allocation per weight class



(c) Highly annoyed people heat map



(d) Highly annoyed people noise level distribution

Figure 2.6: Additional results fuel optimization daytime flight schedule

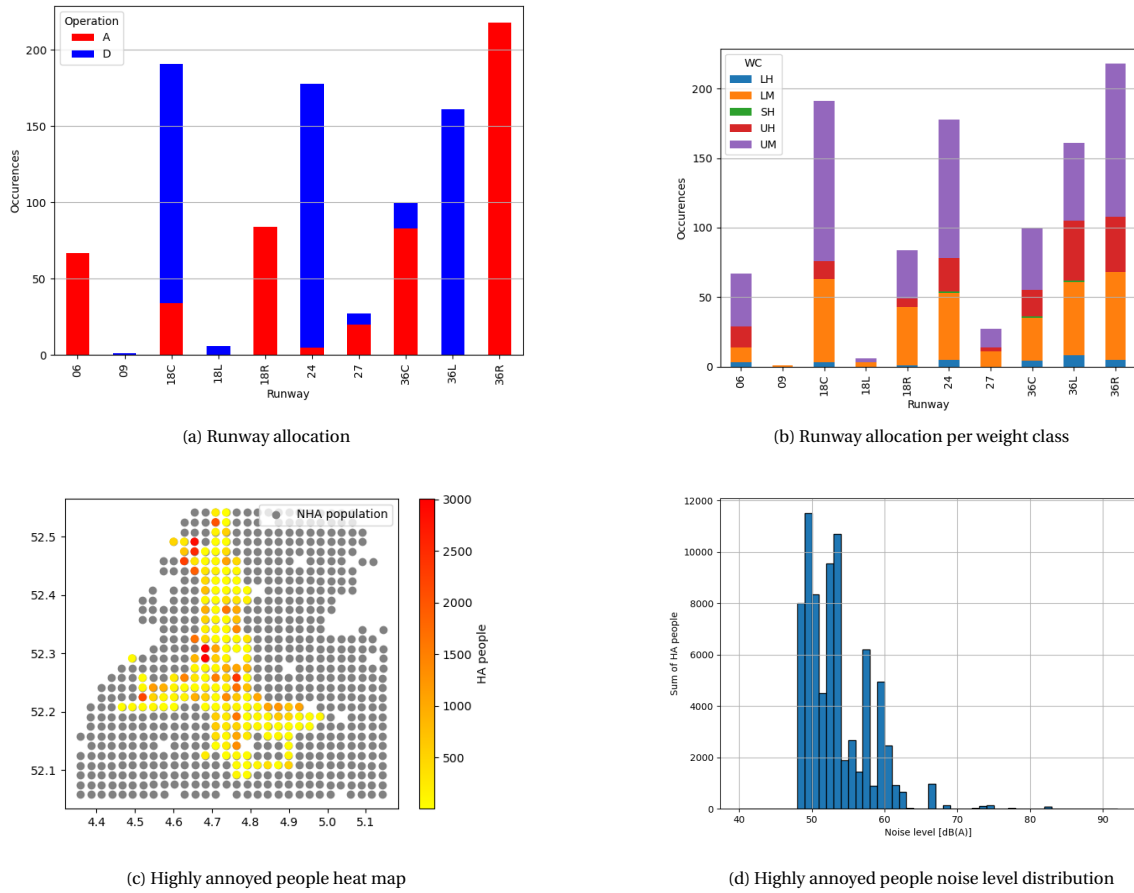


Figure 2.7: Additional results noise optimization daytime flight schedule

2.4. Full day flight schedule

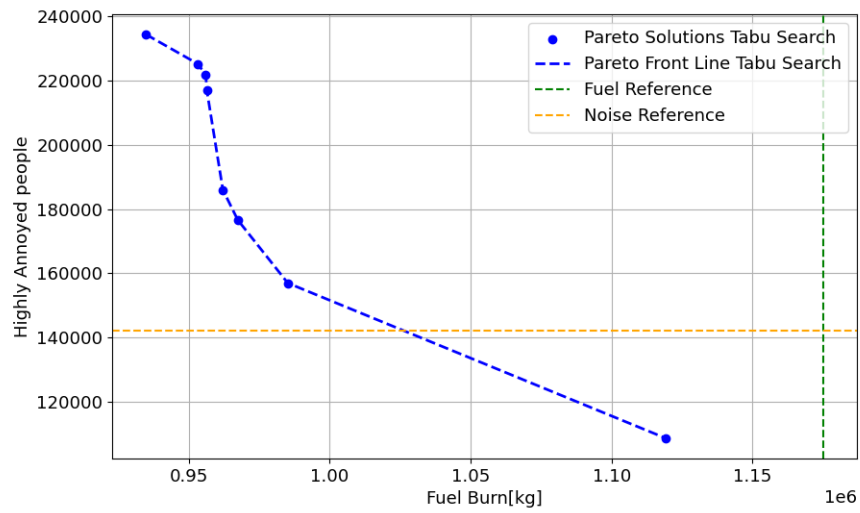
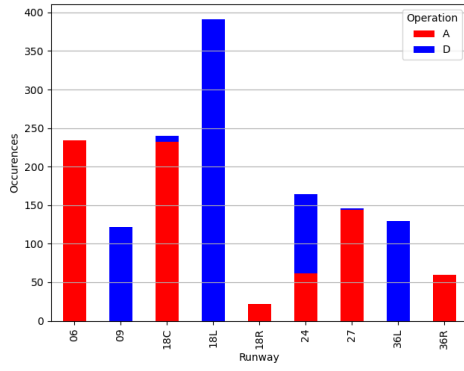
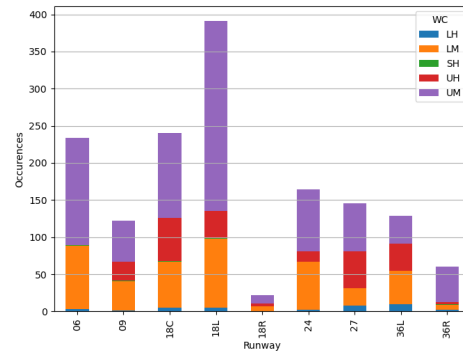


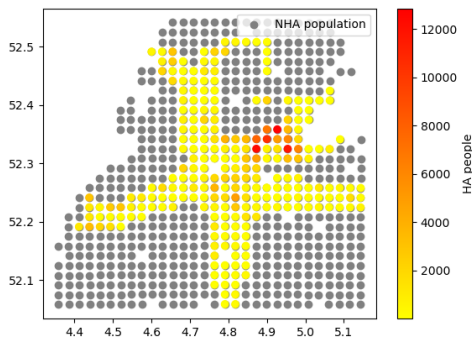
Figure 2.8: Pareto Front full-day flight schedule



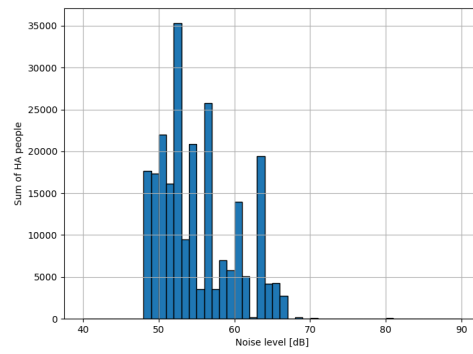
(a) Runway allocation



(b) Runway allocation per weight class

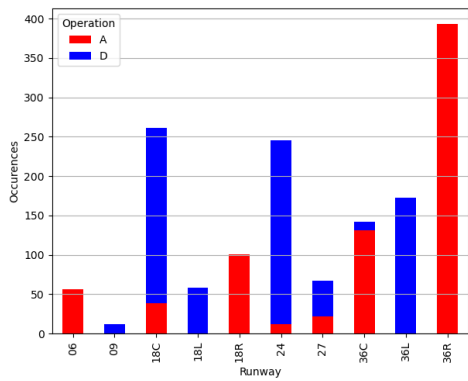


(c) Highly annoyed people heat map

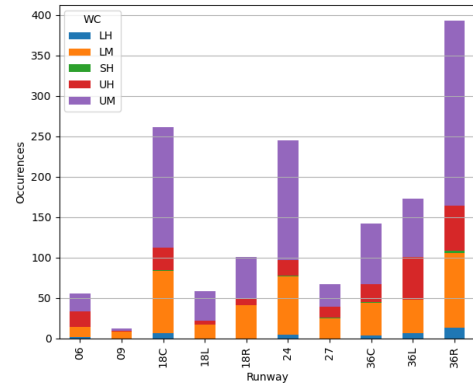


(d) Highly annoyed people noise level distribution

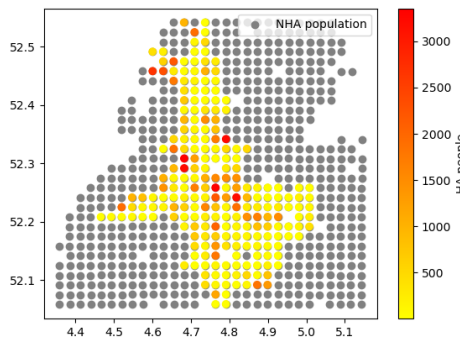
Figure 2.9: Additional results fuel optimization full-day flight schedule



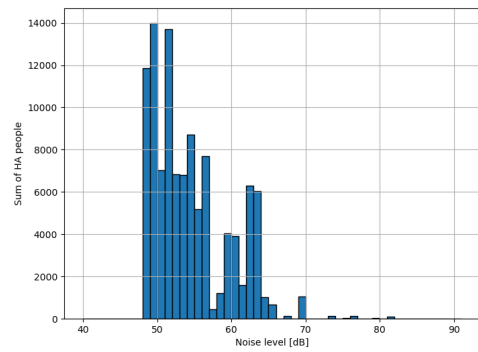
(a) Runway allocation



(b) Runway allocation per weight class



(c) Highly annoyed people heat map



(d) Highly annoyed people noise level distribution

Figure 2.10: Additional results noise optimization full-day flight schedule

3

Verification & Validation

3.1. Verification

The findings presented in the scientific paper have undergone rigorous testing to ensure strict adherence to the model's specified constraints. The verification process encompasses multiple checks aimed at upholding the integrity of the model's outcomes.

An essential verification step guarantees that every flight in the solution adheres to the separation criteria. This is achieved by implementing a separation check and evaluating all solutions generated by the model. The definition returns a true statement when all separation criteria are satisfied; otherwise, it returns false along with details on conflicting flights and runways. Notably, for all solutions produced by the model, the verification yielded a true statement.

Moreover, the model underwent verification to ensure that all flights possess flight consumption data, indicating the assignment of a valid runway. Runways unavailable for operation were assigned a fuel consumption of 0. Importantly, no flight displayed a value of 0 or exceptionally low. This confirmation extends to the assignment of delays, as it also contributes to the overall fuel consumption, affirming the reliability of this aspect of the model.

3.1.1. Separation

To analyze and verify the separation modeling, a small part of the solution of the balanced flight schedule is used. The flight schedule can be seen in [Table 3.1](#) with the flight number, aircraft type, weight class (WC), scheduled time, actual operating time, and runway.

Table 3.1: Part of balanced flight schedule

Flight	AC type	WC	Scheduled time	Operating time	Operation	Runway
15	B738	UM	10:40:00	10:40:00	A	18C
16	B739	UM	10:40:00	10:40:30	D	09
17	B763	LH	10:41:00	10:41:05	A	36R
18	A319	UM	10:42:00	10:42:05	A	18R
19	A332	UH	10:42:00	10:42:00	A	18C
20	E290	LM	10:43:00	10:43:00	D	18L
21	B737	UM	10:44:00	10:44:00	A	06
22	B739	UM	10:44:00	10:44:20	D	18L

The arrival of Flight 15 on Runway 18C establishes a dependency on the departure of Flight 16 from Runway 09R, with a prescribed minimum separation time of 30 seconds for the UM-UM weight class combination. For the subsequent arrivals, Flight 17 and Flight 18, the minimum separation time is contingent upon the activities of flights outside this specific schedule. Notably, when two UH aircraft operate in opposite directions, a minimum separation time of 245 seconds is required. The departure of Flight 22 introduces a separation time dependency on the departure of Flight 20. According to Recat-EU guidelines [91], the weight class combination LM-UM mandates a minimum separation time of 80 seconds. Analyzing the operating times in

Table 3.1 it can be found that the flights adhere to these separation requirements and this part of the model is verified.

3.2. Validation

3.2.1. Handhavingspunten

The noise findings can be verified by referencing the designated "handhavingspunten." An outline of these points is depicted in Figure 3.1. These handhavingspunten are established within the Schiphol Airport Traffic Decision (LVB) and are monitored by the Inspection for Transport and Environment (ILT). Within the LVB, specific limits are outlined for the total noise permissible at AAS. Additionally, the LVB stipulates the maximum noise levels allowed at 35 enforcement locations surrounding AAS. The ILT is responsible for ensuring that the overall annual noise production does not exceed the thresholds set at these enforcement points.

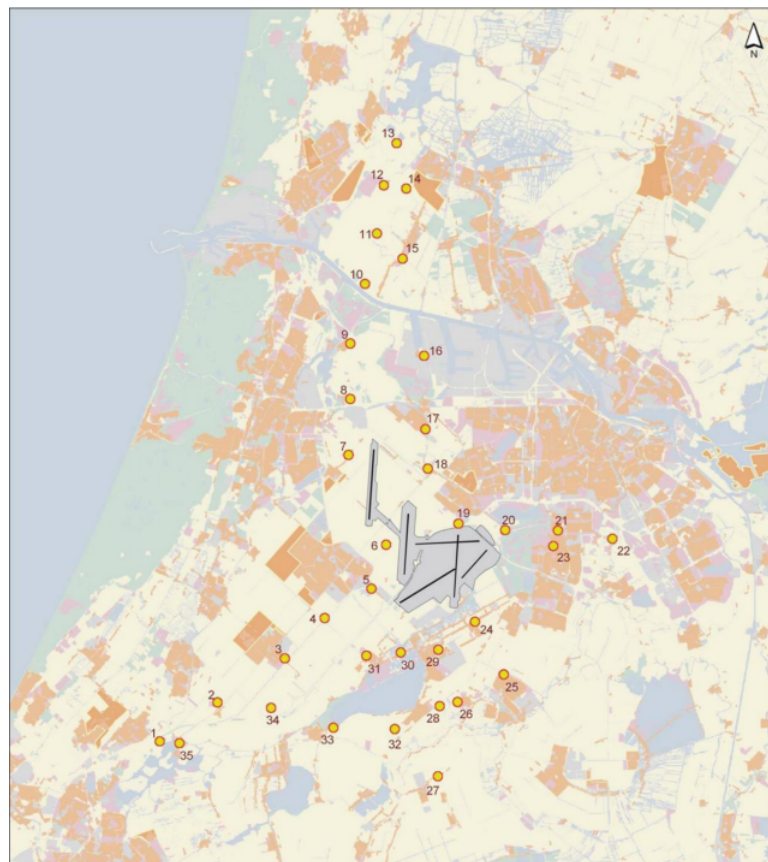


Figure 3.1: Handhavingspunten Amsterdam Airport Schiphol [53]

The noise validation of the model involves comparing simulated noise levels at measurement points with real-world data, as presented in Table 3.2. This comparison indicates that the noise levels closely align with the actual 2019 data. However, it is worth noting that at some measurement points, the noise exceeds the limit set by ILT. This deviation occurs because official regulations require noise level calculations on an annual basis. The simulation computes the L_{DEN} for a full day of operations, potentially allowing for violations on specific days, compensated by lower noise levels on others. As different runway combinations are utilized throughout the year, the daily noise loads on the surrounding areas vary accordingly.

Table 3.2: Validation handhavingspunten full day $\alpha = 0.2$

Location	Limit value	Simulated value	Percentage
	L_{DEN} [dB(A)]	L_{DEN} [dB(A)]	
1	55.85	52.89	50.58%
2	57.58	50.16	18.11%
3	58.61	51.96	21.63%
4	58.08	59.47	137.72%
5	57.74	58.00	106.17%
6	59.44	53.89	27.86%
7	57.63	54.56	49.31%
8	58.60	53.21	28.91%
9	57.04	52.38	34.20%
10	59.23	58.75	89.53%
11	58.77	52.00	21.04%
12	58.46	50.33	15.38%
13	57.47	49.93	17.62%
14	56.80	51.64	30.48%
15	57.95	54.01	40.37%
16	56.71	58.43	148.59%
17	56.47	53.48	50.23%
18	60.76	52.64	15.42%
19	54.27	53.16	77.45%
20	58.35	55.30	49.54%
21	57.88	54.47	45.6%
22	57.81	53.96	41.21%
23	57.21	49.04	15.24%
24	57.65	60.94	213.30%
25	57.94	54.96	50.35%
26	55.69	61.64	162.18%
27	56.41	58.10	147.57%
28	55.91	59.46	226.46%
29	57.18	57.79	279.25%
30	58.22	60.36	163.68%
31	58.93	55.30	43.35%
32	57.17	56.79	91.62%
33	56.50	53.66	52.00%
34	57.24	57.41	103.92%
35	57.02	49.2	16.52%

3.2.2. Fuel flow and AEDT

The aircraft-specific fuel flows are validated using the BADA appendix [28]. By undertaking these checks, the methodologies employed in acquiring the fuel burn characteristics dataset for this research are validated. The dataset related to aircraft-specific noise emission is sourced from the Aviation Environmental Design Tool (AEDT)[59], developed by the FAA. It is assumed that this dataset accurately reflects real-world data to a degree of validity that aligns with the requisites of this research.

Bibliography

- [1] A.W. Abbenhuis. Flexible Runway Scheduling for Complex Runway Systems. Master's thesis, Delft University of Technology, 2021.
- [2] Md Shohel Ahmed, Sameer Alam, and Michael Barlow. A cooperative co-evolutionary optimisation model for best-fit aircraft sequence and feasible runway configuration in a multi-runway airport. *Aerospace*, 5(3):85, 2018.
- [3] Airlines for America. Passenger airlines operating costs, united states, 2019. <https://transportgeography.org/contents/chapter5/air-transport/airline-operating-costs/>, 2020. Accessed: 11-5-2023.
- [4] Airport Research Center. Cast simulation software. <https://arc.de/cast-simulation-software/>, 2023. Accessed: 10-5-2023.
- [5] AirTOP. What is airtop? <https://www.airtop-software.com/>, 2022. Accessed: 3-5-2023.
- [6] Konstantin Artiouchine, Philippe Baptiste, and Juliette Mattioli. The k king problem, an abstract model for computing aircraft landing trajectories: On modeling a dynamic hybrid system with constraints. *INFORMS Journal on Computing*, 20(2):222–233, 2008.
- [7] Norman J. Ashford, Saleh Mumayiz, and Paul H. Wright. *Airport Engineering*. Wiley, 4 2011. ISBN 9780470398555. doi: 10.1002/9780470950074.
- [8] Jason AD Atkin, Edmund K Burke, John S Greenwood, and Dale Reeson. Hybrid metaheuristics to aid runway scheduling at london heathrow airport. *Transportation Science*, 41(1):90–106, 2007.
- [9] Civil Aviation Authority. Airspace Design Guidance: Noise mitigation considerations when designing PBN departure and arrival procedures. Technical report, CAA, 2016. URL www.caa.co.uk, .
- [10] Pasquale Avella, Maurizio Boccia, Carlo Mannino, and Igor Vasilyev. Time-indexed formulations for the runway scheduling problem. *Transportation Science*, 51(4):1196–1209, 2017.
- [11] J Barrer. A new method for modeling complex runway systems. In *Proceedings of the 7th USA/Europe Air Traffic Management Research and Development Seminar*, 2007.
- [12] John Barrer, Peter Kuzminski, and William Swedish. Analyzing the runway capacity of complex airports. In *AIAA 5th ATIO and 16th Lighter-Than-Air Sys Tech. and Balloon Systems Conferences*, page 7354, 2005.
- [13] Ghizlane Bencheikh, Jaouad Boukachour, and Ahmed EL Hilali Alaoui. Improved ant colony algorithm to solve the aircraft landing problem. *International Journal of Computer Theory and Engineering*, 3(2): 224, 2011.
- [14] Julia A. Bennell, Mohammad Mesgarpour, and Chris N. Potts. Airport runway scheduling. *4OR*, 9:115–138, 6 2011. ISSN 1619-4500. doi: 10.1007/s10288-011-0172-x.
- [15] L. Bertsch, M. Snellen, L. Enghardt, and C. Hillenherms. Aircraft noise generation and assessment: executive summary. *CEAS Aeronautical Journal*, 10:3–9, 3 2019. ISSN 1869-5582. doi: 10.1007/s13272-019-00384-3.
- [16] Alfred Blumstein. The landing capacity of a runway. *Operations Research*, 7:752–763, 12 1959. ISSN 0030-364X. doi: 10.1287/opre.7.6.752.
- [17] Justin Boesel, Carla X Gladstone, Jonathan Hoffman, Patricia A Massimini, Camille Shiotsuki, and Brian Simmons. Taam best practices guidelines. Technical report, The MITRE Corporation, 2001.

- [18] Dirk Briskorn and Raik Stolletz. Aircraft landing problems with aircraft classes. *Journal of Scheduling*, 17:31–45, 2014.
- [19] Eurocontrol Experimental Center. User manual for the base of aircraft data. Technical report, Technical report, Eurocontrol, 2004.
- [20] Gerlach Cerfontaine and Paul Riemens. Strategische Milieuverkenning voor de ontwikkeling van Schiphol op middellange termijn. Technical report, Schiphol Group and Luchtverkeersleiding Nederland, 2008. URL https://www.omgevingsraadschiphol.nl/wp-content/uploads/2015/08/20081024_strategische-milieuverkenning-schiphol.pdf.
- [21] Malcolm J Crocker. Fundamentals of acoustics, noise, and vibration. *Handbook of Noise and Vibration Control*, pages 1–16, 2007.
- [22] Richard de Neufville, Amedeo R Odoni, Peter P Belobaba, and Tom G Reynolds. *Airport Systems: Planning, Design, and Management*. McGraw-Hill Education, 2nd edition edition, 2013. ISBN 9780071770583. URL <https://www.accessengineeringlibrary.com/content/book/9780071770583>.
- [23] Roger George Dear. The dynamic scheduling of aircraft in the near terminal area, 1976.
- [24] J.G. Delsen. Flexible Arrival & Departure Runway Allocation. Master's thesis, Delft University of Technology, 2016.
- [25] Doug DuBois and Gerald C. Paynter. "fuel flow method2" for estimating aircraft emissions. *SAE Transactions*, 115:1–14, 2006. ISSN 0096736X, 25771531. URL <http://www.jstor.org/stable/44657657>.
- [26] Heinz Erzberger, Thomas J Davis, and Steven Green. Design of center-tracon automation system. *AGARD, Machine Intelligence in Air Traffic Management*, 1993.
- [27] Eurocontrol. Enhancing Airside Capacity, 2003.
- [28] Eurocontrol. Aircraft performance summary tables: Base of aircraft data, 2019. URL <https://www.eurocontrol.int/node/10065>.
- [29] FAA. Airport capacity criteria used in preparing the national airport plan. *Journal of Travel Research*, 12:28–28, 10 1973. ISSN 0047-2875. doi: 10.1177/004728757301200241.
- [30] FAA. Integrated noise model (inm). https://www.faa.gov/about/office_org/headquarters_offices/apl/research/models/inm_model/, 2019. Accessed: 19-5-2023.
- [31] Alain Faye. Solving the aircraft landing problem with time discretization approach. *European Journal of Operational Research*, 242:1028–1038, 5 2015. ISSN 03772217. doi: 10.1016/j.ejor.2014.10.064.
- [32] Gil Felix Greco. *A computational investigation of jet-plate interaction noise using a Lattice-Boltzmann based method*. PhD thesis, Universidade Federal de Santa Catarina, 12 2018.
- [33] Antonio Filippone. Aircraft noise prediction. *Progress in Aerospace Sciences*, 68:27–63, 7 2014. ISSN 0376-0421. doi: 10.1016/J.PAEROSCI.2014.02.001.
- [34] Ahmed Ghoniem and Farbod Farhadi. A column generation approach for aircraft sequencing problems: a computational study. *Journal of the Operational Research Society*, 66(10):1717–1729, 2015.
- [35] E.P. Gilbo. Airport capacity: representation, estimation, optimization. *IEEE Transactions on Control Systems Technology*, 1(3):144–154, 1993. doi: 10.1109/87.251882.
- [36] Royal Schiphol Group. Capacity declaration summer season 2023. <https://slotcoordination.nl/wp-content/uploads/2022/09/Capacity-Declaration-Amsterdam-Airport-Schiphol-Summer-season-2023-V1.0.pdf>, 2022. Accessed: 4-4-2023.
- [37] Rainer Guski, Dirk Schreckenber, and Rudolf Schuemer. Who environmental noise guidelines for the european region: A systematic review on environmental noise and annoyance. *International journal of environmental research and public health*, 14(12):1539, 2017.

- [38] Gulsah Hancerliogullari, Ghaith Rabadi, Ameer H Al-Salem, and Mohamed Kharbeche. Greedy algorithms and metaheuristics for a multiple runway combined arrival-departure aircraft sequencing problem. *Journal of Air Transport Management*, 32:39–48, 2013.
- [39] James V. Hansen. Genetic search methods in air traffic control. *Computers Operations Research*, 31(3):445–459, 2004. ISSN 0305-0548. doi: [https://doi.org/10.1016/S0305-0548\(02\)00228-9](https://doi.org/10.1016/S0305-0548(02)00228-9). URL <https://www.sciencedirect.com/science/article/pii/S0305054802002289>.
- [40] Richard M Harris. Models for runway capacity analysis. Technical report, MITRE CORP MCLEAN VA, 1972.
- [41] S.J. Heblj and J. Derei. Methodenrapport doc29. Technical report, National Aerospace Laboratory NLR, 2019.
- [42] Philip G. Hill and Carl R. Peterson. *Mechanics and thermodynamics of propulsion (2nd revised and enlarged edition)*. Pearson, 1992.
- [43] Stephen L.M. Hockaday and Adib K. Kanafani. Developments in airport capacity analysis. *Transportation Research*, 8:171–180, 8 1974. ISSN 0041-1647. doi: 10.1016/0041-1647(74)90004-5.
- [44] Robert Horonjeff, Francis X McKelvey, William J Sproule, and Seth B Young. *Planning and design of airports*. McGraw-Hill Education, 2010. ISBN 0071446419.
- [45] Xiao-Bing Hu and Wen-Hua Chen. Receding horizon control for aircraft arrival sequencing and scheduling. *IEEE Transactions on Intelligent Transportation Systems*, 6(2):189–197, 2005. doi: 10.1109/TITS.2005.848365.
- [46] Xiao-Bing Hu and Ezequiel A Di Paolo. A ripple-spreading genetic algorithm for the aircraft sequencing problem. *Evolutionary Computation*, 19(1):77–106, 2011.
- [47] IATA. Jet fuel price monitor. <https://www.iata.org/en/publications/economics/fuel-monitor/>, 2023. Accessed: 11-5-2023.
- [48] IATA. Global outlook for air transport: A local sweet spot, 2023.
- [49] ICAO. Icao document 9184, airport planning manual, part 2land use and environmental control. Technical report, ICAO, 2018.
- [50] ICAO. Balanced Approach to Aircraft Noise Management. <https://www.icao.int/environmental-protection/pages/noise.aspx>, 2022. Accessed: 24-5-2023.
- [51] ICAO. Reduction of noise at source. <https://www.icao.int/environmental-protection/Pages/Reduction-of-Noise-at-Source.aspx>, 2022. Accessed: 24-5-2023.
- [52] Sana Ikli, Catherine Mancel, Marcel Mongeau, Xavier Olive, and Emmanuel Rachelson. The aircraft runway scheduling problem: A survey. *Computers & Operations Research*, 132:105336, 8 2021. ISSN 03050548. doi: 10.1016/j.cor.2021.105336.
- [53] Inspectie Leefomgeving en Transport. Handhavingsrapportage schiphol 2019, 2020. URL <https://www.ilent.nl/documenten/rapporten/2020/02/05/handhavingsrapportage-schiphol-2019>.
- [54] Yu Jiang, Zhaolong Xu, Xinxing Xu, Zhihua Liao, and Yuxiao Luo. A schedule optimization model on multirunway based on ant colony algorithm. *Mathematical Problems in Engineering*, 2014, 2014.
- [55] Amy Kim and Mark Hansen. Validation of runway capacity models. *Transportation research record*, 2177(1):69–77, 2010.
- [56] Peter C Kuzminski. An improved runwaysimulatorsimulation for runway system capacity estimation. In *2013 Integrated Communications, Navigation and Surveillance Conference (ICNS)*, pages 1–11. IEEE, 2013.

- [57] M.F Lamers. Enhanced Runway Capacity at Airports with Complex Runway Layouts. Master's thesis, Delft University of Technology, 2016.
- [58] TX Le. Total airportsim: A new generation airport simulation model. *Transportation Research Circular*, 2002.
- [59] C Lee, TT Thrasher, E Boeker, R Downs, S Gorshkov, A Hansen, S Hwang, et al. Aviation environmental design tool (aedt) version 3e technical manual, 2022.
- [60] David A Lee, Peter F Kostiuk, Robert V Hemm Jr, Earl R Wingrove III, and Gerald Shapiro. Estimating the effects of the terminal area productivity program. Technical report, NASA, 1997.
- [61] Joosung J Lee, Ian A Waitz, Brian Y Kim, Gregg G Fleming, Lourdes Maurice, and Curtis A Holsclaw. System for assessing aviations global emissions (sage), part 2: uncertainty assessment. *Transportation Research Part D: Transport and Environment*, 12(6):381–395, 2007.
- [62] Minwoo LEE, Larry K.B. LI, and Wenbin SONG. Analysis of direct operating cost of wide-body passenger aircraft: A parametric study based on hong kong. *Chinese Journal of Aeronautics*, 32:1222–1243, 5 2019. ISSN 1000-9361. doi: 10.1016/J.CJA.2019.03.011.
- [63] P van Leeuwen and NCBP van Hanxleden Houwert. Scheduling aircraft using constraint relaxation. *Electronic Notes in Theoretical Computer Science*, 2003.
- [64] Man Liang. *Aircraft route network optimization in terminal maneuvering area*. PhD thesis, Université Paul Sabatier (Toulouse 3), 2018.
- [65] Gerald J Lieberman and Frederick S Hillier. *Introduction to operations research*, volume 11. McGraw-Hill New York, NY, USA, 2021.
- [66] Alexander Lieder and Raik Stolletz. Scheduling aircraft take-offs and landings on interdependent and heterogeneous runways. *Transportation Research Part E: Logistics and Transportation Review*, 88:167–188, 4 2016. ISSN 13665545. doi: 10.1016/j.tre.2016.01.015.
- [67] Junhao Liu, Qing Cheng, Yuanji Wang, Changqi Yang, Rui Zhou, Xinpeng Zhu, Di Yao, Junjie Zhou, Yaqian Du, and Shanshan Yang. An improved genetic algorithm-based traffic scheduling model for airport terminal areas. *Journal of Sensors*, 2022, 2022.
- [68] LVNL. Weather conditions. <https://en.lvnl.nl/safety/achieving-safety/weather-conditions/>, 2022. Accessed: 11-4-2023.
- [69] Kerry Marie Malone. *Dynamic queueing systems: behavior and approximations for individual queues and for networks*. PhD thesis, Massachusetts Institute of Technology, 1995.
- [70] Julio Martinez, Antonio Trani, and Photios Ioannou. Modeling airside airport operations using general-purpose, activity-based, discrete-event simulation tools. *Transportation Research Record*, 1744:65–71, 01 2001. doi: 10.3141/1744-08.
- [71] Henk M Miedema and Catharina G Oudshoorn. Annoyance from transportation noise: relationships with exposure metrics dnl and denl and their confidence intervals. *Environmental health perspectives*, 109(4):409–416, 2001.
- [72] Bojana Mirkovic and Vojvode Stepe. Airfield modellingstate of the art. *Faculty of Transport and Traffic Engineering, University of Belgrade, Safety DoAaAT*, 2011.
- [73] Nicolas Molin. Airframe noise modeling and prediction. *CEAS Aeronautical Journal*, 10:11–29, 3 2019. ISSN 1869-5582. doi: 10.1007/s13272-019-00375-4.
- [74] A Montlaur and L Delgado. Delay assignment optimization strategies at pre-tactical and tactical levels. *Fifth SESAR Innovation Day*, 2015.
- [75] Frank Neuman and Heinz Erzberger. *Analysis of delay reducing and fuel saving sequencing and spacing algorithms for arrival traffic*. National Aeronautics and Space Administration, Ames Research Center, 1991.

- [76] Noise Quest. Noise basics. <https://www.noisequest.psu.edu/noisebasics-noisemodels.html>, 2022. Accessed: 10-5-2023.
- [77] A Nuic and V Mouillet. User manual for the base of aircraft data (bada) family 4, eec technical/scientific report. *Eurocontrol Experimental Centre, Bretigny-sur-Orge, France*, 86, 2014.
- [78] Angela Nuic, Damir Poles, and Vincent Mouillet. Bada: An advanced aircraft performance model for present and future atmsystems. *International Journal of Adaptive Control and Signal Processing*, 24: 850–866, 10 2010. ISSN 08906327. doi: 10.1002/ACS.1176.
- [79] Amedeo R Odoni, Jeremy Bowman, Daniel Delahaye, John J Deyst, Eric Feron, R John Hansman, Kashif Khan, James K Kuchar, Nicolas Pujet, and Robert W Simpson. Existing and required modeling capabilities for evaluating atm systems and concepts. Technical report, Massachusetts Institute of Technology, 1997.
- [80] International Civil Aviation Organization. *Environmental Protection: Annex 16 to the Convention on International Civil Aviation*. International Civil Aviation Organization, 2008.
- [81] International Civil Aviation Organization. *Guidance on the balanced approach to aircraft noise management*, volume 9829. International Civil Aviation Organization, 2008.
- [82] International Civil Aviation Organization. *Procedures for Air Navigation Services Air Traffic Management (Doc 4444)*. ICAO, 16th edition, 2016.
- [83] Stanislav Pavlin, Mario ui, and Stipe Pavii. Runway occupancy time as element of runway capacity. *Promet-Traffic & Transportation*, 18:293–299, 2006. ISSN 1848-4069.
- [84] Rakesh Prakash, Rajesh Piplani, and Jitamitra Desai. An optimal data-splitting algorithm for aircraft scheduling on a single runway to maximize throughput. *Transportation Research Part C: Emerging Technologies*, 95:570–581, 2018.
- [85] Marco Pretto, Pietro Giannattasio, Michele De Gennaro, Alessandro Zanon, and Helmut Kühnelt. Web data for computing real-world noise from civil aviation. *Transportation Research Part D: Transport and Environment*, 69:224–249, 2019. ISSN 1361-9209. doi: <https://doi.org/10.1016/j.trd.2019.01.022>. URL <https://www.sciencedirect.com/science/article/pii/S1361920918306254>.
- [86] Harilaos Nicholas Psarftis. A dynamic programming approach to the aircraft sequencing problem. Technical report, Cambridge, Mass.: Massachusetts Institute of Technology, Flight , 1978.
- [87] Nikolas Pyrgiotis, Kerry M Malone, and Amedeo Odoni. Modelling delay propagation within an airport network. *Transportation Research Part C: Emerging Technologies*, 27:60–75, 2013.
- [88] A Rodríguez-Díaz, Belarmino Adenso-Díaz, and Pilar Lourdes González-Torre. Minimizing deviation from scheduled times in a single mixed-operation runway. *Computers & Operations Research*, 78:193–202, 2017.
- [89] P.C. Roling. AE4446 Airport Operations Lecture Slides Airside, 2021. <https://brightspace.tudelft.nl/d21/le/content/398027/viewContent/2283974/View>.
- [90] P.C. Roling. AE4446 Airport Operations Lecture Slides Delay and ATM, 2021. <https://brightspace.tudelft.nl/d21/le/content/398027/viewContent/2283974/View>.
- [91] Frédéric Rooseleer, Vincent Treve, and David Phythian. "RECAT-EU" European Wake Turbulence Categorisation and Separation Minima on Approach and Departure, 2018. URL www.eurocontrol.int.
- [92] Safrilah and J C P Putra. Review study on runway capacity parameters and improvement. *IOP Conference Series: Materials Science and Engineering*, 209:012108, 6 2017. ISSN 1757-8981. doi: 10.1088/1757-899X/209/1/012108.
- [93] Amir Salehipour, L Moslemi Naeni, and Hamed Kazemipoor. Scheduling aircraft landings by applying a variable neighborhood descent algorithm: Runway-dependent landing time case. *Journal of Applied Operational Research*, 1(1):39–49, 2009.

- [94] Amir Salehipour, Mohammad Modarres, and Leila Moslemi Naeni. An efficient hybrid meta-heuristic for aircraft landing problem. *Computers & Operations Research*, 40(1):207–213, 2013.
- [95] Marcella Samà, Andrea D’Ariano, Dario Pacciarelli, Konstantin Palagachev, and Matthias Gerdts. Optimal aircraft scheduling and flight trajectory in terminal control areas. In *2017 5th IEEE International Conference on Models and Technologies for Intelligent Transportation Systems (MT-ITS)*, pages 285–290. IEEE, 2017.
- [96] David A. Senzig, Gregg G. Fleming, and Ralph J. Iovinelli. Modeling of terminal-area airplane fuel consumption. *Journal of Aircraft*, 46:1089–1093, 7 2009. ISSN 0021-8669. doi: 10.2514/1.42025.
- [97] D.G. Simons and M. Snellen. Part a: Introduction to general acoustics and aircraft noise, 2021.
- [98] Dick G. Simons, Irina Besnea, Tannaz H. Mohammadloo, Joris A. Melkert, and Mirjam Snellen. Comparative assessment of measured and modelled aircraft noise around amsterdam airport schiphol. *Transportation Research Part D: Transport and Environment*, 105:103216, 4 2022. ISSN 1361-9209. doi: 10.1016/J.TRD.2022.103216.
- [99] Bulent Soykan and Ghaith Rabadi. *A Tabu Search Algorithm for the Multiple Runway Aircraft Scheduling Problem*, pages 165–186. Springer International Publishing, Cham, 2016. ISBN 978-3-319-26024-2. doi: 10.1007/978-3-319-26024-2_9. URL https://doi.org/10.1007/978-3-319-26024-2_9.
- [100] Bulent Soykan and Ghaith Rabadi. A simulation-based optimization approach for multi-objective runway operations scheduling. *Simulation*, 98:991–1012, 11 2022. ISSN 17413133. doi: 10.1177/00375497221099544/ASSET/IMAGES/LARGE/10.1177_00375497221099544-FIG2.JPEG. URL <https://journals-sagepub-com.tudelft.idm.oclc.org/doi/10.1177/00375497221099544>.
- [101] Miltiadis A. Stamatopoulos, Konstantinos G. Zografos, and Amedeo R. Odoni. A decision support system for airport strategic planning. *Transportation Research Part C: Emerging Technologies*, 12:91–117, 4 2004. ISSN 0968-090X. doi: 10.1016/J.TRC.2002.10.001.
- [102] Jiaming Su, Minghua Hu, Yingli Liu, and Jianan Yin. A large neighborhood search algorithm with simulated annealing and time decomposition strategy for the aircraft runway scheduling problem. *Aerospace*, 10, 2 2023. ISSN 22264310. doi: 10.3390/aerospace10020177.
- [103] William J Swedish. Upgraded faa airfield capacity model. volume 1. supplemental user’s guide. Technical report, MITRE CORP MCLEAN VA METREK DIV, 1981.
- [104] Daichi Toratani, Daniel Delahaye, S Ueno, and T Higuchi. Merging optimization method with multiple entry points for extended terminal maneuvering area. In *EIWAC 2015, 4th ENRI International Workshop on ATM/CNS*, 2015.
- [105] Joey van der Klugt. Calculating capacity of dependent runway configurations. Master’s thesis, Delft University of Technology, 2012.
- [106] S.A. van der Meijden. Improved Flexible Runway Use Modeling. Master’s thesis, Delft University of Technology, 2017.
- [107] D Welkers, A Sahai, E van Kempen, and R Helder. Analyse gelijkwaardigheidscriteria schiphol. Technical report, Rijksinstituut voor Volksgezondheid en Milieu RIVM, 2021.
- [108] Tim Tim Alan Yoder. *Development of aircraft fuel burn modeling techniques with applications to global emissions modeling and assessment of the benefits of reduced vertical separation minimums*. PhD thesis, Massachusetts Institute of Technology, 2007.
- [109] Oleksandr Zaporozhets. Aircraft noise models for assessment of noise around airports improvements and limitations. *Environmental Report: Aviation and climate change*, pages 50–56, 2016.
- [110] Oleksandr Zaporozhets. Balanced approach to aircraft noise management. In *Aviation Noise Impact Management: Technologies, Regulations, and Societal Well-being in Europe*, pages 29–56. Springer International Publishing Cham, 2022.

- [111] Zhi-Hui Zhan, Jun Zhang, Yun Li, Ou Liu, S. K. Kwok, W. H. Ip, and Okyay Kaynak. An efficient ant colony system based on receding horizon control for the aircraft arrival sequencing and scheduling problem. *IEEE Transactions on Intelligent Transportation Systems*, 11(2):399–412, 2010. doi: 10.1109/TITS.2010.2044793.
- [112] Zhi-Hui Zhan, Jun Zhang, Yun Li, Ou Liu, SK Kwok, WH Ip, and Okyay Kaynak. An efficient ant colony system based on receding horizon control for the aircraft arrival sequencing and scheduling problem. *IEEE Transactions on Intelligent Transportation Systems*, 11(2):399–412, 2010.
- [113] Wenjing Zhao, Richard Curran, and Hussein A Abbass. Dynamic capacity-demand balance in air transport systems using co-evolutionary computational red teaming. *Air Transport and Operations*, pages 1–11, 2015.
- [114] Hang Zhou and Xinxin Jiang. Multirunway optimization schedule of airport based on improved genetic algorithm by dynamical time window. *Mathematical Problems in Engineering*, 2015:1–12, 2015. ISSN 1024-123X. doi: 10.1155/2015/854372.